A Configuration for a Stepped Planing Boat Having Minimum Drag (Dynaplane Boat)

Eugene P. Clement

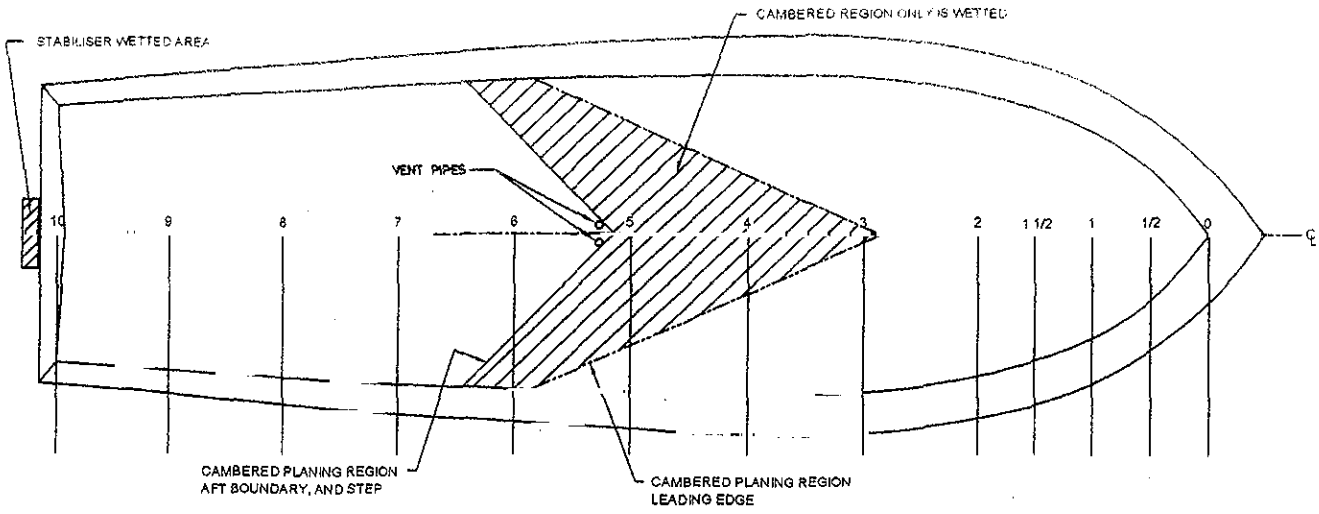

PLAN

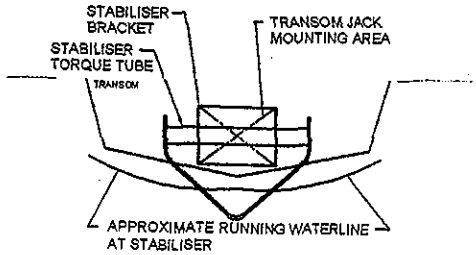

STABILISER-STERN VIEW
(SURFACE PIERCING VEE HYDROFOIL)

Second Edition

Contents

Nomenclature i

Introduction 1

Chapter 1
The "Airplane-Configuration," or "Dynaplane"
Stepped Planing Boat 2

Chapter 2
Prismatic Planing Surfaces with Square Trailing Edges -
As Applied to Stepped Planing Boats 12

Chapter 3
Prismatic Planing Surfaces with Sweptback Trailing Edges -
As Applied to Stepped Planing Boats 22

Chapter 4
Design Procedure for a Planing Surface Having Camber 29

Chapter 5
Design of a Step and Afterbody, and Drag at the Hump 48

Chapter 6
A Surface-Piercing Vee Hydrofoil as the Trim-Control Device
for a Stepped Planing Boat 52

Appendix A
Drawings and Test Results for a Model of an Airplane-Configuration
Stepped Planing Boat - DTMB Model No. 5115 58

Appendix B
Results of Tests of a Planing Surface Model
with the Johnson 3-Term Camber 63

References 71

Nomenclature

A or A.R.	aspect ratio, b^2/S
A_P	projected bottom area of a hull (excluding external spray strips)
B_{PX}	maximum breadth over chines of a hull (excluding external spray strips)
b	breadth of planing surface, ft
C_D	drag coefficient normalized on area, $D/\frac{1}{2}\rho v^2 S$
C_{Lb}	lift coefficient normalized on beam, $L/\frac{1}{2}\rho v^2 b^2$
C_{Lb_0}	lift coefficient, zero deadrise
C_{Lb_β}	lift coefficient, deadrise surface
C_L	lift coefficient normalized on area, $L/\frac{1}{2}\rho v^2 S$
$C_{L,d}$	two-dimensional design lift coefficient for a cambered planing surface
C_f	skin friction coefficient
c	chord length of camber curve
D	drag, lb
F_∇	Froude number based on volume of water displaced at rest, $v/\sqrt{g\nabla^{1/3}}$
g	acceleration due to gravity, 32.16 ft/sec ^{2}
L	lift, lb
ℓ_{cp}	distance of center of pressure forward of trailing edge of planing surface, ft
ℓ_r	root-chord wetted length (i.e., keel wetted length)
ℓ_t	tip-chord wetted length (i.e., chine wetted length)
ℓ_m	mean wetted length
$\ell_{\frac{1}{4}}$	distance from step to spray-root line, measured along a ¼ beam buttock line
R	resistance, lb
Re	Reynolds number
S	projected wetted area bounded by spray-root lines, chines and step, measured on a plane normal to the centerline and containing the keel, ($b\ell_m$) sq ft
V	horizontal velocity, mph, or knots, as indicated
v	horizontal velocity, fps
W	weight of boat, lb
α	angle of attack, deg
β	deadrise angle, deg
ϕ	sweepback angle of 50% chord line, projected on a plane containing the keel, deg
γ	angle between a spray-root line and the centerline, projected on a plane containing the keel, deg
θ	sweepback angle of the step, projected on a plane containing the keel, deg
ρ	mass density of water, slugs per cu ft
τ	trim angle, angle between straight portion of forebody keel and horizontal, deg
∇	volume of water displaced at rest, cu ft

A Configuration for a Stepped Planing Boat Having Minimum Drag
(Dynaplane Boat)

By Eugene P. Clement

Introduction

The type of planing motorboat that is present in the largest numbers throughout the world is the deep-vee type, with longitudinal spray rails. This type has proven to be very suitable for offshore operation, or wherever sizeable waves will be encountered. It is less suitable, however, for operation on the sheltered waters of rivers and lakes, because the type has high drag. Accordingly, it requires large amounts of installed power and is wasteful in regard to fuel consumption. The design continues to be popular because it has the appeal of being patterned after the design of successful offshore racers. Also, the high-horsepower engines required are readily available, and relatively inexpensive, and for the time being the same factors obtain for the fuel. With the emphasis now on reducing motorboat fuel consumption rates and pollution effects, the stepped type of hull, although more complex to design and to build, deserves, because of its very low drag, to find a number of applications. Figure 1-1 shows a comparison of values of resistance/weight ratio, versus an appropriate speed coefficient, from model tests of a number of hull types - including the deep-vee and the stepped types of hulls. (The speed coefficient used, F_{∇}, or volume Froude number, is highly appropriate for comparing the performances of different ships and boats. It realistically adopts gross weight, rather than length, as the significant index of size, and compares different craft on the basis of equal weight and equal speed. The nomograph in Figure 1-2 shows the relationship of F_{∇}, to craft speed and craft gross weight. This nomograph is for salt water, but the values for fresh water are only slightly different.)

Contemporary planing boats generally correspond to either the one or the other of the two unstepped types for which performance data are given in Figure 1-1. Davidson Lab Model No. 2879 was a model of a Ray Hunt deep-vee hull design. DTMB Model No. 4667-1 was the parent hull form for the DTMB unstepped planing boat Series 62. The particulars about that series are given in Reference 1. The Swedish tank-test data for a stepped hull are taken from Reference 2. That reference reported the results from model tests of twenty-seven different single-step hull configurations. The features varied were the deadrise, height of the step, angle between the fore- and after-body keel lines, and length of the afterbody. The data points given in the graph are for the configuration that had the least drag and that also ran stably. (Seventeen of the configurations porpoised when they were run relatively fast). DTMB Model 5115 (which is represented in Figure 1-1) also had a single step; in addition, however, it had a cambered planing surface near amidships, and an adjustable planing stabilizer at the stern for control of the running trim angle. Complete particulars of Model 5115 are given in the Design Data Sheet for that model, which is included as Appendix A.

The desired top speed for a planing boat will generally correspond to a value of the speed coefficient F_{∇} of about 4.5 (or higher). Figure 1-1 shows that at a speed

coefficient of 4.5, hull drag (at equal weight) for the better of the two types of stepped hulls would be approximately one-half the hull drag of the better of the two types of unstepped hulls. This comparison of the two types on the basis of equal weight indicates that horsepower required and fuel consumption rate would be approximately half as much for a stepped boat as for a comparable unstepped boat. However, if a comparison is more appropriately made, between two boats which are designed for the same mission or purpose, the stepped boat would be considerably the lighter in weight (because of its smaller engines and lighter fuel load), and this would lead to further reductions in its drag, horsepower required, and fuel consumption rate. The significant final result is that fuel consumption rate and fuel cost (and also pollution caused) would be less than half as much for an optimized stepped boat as for a comparable unstepped boat. Furthermore, the efficient stepped type has sufficiently low drag that it could be used in the future for planing runabouts powered by fuel-cell-powered drive trains of the size and type presently being developed for automobiles.

Chapter 1
The "Airplane-Configuration," or "Dynaplane" Stepped Planing Boat

A variety of types of stepped planing boats are feasible, such as single-step, multi-step, catamaran, canard, and "airplane-configuration." (or "Dynaplane"). The studies and comparisons of those different types show that the Dynaplane configuration will be the superior type for numerous applications. (Dynaplane refers to a configuration for which, as is the case for an airplane, most of the lift is provided by a cambered, relatively high-aspect-ratio lifting surface located near the center of gravity, and an adjustable lifting surface aft provides stability and control of the angle of attack.) Because of the points of similarity between this type of stepped planing boat and a modern monoplane airplane, an appropriate design procedure for the boat can borrow extensively from the design concepts and procedures that are used for an airplane.

DTMB Model 5115, which is represented in Figure 1-1, is a model of a stepped boat of the "airplane," or "Dynaplane" type. The performance comparison of Figure 1-1 indicates the superiority of the type. Also, a comparison of the performances of Models 4667-1 and 5115 illustrates the significant differences in the performances of unstepped and stepped planing boats. Typically, the stepped boat has more drag in the lower part of the speed range, and there is a hump in its drag curve. At values of the speed coefficient F_{∇} of about 3 and higher the stepped type of hull has the lower drag, and the resistance difference increases markedly with increase in speed. Accordingly, if the speed coefficient of a projected new design is about 3.5 or higher, a stepped configuration can be expected to have appreciably less drag than a corresponding unstepped configuration.

A striking fact about the potential of the Dynaplane-type of stepped planing boat is that as the design speed increases, the hydrodynamic hull drag remains practically the same (and in some cases actually decreases). For example, an optimum Dynaplane-type of boat, designed for, and running at, a speed of 45 mph will usually have lower hydrodynamic hull drag than a corresponding Dynaplane boat (of equal weight) designed

for, and running at, a speed of only 35 mph. Appendage drag and air drag will, however, be greater for the faster boat.

The majority of what follows is devised to guide the design of the Dynaplane-type of stepped planing boat. However, design information for different types of planing surfaces is included that can be used for designing the planing surfaces of the other types of stepped boats as well.

The building and testing of a number of models and full-scale boats of the stepped type has resulted in the development of a configuration having highly satisfactory performance. An example of the type of configuration that has been developed is shown in Figure 1-3. An essential feature is a step, near mid-length, which will cause the flow to separate from the afterbody bottom, thereby reducing the amount of the bottom wetted area and accordingly also, the frictional resistance. The shape adopted for the chine line in plan view is important. The relatively narrow stern tends to give low drag in the lower part of the speed range, and the wide forebody provides good transverse stability in the high-speed planing condition. The hull form of Figure 1-3 consists entirely of developable surfaces. A result of this is that the bow sections have the convex shape which is desirable for good rough-water performance. Another result is that the skin of a corresponding full-scale boat can be economically made from large sheets of either aluminum or plywood.

The best results are obtained for a Dynaplane-type of boat if the forebody deadrise angle is not more than about 15 degrees. For the case shown in Figure 1-3 the forebody deadrise angle is 12.5 degrees. Both the step and the center of gravity are near midlength. The reason for sweep-back of the step will be explained subsequently. The afterbody is tilted up with respect to the forebody, so that it will run clear of the water at high speed. It is convenient during the design procedure to draw the buttock lines of the forebody bottom, from the step, and for some distance forward of it, initially straight, and parallel to the baseline. Then, when final values for the speed and weight of the boat have been determined, a suitable design for the forebody's cambered region can be developed, and conveniently grafted onto the flat regions adjacent to the step. The afterbody bottom should be a simple vee shape (with straight and parallel buttock lines), so that it will perform its needed function of providing a significant proportion of the lift at intermediate speeds, and particularly at the hump.

The overall dimensions of a design for a Dynaplane-type of boat can be derived in the same manner as for the case of designing a conventional (unstepped) planing motorboat. Accordingly, with the boat's purpose and desired speed specified, estimates of the length, the beam, and the weight can be made in the usual way. Examples of previous successful stepped and unstepped designs should be referred to in order to arrive at suitable values for the length and beam of a projected new design.

The succeeding steps in the design of a Dynaplane-type of boat should be directed towards achieving minimum drag at the selected high-speed design point. At this high-

speed design point the boat is to be supported by a main planing region (appropriately located with respect to the center of gravity), together with an adjustable small lifting device at the stern. Those features are analogous to the wing and stabilizer of an airplane. Accordingly, application of a design procedure similar to that for designing an airplane is appropriate. The concepts and ideas that are appropriate for designing the hull-form of a conventional, unstepped, boat are unsuitable for designing an efficient main lifting surface, and a suitable stabilizer, for an optimum (Dynaplane) stepped boat. This is an extremely important point to realize! It is essential to "shift gears," mentally, and to think and operate in different terms in order to be able to proceed satisfactorily with the design of an optimized stepped planing boat. Helpful guidance can be obtained, however, by thinking in terms of the analogy between an efficient stepped planing boat and a modern monoplane airplane. This analogy is valid because both are supported by dynamic lift, and therefore the factors affecting the lift and the drag of the two types arise from similar effects. (An important difference, of course, is the relative densities of the mediums in which the two different types operate.) A significant consideration in proposing this analogy is that the configuration and the design methods for the modern monoplane airplane have resulted from development work which has extended over the past century. A goal of that work was to derive configurations which would produce a specified amount of dynamic lift, would run stably, and would cause a minimum amount of drag. The goal when designing an efficient stepped planing boat is very similar. It is pertinent to point out that although the configuration and the basic design methods for the modern monoplane airplane are now so familiar as to be considered obvious, that was not always the case. Instead, both the design and the design methods were adopted after a period of trial and error during which a variety of other configurations and methods were tried and rejected. The undertaking of developing designs (and design methods) for efficient stepped planing boats can benefit from this history of the development of the modern monoplane airplane. That is, instead of undertaking a long and expensive trial and error process in order to find the best configurations, and the best design procedures, for producing efficient stepped boats, configurations and design methods analogous to those that have been developed for the case of the modern monoplane airplane can confidently be adopted.

An essential (and now obvious) feature of a modern monoplane airplane is a wing (located close to the center of gravity) that has been carefully designed to provide a needed amount of dynamic lift with a minimum amount of drag. It was learned in the very early stages of the development of the airplane that to obtain satisfactory performance it was essential to give an airplane wing a suitable camber curvature. Camber curvature can provide similar important benefits when incorporated into the main lifting surface of a stepped planing boat.

The center of gravity of an airplane is located close to the mid-length point of the fuselage, so that the full length of the internal volume can be utilized for carrying useful items of payload. Similarly, the center of gravity of a stepped planing boat that is intended to be efficient and useful should be located close to the mid-length point of the hull. (This is in contrast to the case for conventional unstepped planing boats, for which the center of

gravity is usually located an appreciable distance aft of amidships, in order to achieve some reduction in wetted bottom area when planing.) Another distinctive feature of the modern monoplane airplane is an adjustable stabilizer at its stern (much smaller than the wing), to provide stability, and to make it possible to adjust the trim angle of the craft so that the wing will run at its optimum angle of attack. Similarly, if a stepped planing boat is to operate stably and with maximum efficiency, it also requires a small adjustable stabilizer at the stern.

The chief features of an efficient stepped planing boat are illustrated in Figure 1-3. These are, a cambered main planing surface, a sweptback step located at approximately mid-length, and an adjustable lifting device at the stern. Vent pipes should be provided just behind the step, adjacent to the centerline, as indicated in the figure. With the aid of a flow of air through the vent pipes, water will separate from the hull bottom at a relatively low speed, beginning at the step. At high speed the entire hull bottom aft of the step will run clear of the water, and the frictional resistance will accordingly be significantly reduced. At the high speed design point most of the weight of the boat will be carried by a relatively small bottom area beginning at the step and extending a short distance forward of it. A small adjustable stern lifting device will carry the remainder of the weight. The amidships lifting area is, of course, analogous to the wing of an airplane. Because of the very high density of the fluid medium in the case of the boat (approximately 800 times the density of the fluid medium for the case of an airplane), the lifting area needed for the boat is extremely small. The initiate to the art of designing a Dynaplane-type of stepped boat is likely to be extremely surprised to find how small an appropriately designed main planing surface will be. A hull bottom width of the usual size will accordingly provide the needed span dimension, and a relatively short wetted length will provide the needed fore-and-aft dimension. (The possibility of developing a planing boat design analogous to a "tailless" airplane obviously suggests itself. However, experience has shown that a short planing surface running by itself will not operate stably. It has further been found that if approximately 90% of the weight of a stepped planing boat is carried by a short planing area located near amidships, and the remainder of the weight is carried by a small lifting area at the stern, this will result in a configuration which will run stably.)

The amidships planing region can be optimized for minimum drag by incorporating camber curvature of the type that has been developed for the lower surfaces of supercavitating hydrofoils. Alternatively, the main planing surface of a stepped hull can in some cases be a simple prismatic surface with a square trailing edge, and in other cases a prismatic surface with a swept-back trailing edge. The three types of planing surfaces are treated, separately, in the three succeeding chapters.

It was mentioned previously that the center of gravity should be located close to the midlength point of the hull. This will result in a suitable floating angle (angle of the straight portion of the forebody keel with the horizontal) of between zero and one degree by the stern.

It is helpful in designing such important features as the position and height of the

step, and the angle between the forebody and afterbody keels, to refer to previous successful designs. The mean step position has typically been at about 55% of the chine length from the bow, and the height of the step typically equal to about 1% of the beam of the main planing surface. (The step edge must be sharp.) The angle between the forebody and afterbody keels should be such that when the forebody keel is trimmed to its design running angle the afterbody keel will be approximately horizontal. The downwash from the step will typically be about 2 degrees, and this will provide the needed clearance between the afterbody and the water surface.

The adjustable rear lifting surface of the Dynaplane-type of boat introduces a complication, but this makes it possible to maintain the trim of the boat at the angle for minimum drag, and also makes it possible to avoid two types of misbehavior to which a stepped boat with a fixed rear lifting surface is susceptible - porpoising, and nosediving in a following sea. Regarding porpoising, the Introduction has explained that interesting evidence regarding that problem is available in **Reference 2**. The possibility of nosediving in a following sea also needs to be a concern, since that type of misbehavior has occurred in the case of a number of stepped boats of the past which had fixed sterns. This event can occur when the forward planing surface of a stepped boat encounters the downward-moving water particles in the back of a wave, and therefore loses lift, while at the same instant the rear planing surface is developing a relatively high lift. The combined effect is that the boat may be trimmed down to such a dangerously low angle that it buries itself in the back of a wave. This likelihood can be avoided with an adjustable rear lifting surface, which can be used to trim the boat to a suitably high and safe angle when running in a following sea. An adjustable rear surface can also be utilized to prevent porpoising.

The stern device (for trim-control and stabilization) that recommends itself for an optimum stepped boat is a surface-piercing Vee hydrofoil. Such a foil is illustrated in Figure 1-3. This foil will typically carry about 10 percent of the weight of the boat at the design speed. It will provide inherent stabilization in heave and trim when fixed in position. However, provision should be made for vertical adjustment of the foil to cater for variations in boat weight and LCG location. (It is proposed that the vertical adjustment be provided by mounting the hydrofoil on a power-actuated transom jack of the type used for adjusting the heights of outboard motors.) Results from the tank testing of some Vee hydrofoils, at different depths of submersion, and up to high speeds, were given in **Reference 3**. Results from that reference which are of interest for the present case are given in Chapter 6. That chapter also includes guidelines to foil design that have been learned from the experiences of enterprising entrepreneurs who have designed, built, and tested hydrofoil-supported motorboats.

There is a significant point to be made about the trim-control feature in relation to the highly important factor of marketing. Particular enjoyment and satisfaction are to be derived from the operation of a fast runabout when the pilot is able to adjust the angle of attack of his craft. The experience of skimming over the water on an efficient small planing area, and, with the throttles fixed, adjusting the position of the stern hydrofoil up

or down to find the optimum running angle of attack (as shown by the speed gauge and the tachometer) is outstanding fun! This is in marked contrast to the case for a conventional (unstepped) boat with adjustable stern trim flaps. Such flaps are only useful at low speeds for getting over the hump. At planing speeds such a craft runs at a low, and inefficient, angle of attack, and activation of the stern flaps will lower the running trim angle further and make the craft even more inefficient. Therefore, at planing speeds such flaps are usually retracted clear of the water.

Succeeding chapters of this booklet explain how to design the different types of planing surfaces that can be utilized for the main (forward) planing surface of a single-step boat. A chapter is included that gives pointers about designing a step and an afterbody, and also explains how to predict the drag at the "hump." Finally, there is a chapter that gives the particulars of a hydrofoil that will serve as an efficient stern trim control device.

It should be noted that this booklet is not a complete text on how to design a Dynaplane-type of stepped motorboat. Its intention, instead, is to supply the additional information that will enable an experienced motorboat designer to design a successful boat of that type. A design produced on the basis of the information given here, by someone other than an experienced motorboat designer, should be thoroughly checked by a suitably-qualified person, before construction of a boat.

Limitations on the range of applicability of the Dynaplane design should also be explained. The type of surface-piercing hydrofoil recommended here for the stern trim-control device is limited to a top speed of approximately 50 mph. At higher speeds cavitation or ventilation is likely to occur, with significantly adverse effects on the performance of the hydrofoil. Adopting a speed limit of 50 mph makes it possible to calculate appropriate limits on installed hp for ranges of values of weight and deadrise angle. The recommended limits on installed power are shown in Figure 1-4.

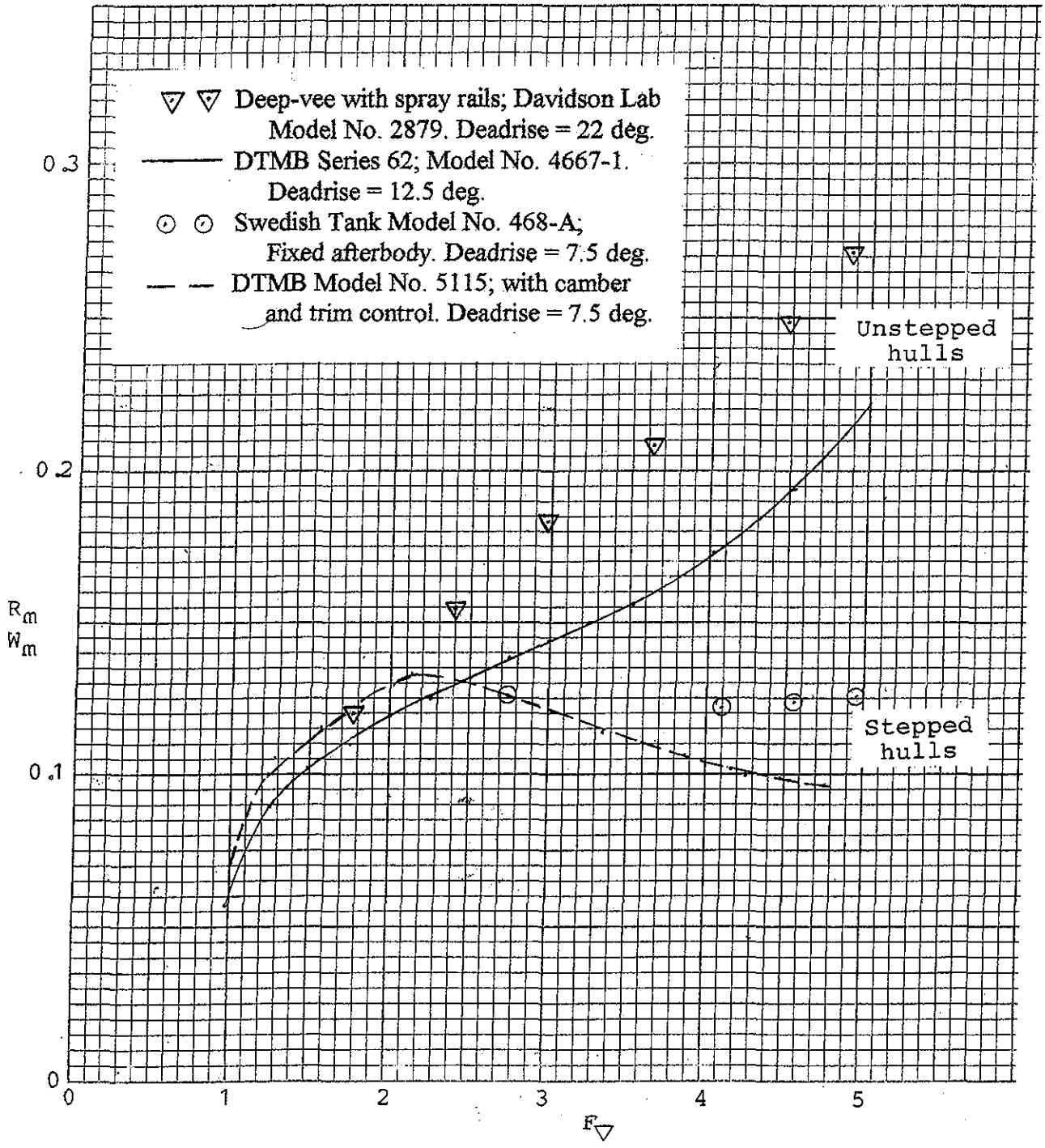

Figure 1-1 - Values of Model Resistance/Weight Ratio, Versus Speed Coefficient, for Different Types of Planing Hulls.

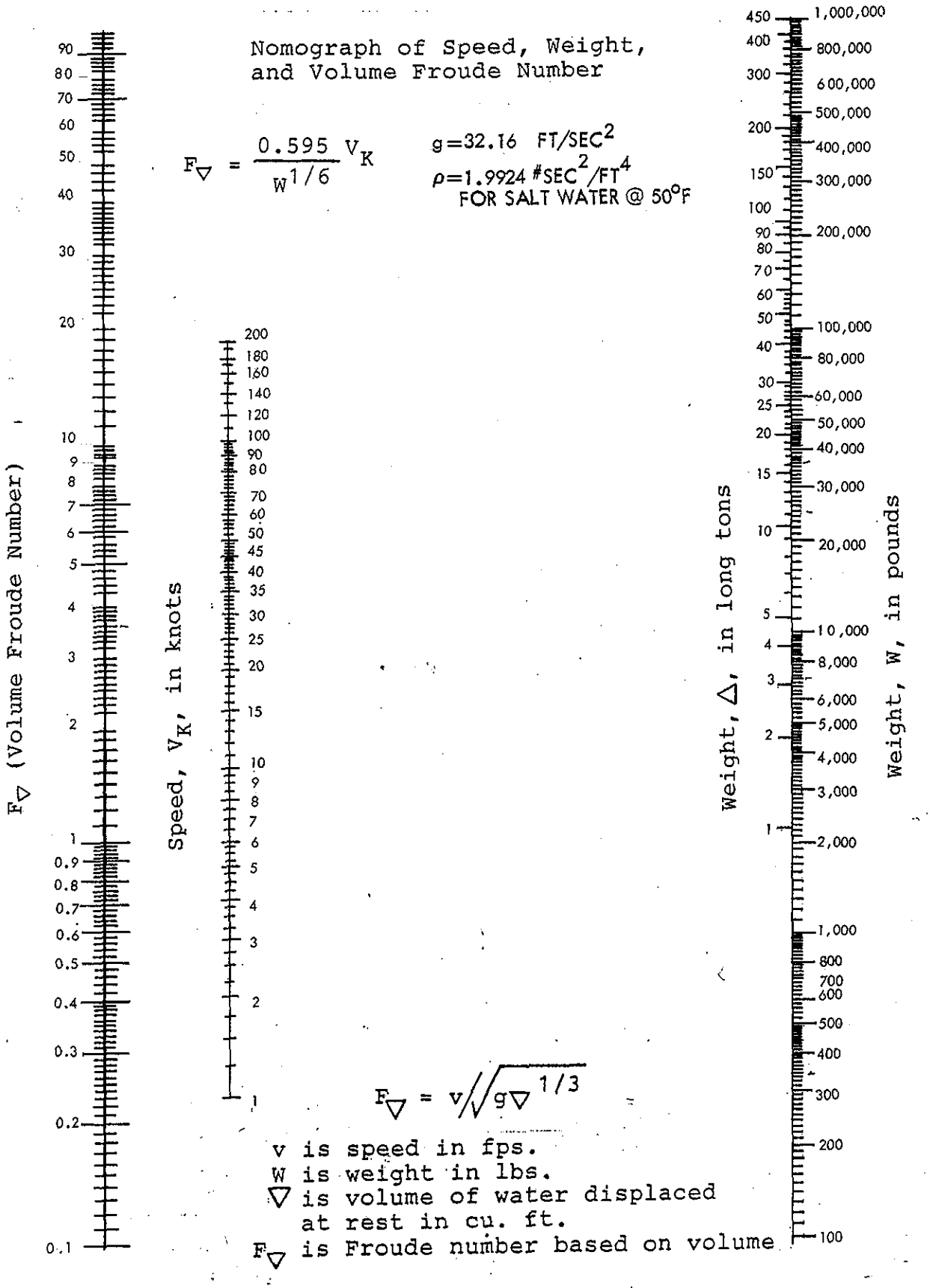

Figure 1-2 - Nomograph of Speed, Weight, and Volume Froude Number.

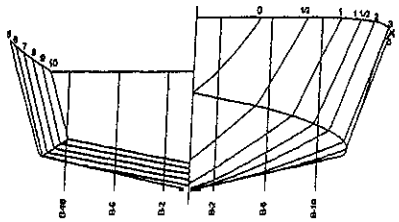

BODY PLAN

CAMBER NOT SHOWN IN THIS VIEW

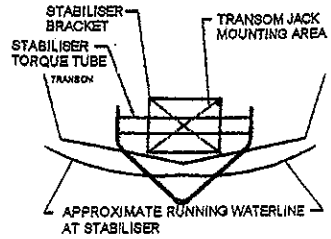

STABILISER-STERN VIEW

(SURFACE PIERCING VEE HYDROFOIL)

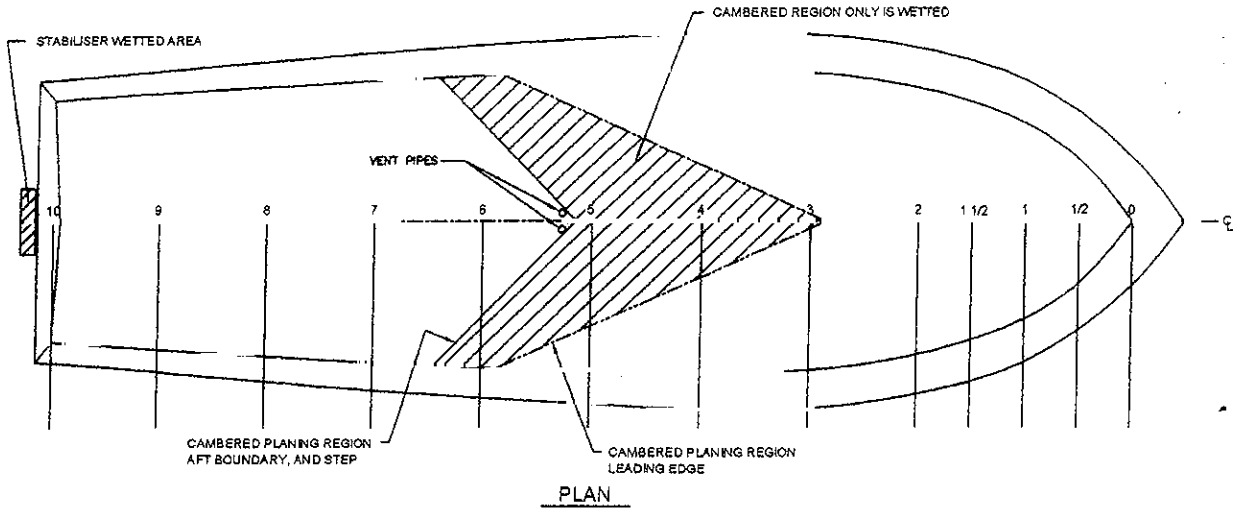

PLAN

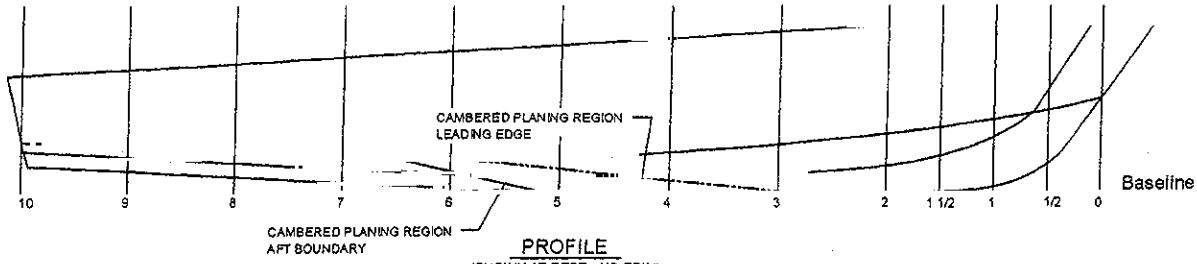

PROFILE

(SHOWN AT REST - NO TRIM)

CAMBER NOT SHOWN IN THIS VIEW, SEE ENLARGED CAMBER PROFILE FOR BUTTOCK SHAPE IN THE CAMBERED REGION.

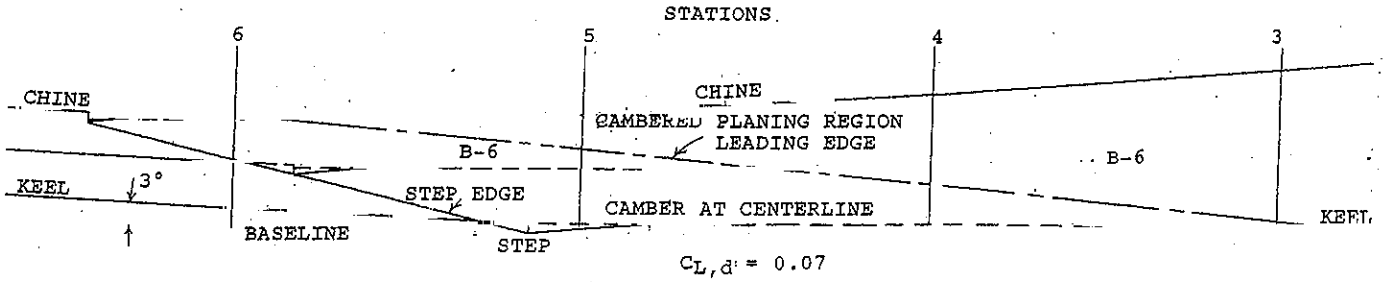

CAMBER PROFILE

Figure 1-3 - Example of a Design for a Stepped Planing Boat having Minimum Drag.

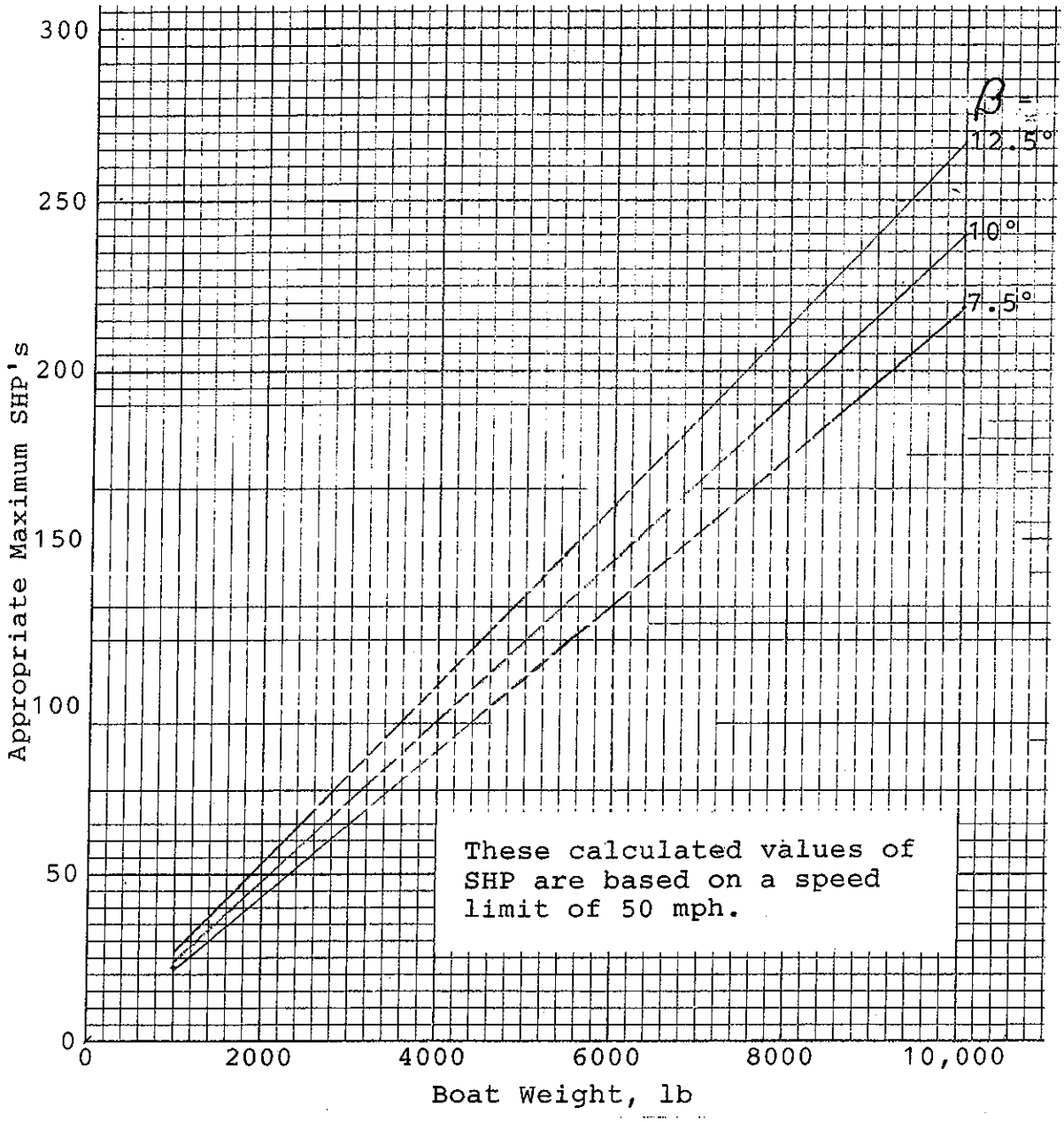

Figure 1-4 - Appropriate Maximum Values of Installed Horsepower for Dynaplane-Configuration Stepped Planing Boats.

Chapter 2
Prismatic Planing Surfaces with Square Trailing Edges - As Applied to Stepped Planing Boats

A great many stepped planing motorboats have been built during the past century. In most cases such boats have been the single-step type, and have utilized a simple prismatic surface with a square trailing edge for their main (forward) planing surfaces. The afterbodies of such boats have almost invariably been fixed. Stepped boats of that type are limited with regard to performance and range of applicability. The Introduction has referred to the series of 27 models of stepped planing hulls which were tested in Sweden. Those models were representative in form of many of the stepped boats built during the past century. The susceptibility of the type to porpoising is indicated by the fact that the majority of the models of the series tested in Sweden porpoised when running relatively fast. The model from the Swedish series which is represented in Figure 1-1 ran stably at particular conditions of weight and CG location, but would be liable to porpoise at other conditions. Furthermore, Figure 1-1 indicates that the resistance of the type at high speed is more than 25 percent higher than the resistance of an available alternative type of stepped hull.

For those cases when the familiar stepped type of the past has run without porpoising it has shown an improvement in performance over that of an unstepped boat. A suitably-sharp step will result, at a relatively low speed, in the flow separating from the bottom of the afterbody immediately behind the step; then, as the speed increases, the extent of the region of the afterbody bottom from which the flow is separated also increases, and at high speed only the aft-most portion of the bottom of the afterbody remains in contact with the water. The extent of the afterbody wetted area, and therefore also the amount of the frictional resistance of the afterbody, are therefore substantially reduced. (The region of the forebody bottom that is wetted at planing speed is also less than when the boat is at rest, whether a planing hull is stepped or unstepped.) A typical planing configuration for such a boat (with the areas wetted at high speed indicated) is shown in Figure 2-1.

When running at high speed most of the weight of a single-step boat (typically about 90% of the weight) will be supported by the main (forward) planing surface. The small wetted region of the hull bottom near the stern will therefore be carrying about 10% of the weight. Accordingly, the index of the performance of such a design (i.e., the hull lift/drag ratio), can be assumed to be very close to the value of the lift/drag ratio of just the forward planing surface. A design goal for such a craft will, of course, be to minimize its high-speed resistance. Achievement of this will require that the important forward planing surface consistently operate at such an angle of attack that it develops the needed lift, together with a minimum amount of drag. That is, the forward planing surface should consistently run (at the different speed and loading conditions of the boat) at its optimum angle of attack. Now, the angle of attack at which the forebody runs is largely determined by the position of the afterbody. The requirement that the forebody run at its optimum angle of attack cannot be fulfilled by the usual type of stepped boat, having a fixed

afterbody, since the positioning of the afterbody that will cause the forebody to run at its optimum angle of attack varies with the speed, weight, and CG location of the boat. With an adjustable rear lifting surface, however (i.e., with an "airplane-type" of boat), the forward planing surface can be constrained to operate at its optimum angle of attack, and minimum resistance can be attained for a wide range of conditions of operation.

It has been pointed out that to attain optimum performance with a stepped planing boat the forward planing surface should run at its optimum angle of attack. It was also explained that knowing the resistance/weight ratio of the forward planing surface provides a close approximation to the hydrodynamic resistance/weight ratio of the complete craft. Accordingly, points of interest for a stepped planing boat are the angle of attack at which the forebody should run for least drag, and the resulting resistance in the high-speed planing condition . Those and other interesting details can be determined from the available extensive literature on the subject of planing surfaces. Very comprehensive particulars regarding the performance characteristics of prismatic planing surfaces with square trailing edges are given by the equations and graphs to be found in **References 4 and 5**. Those equations and graphs are based on extensive testing of planing surfaces by NACA (now NASA) in its seaplane towing tank.

It has been pointed out previously that the methods and concepts used for designing a conventional unstepped planing boat are not appropriate for designing an efficient stepped planing boat. It is essential to put the conventional methods aside, and to utilize instead concepts and methods that are appropriate for designing a craft that is intended to develop dynamic lift in an optimum manner (i.e, with a minimum amount of drag). The analogy to the case of designing an airplane is apparent, and was pointed out previously. The following performance particulars for prismatic planing surfaces with square trailing edges are intended to be useful for designing efficient forward planing surfaces of stepped boats. Therefore, those particulars are presented in terms borrowed from airplane design - i.e., in terms of aspect ratio, lift coefficient, and optimum angle of attack.

Now, the range of aspect ratios for the main (forward) planing surfaces of single-step boats (when planing) is generally in the range of about 1.5 to 2.5. The graphs given in **Reference 5** reveal that for this range of values of aspect ratio the optimum angle of attack of a planing surface having a particular value of deadrise angle remains essentially constant with variation in aspect ratio. The graphs of that reference also show what those optimum angles of attack are for different angles of deadrise. Those graphs show that for a prismatic planing surface with 5 deg deadrise, the optimum angle of attack is almost exactly 3 deg, with 10 deg deadrise, it is almost exactly 4 deg, and with 15 deg deadrise it is very close to 4.5 deg.

The graphs of **Reference 5** also display the interesting fact that for deadrise angles of 10 deg and 15 deg, planing efficiency (i.e., resistance/weight ratio, R/W) does not change, with change in aspect ratio, in the aspect ratio range which is applicable for stepped hulls. For 5 deg deadrise there is some decrease in R/W with increase in aspect

ratio. Those facts make it possible to distill, for the stepped-hull case, the very extensive planing surface performance characteristics which are given in **Reference 5** into only the four curves of resistance/weight ratio (R/W) given in Figure 2-2.

In what follows the term "trim angle," tau (τ), is introduced, and is used interchangeably with "angle of attack," alpha (α). This is for convenience in incorporating material from various references.

Complete particulars of the forward planing surfaces of single-step boats (of deadrise angles of 5, 10, and 15 degrees), when they are running at their optimum trim angles, can be determined from the graphs presented here. Figure 2-3 shows the relationship between lift coefficient and aspect ratio, for deadrise angles of 5, 10, and 15 degrees, at the optimum trim angle for each deadrise angle. It was prepared by utilizing information given in **Reference 5**. For a particular design case the lift coefficient based on the square of the bean can be calculated, and the value of the aspect ratio can then be read from Figure 2-3. With the aspect ratio known, the mean wetted length at the planing point can be calculated from the relationship that aspect ratio equals b/ℓ_m, so that ℓ_m equals b/(AR). The angle between the spray-root line and the centerline of the boat, in plan view (angle γ), can be read from Figure 2-4, or can be calculated using the equation given there. (The spray-root line is the forward boundary of the region of the bottom that is wetted by solid water - i.e., the forward boundary of the region that contributes the planing lift.)

As an example of the use of the foregoing graphs and relationships, assume the case of a main (forward) planing surface for a stepped boat having a chine beam of 6 feet and a deadrise angle of 10 deg. This forward planing surface is to provide 4500 pounds of lift at a speed of 40 mph (i.e., 58.7 fps). Assume fresh water, for which rho (ρ, which is equal to w/g) equals 1.94. The value of the lift coefficient based on the square of the beam can now be calculated:

$$C_{Lb} = L/(1/2\,\rho\, v^2 b^2)$$

$$= 0.037$$

As explained previously, a 10 deg deadrise planing surface being utilized for the main (forward) lifting surface of a stepped boat should run at an angle of attack of 4 deg (so that it will have minimum drag). This is to be achieved either by appropriate design of a fixed rear planing surface, or by proper positioning of an adjustable rear lifting surface. With the foregoing values for C_{Lb} and deadrise, Figure 2-3 can be entered to find that the aspect ratio will be 1.7. Figure 2-2 can then be entered to find that the resistance/weight ratio will be 0.12. If the total boat weight is 5000 lb, then hydrodynamic hull drag can be taken to be 12% of that weight, or 600lb. The remaining particulars of the forward planing surface at the design point can also now be determined. Since the beam is 6 ft, and the aspect ratio is 1.7, the mean wetted length, ℓ_m, can be calculated to be 3.53 ft. The angle gamma (γ), between the spray-root line and the centerline, in plan view, will be found, as explained above, to be equal to 32.4 deg.

The planing configuration can then be drawn, as depicted in Figure 2-5, either by laying off the mean wetted length, ℓ_m, and drawing a straight line through its forward end at the proper angle (γ) with the centerline, or, alternatively, by determining the root-chord and tip-chord wetted lengths from the relationships given on the figure.

It is important to know the location of the center of pressure on the bottom of a planing surface that is to be utilized for a stepped boat. The graphs of **Reference 5** show that for the design region applicable to stepped boats (aspect ratios above about 1.5) the center of pressure on the bottom of planing surfaces having deadrise angles of 5, 10, or 15 deg (at the optimum trim angle in each case) will be at 84% of the mean wetted length forward of the trailing edge.

In designing a stepped boat care must be taken to prevent a particular type of spray produced by the forebody from wetting the afterbody, and causing a large drag rise. It is this consideration which limits the range of applicability of the planing surface with a square trailing edge. Examples from model tests of the occurrence of this drag rise were presented in **Reference 6**. The phenomenon can be explained by reference to Figure 2-1. When a stepped hull is planing on the surface of the water, the forebody bottom (i.e., the region ahead of the step) is wetted by two different types of flow. There is a region beginning at the step and extending some distance forward of it which is wetted by solid water. This is a region of relatively high pressure which supports most of the weight of the boat. The forward boundary of this region is the "spray-root" line. Typically, in the planing condition, the forebody of a stepped boat will support approximately 90% of the weight of the boat, with the remaining weight carried either by the stern portion of the afterbody bottom , or, preferably, by an adjustable lifting device at the stern. When planing, all or most of the afterbody bottom should be clear of the water in order to reduce the frictional component of the hull drag. Forward of the region of the forebody which is wetted by solid water there is a region which is wetted by a thin sheet of "whisker spray." A second type of spray is also produced by the forebody - a pair of "main spray blisters." Details of the origin and shape of this spray formation have been given in **Reference** 7. It is this latter spray formation which can produce an objectionable large drag rise. As indicated in the figure, the main spray blisters ordinarily originate at the intersection of the spray root lines with the chines of the boat. They are jets of water which shoot upward and outward from their points of origin, forming approximately the shapes of cones. The spray root lines on the bottom of the forebody are lines of high pressure, so it is readily understandable that strong jets of water will occur at the chines, where the high pressures are released. Now, the spray root lines are near the bow at the lower planing speeds, and move progressively aft as the speed increases. This shift occurs because the lift per unit of area on the bottom of the forebody is proportional to the square of the speed, so that as the speed increases, less and less bottom area is required for it to provide its needed proportion of lift. In other words, the forward boundary of the wetted region moves aft in such a way as to maintain a balance between the downward weight and the planing lift. Eventually, when a relatively high speed is reached, the chine ends of the spray root lines come close to the step. This condition is shown in Figure 2-6. Then, with further increase in speed, the spray root lines

will intersect the step rather than the chines. The points of origin of the main spray blisters will now be under the bottom of the afterbody. Accordingly, each upward-shooting cone of water will now wet a portion of the afterbody bottom, and will thereby produce a substantial increase in drag. Since in this condition the width of the hydrodynamic pressure area supporting the weight of the boat is diminished, the transverse stability will also deteriorate. A further highly undesirable effect of the afterbody-wetting phenomenon is that it tends to cut off the flow of ventilating air to the step and the afterbody. In some instances a subsequent result of this effect is that a reduced pressure is produced on the afterbody bottom. The hull will then be sucked down, and the entire afterbody bottom will become wetted. The drag rise in this condition will, of course, be very great indeed. It will readily be appreciated, too, that when a stepped boat is running in even small waves the spray-root lines on the bottom of the forebody will be continuously moving back and forth. If those spray-root lines cross the step, then, intermittently, large increases in drag will occur.

It will be apparent from Figures 2-1 and 2-6 that, to avoid the problems explained above, it is necessary that the spray-root lines consistently intersect the chines an adequate distance forward of the step. Or, in other words, it is necessary that, at the intended operating conditions, there is an adequate value of tip-chord wetted length. Figure 2-7 (which is based on the NACA research results) makes it easy to determine if there will be an adequate amount of tip-chord wetted length at the intended operating point for a proposed new design. The graph gives values of lift coefficient versus deadrise, at best trim, for various values of tip-chord wetted length. When the values of beam, weight, and speed give a value of lift coefficient such that the tip-chord wetted length is zero, the spray-root lines at the chines are at the step. A greater speed (or a smaller weight) would then result in the main spray blisters originating at the step and inboard of the chines (i.e., under the afterbody), thereby producing a large drag rise. It can be seen from Figure 2-7 that the lift coefficient value for the example given previously in the text (0.037), with a deadrise of 10 deg, will give a tip-chord wetted length at the high-speed design point of approximately 0.2b. However, if the design speed was increased from 40 mph to 45 mph, then the value of the lift coefficient would become 0.03, and it can be seen from the graph that the value of the tip-chord wetted length would then be close to zero. It is considered that a suitable minimum value for tip-chord wetted length, at the high-speed design point, for a boat intended to be run in waves, is about 0.2b. Chapter 3 will explain that for a stepped boat intended to be operated at high speed, an adequate value of tip-chord wetted length can be maintained by giving the step an angle of sweep-back.

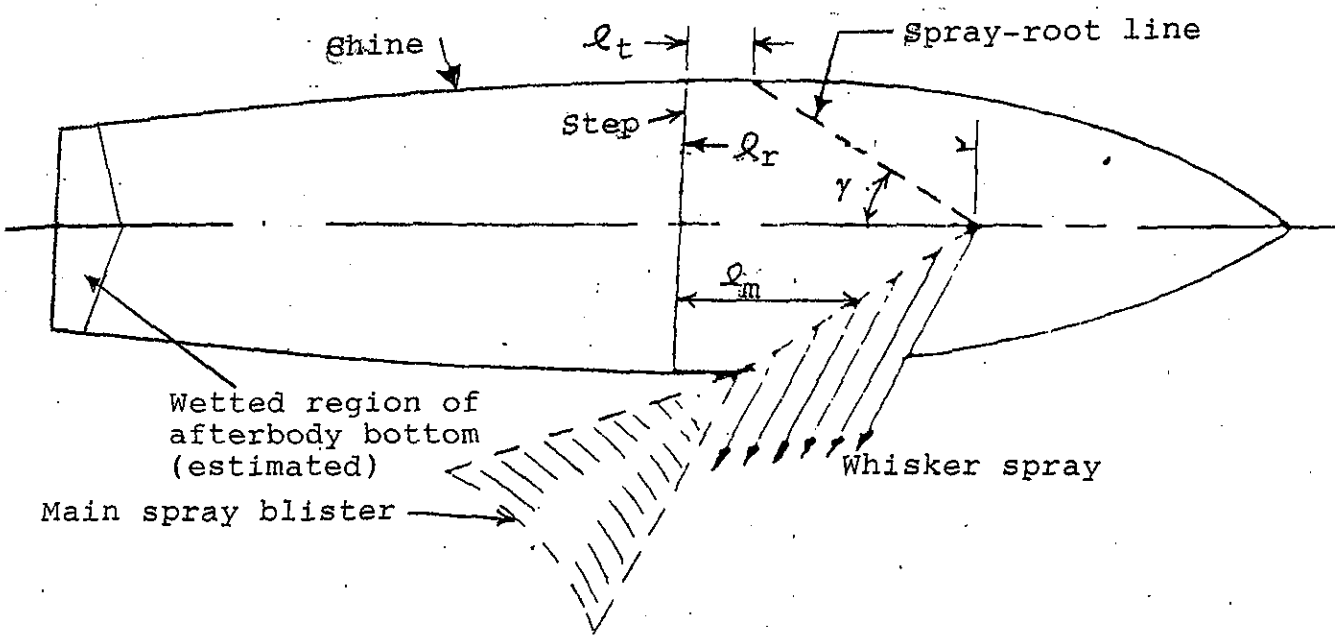

Figure 2-1 - Typical Planing Configuration for the Case of a Stepped Boat With a Main Planing Surface Having a Square Trailing Edge, When Running at High Speed.

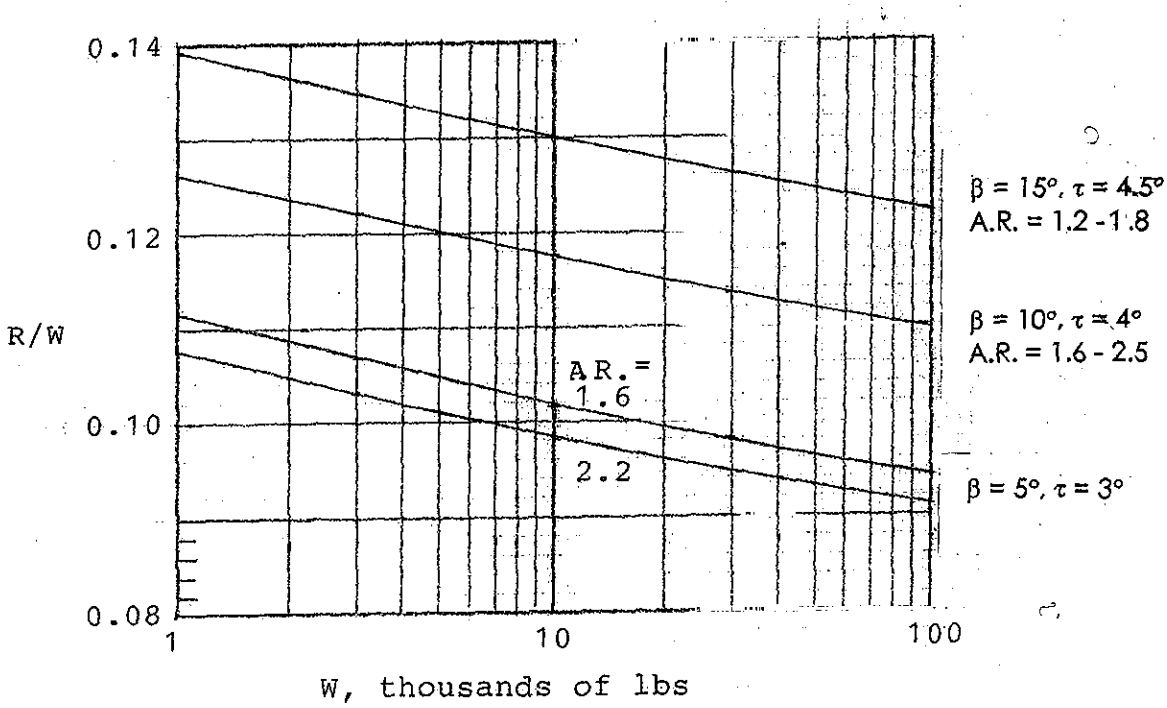

Figure 2-2 - Resistance/Weight Ratio Versus Weight for Prismatic Planing Surfaces with Square Trailing Edges.

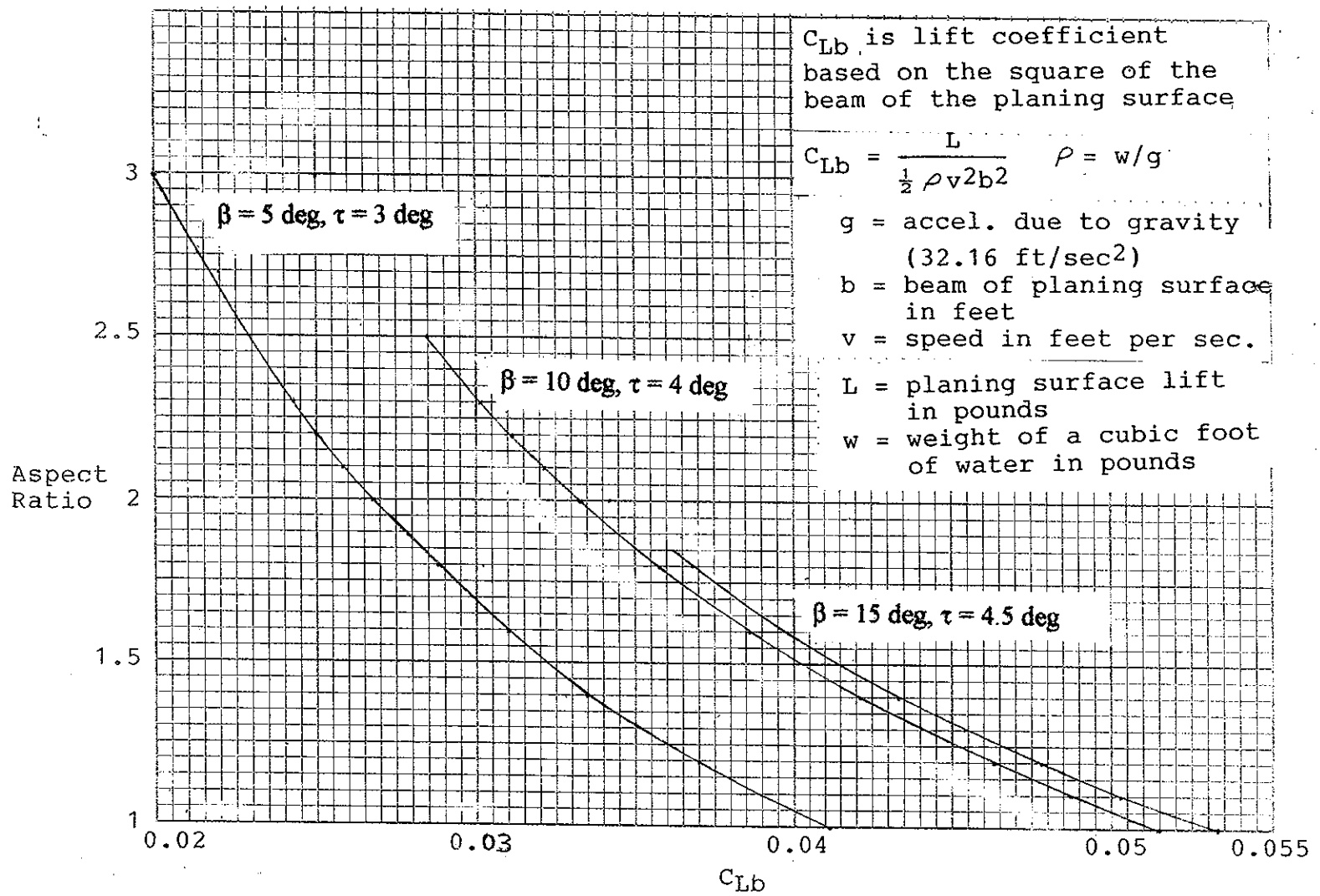

Figure 2-3 - Aspect Ratio versus Lift Coefficient for Planing Surfaces with Square Trailing Edges.

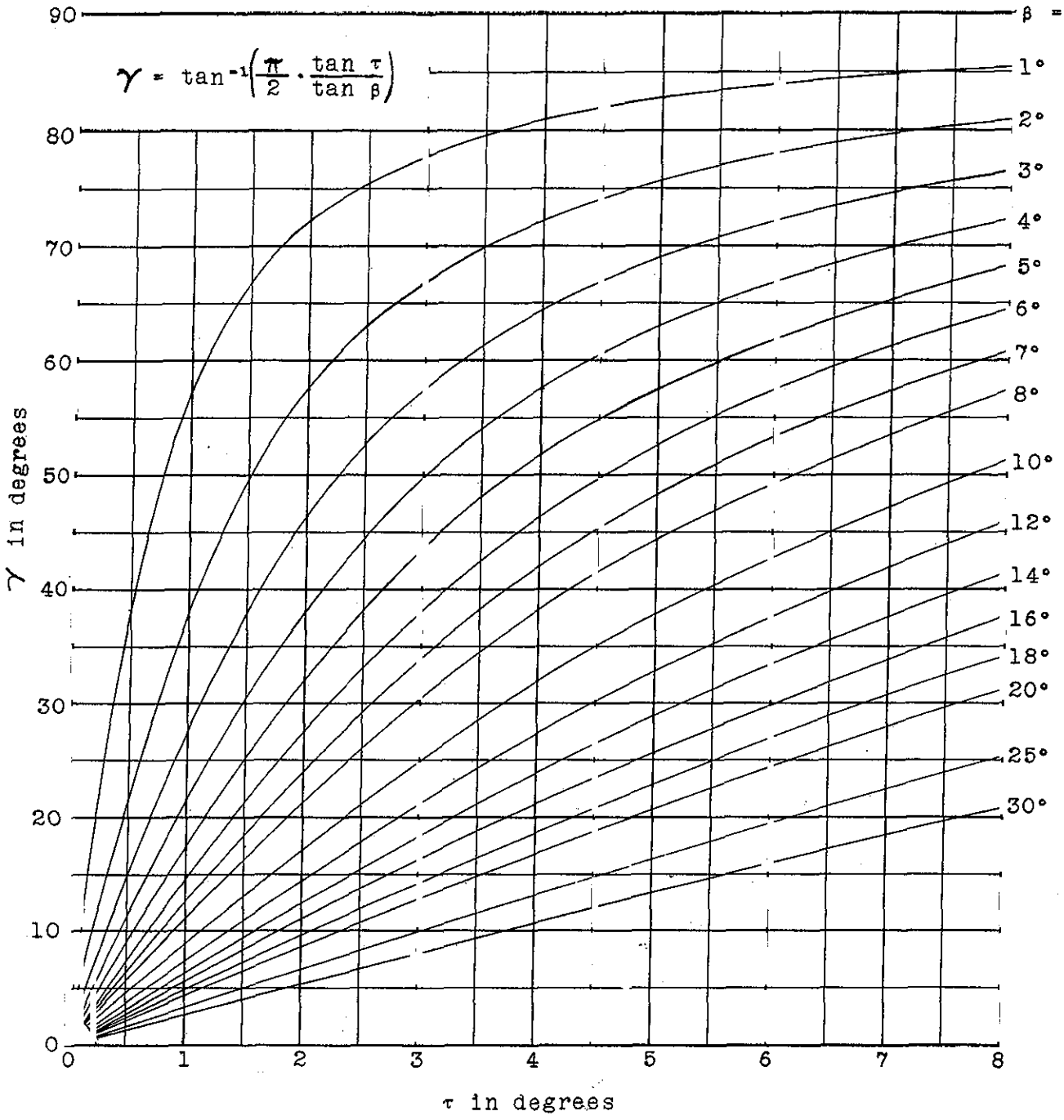

Figure 2-4 - Angle Gamma (γ) Between Spray-Root Line and Centerline, in Plan View, for Prismatic Planing Surfaces with Square Trailing Edges.

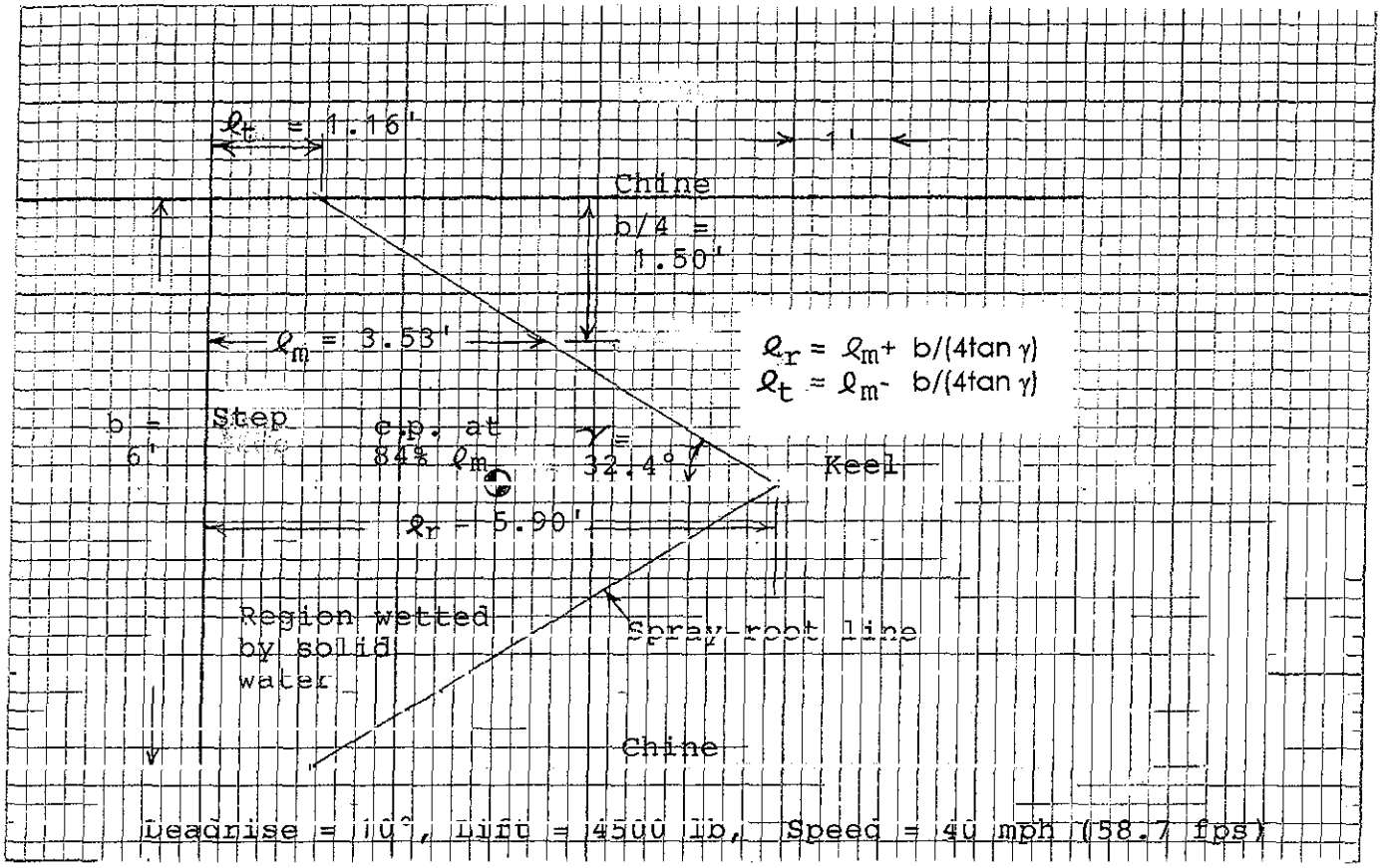

Figure 2-5- Forward Planing Surface of a Stepped Boat, Running at Design Speed.

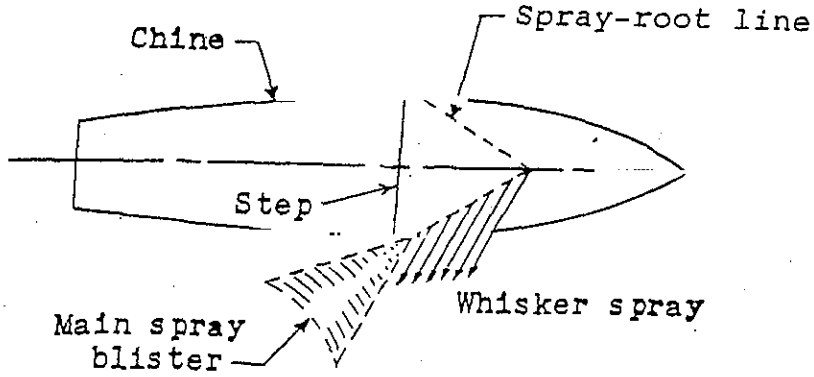

Figure 2-6 - Planing Configuration with the Chine Ends of the Spray-Root Lines Close to the Step.

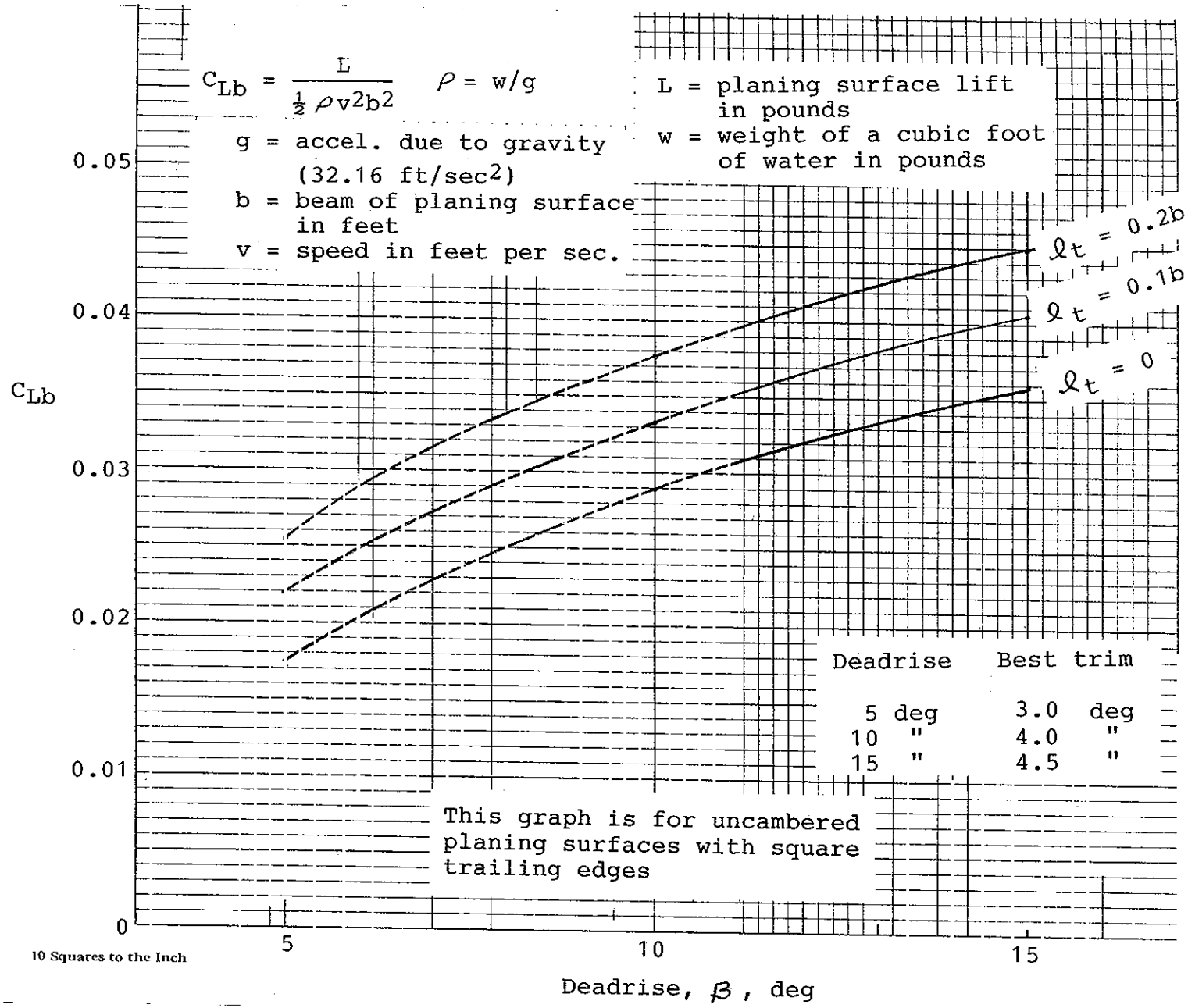

Figure 2-7 - Lift Coefficient versus Deadrise, at Best Trim, for Tip-Chord Wetted Lengths of Zero, 0.1b, and 0.2b.

Chapter 3

Prismatic Planing Surfaces With Sweptback Trailing Edges - As Applied to Stepped Planing Boats

The potential problem for a stepped hull of spray wetting the bottom of the afterbody, and causing a large drag rise, was explained in Chapter 2 (and previously in **Reference 6**). This problem can be overcome by adopting sweep-back of the step, as was proposed in **Reference 8.** By sweeping the step back, good planing efficiency can be maintained up to very high speeds. A planing surface with a sweptback trailing edge (for a stepped boat) can be either a prismatic surface, with straight buttock lines, or a cambered surface. For many cases the best result will be obtained when camber is utilized. For some cases, however, it will be preferable to dispense with the feature of camber, and to make the forebody bottom a simple prismatic surface (but with a sweptback trailing edge). Those latter cases include the instance where the boat to be designed is quite fast and light, so that the incorporation of camber would result in an undesirably short wetted length, and also the instances where the deadrise is above about 15 degrees, where camber is apparently not suitable. This chapter explains the procedure for designing prismatic planing surfaces (i.e., without camber) but having deadrise and trailing edge sweepback. The method of *designing planing surfaces having both camber and trailing edge sweepback is given in Chapter 4.*

Some of the alternative plan-form configurations that can be adopted for a swept-back step are shown in Figure 3-1. If the step is given an appropriate sweepback angle, then boat speed can be increased to a high value (when the wetted bottom area of the forebody will decrease to a low value) without producing wetting of the afterbody by the main spray blisters produced by the forebody. Accordingly, high speeds can be attained, and, also, waves can be negotiated, without encountering the drag-rise produced by impingement of spray on the bottom of the afterbody. If the step is swept back so that it is parallel to the spray-root line, then as the speed increases the supporting wetted area can decrease almost to zero without producing wetting of the afterbody by the main spray blisters (step a in Figure 3-1). However, a configuration similar to b is generally preferable, because a highly swept-back step causes some reduction in lift/drag ratio, and also may be difficult to ventilate adequately. Alternatively, the step can be curved in plan view, like c.

It is of significance that for the case of a transverse step, or a pointed step with the point aft, the aspect ratio will increase with increase in speed only up to the point where the forward boundary of the region wetted by solid water intersects the step. With further increase in speed the aspect ratio remains constant. With a sweptback step, on the other hand, the aspect ratio can continue to increase up to a higher speed. High values of planing aspect ratio can therefore be attained, and the planing efficiency will be improved by this factor as well as by elimination of the afterbody wetting.

Experimental and analytical work by Brown, at the Davidson Laboratory, provide the *tools needed to design prismatic planing surfaces with straight sweptback trailing edges for a fast* stepped boat. Brown tested planing surface models having various angles of deadrise and of trailing edge sweepback. Then, utilizing the experimental data, he derived formulae for the performance characteristics of such planing surfaces, which he presented in **Reference 9**. Brown's equations were utilized to prepare a set of graphs giving the lift characteristics of planing surfaces with straight sweptback trailing edges, for extensive ranges of values of deadrise angle and step sweep-back angle. Those graphs are given in **Reference 10.** The procedures used for deriving the graphs are given there also.

Examples of the graphs in **Reference 10**, for a deadrise angle of 10 deg, and for several trailing edge sweepback angles, are given here in Figure 3-2. An example of the design procedure, including the method for calculating the resistance, is given at the end of this chapter. As before, it is assumed that the type of boat to be designed is to be of the airplane-configuration, and that the main (forward) planing surface is to carry 90% of the weight of the boat at the high-speed design point. The weight, speed, beam, and deadrise angle for the new design need to be selected. The value of the lift coefficient based on the square of the beam for the main planing surface (C_{Lb}) can then be calculated. The angle of attack should be selected to be the optimum for the angle of deadrise adopted. Optimum angles of attack have been determined for the case of planing surfaces with square trailing edges, and, provisionally, are considered applicable for the present case also. Those optimum angles of attack are 3 deg with 5 deg deadrise, 4 deg with 10 deg deadrise, and 4.5 deg with 15 deg deadrise. Figure 3-2 can now be entered (with the inverse of C_{Lb}) to find the step sweepback angle that will give a tip-chord wetted length equal to at least 20% of the beam. Figure 3-2 reveals that this result can be attained by adopting a trailing edge sweepback angle of 40 deg.

A plan-view drawing for this design example, together with the related equations from Brown, are given in Figure 3-3. Also, Brown found that the location of the center of pressure for the configurations which he tested was at 70% of the mean wetted length forward of the mean step position.

Reference 11 gives details of the design, construction, and successful operation, of a high-speed airplane-configuration boat that had a prismatic main (forward) planing surface and a sweptback step that were designed by utilizing the results of Brown's work. The boat was built in 1979, for research purposes, for the British Petroleum Corporation. Design particulars for the boat were a weight of three tons, a deadrise angle of 15 degrees, a chine beam of five feet, and a speed of 80 mph. The design developed for the main planing surface of the boat (which was to carry 90 percent of the weight) is shown in Figure 3-4. A running trim angle of 4 deg was selected. Graphs developed from Brown's equations, like those in Figure 3-2 here (but for a deadrise angle of 15 deg), were utilized to arrive at a step sweepback angle of 60 deg. The curved line of the forward boundary of the wetted region which was predicted, for the design speed, using Brown's equations, is shown. The straight-line step configuration shown was assumed for the calculations. It was decided, however, that an "equivalent" curved step would be preferable for the actual boat, and therefore the one shown was designed. This curved step was drawn so that the lifting area encompassed would be the same as for the step configuration formed by two straight lines.

An advantage of the curved step that was adopted is that the speed of the boat could then be increased considerably above the design speed of 80 mph (or, alternatively, the boat can be run at a lighter weight) without having the forward boundary of the wetted region intersect the step. (That would lead to wetting of the afterbody and a considerable increase in drag). Another advantage of the curved step is that it would tend to eliminate the ridge of water down the center of the wake which is known from model tests to occur in the case of a planing surface with a large trailing edge sweep-back angle. Such a ridge of water would lead to unnecessary additional wetting of a centerline mounted shaft-strut, and also to additional wetting of the center portion of the afterbody bottom during "takeoff."

A model of the planing surface configuration having the curved step was tested in a towing tank of the British Hovercraft Corporation. The model tests were made at a fixed trim of 4 degrees, with the model free to heave, and carrying a load corresponding to 6048 pounds, full-scale (i.e., 90% of the estimated total weight of 3 tons). Drag, and the forward boundaries of the regions

wetted by solid water were determined at test speeds corresponding to 60, 80, and 90 mph, full-scale. The values of full-scale resistance derived from the model testing are shown in Figure 3-5. The value of resistance of 765 pounds at the design speed of 80 mph compared closely to the value of 760 pounds that was calculated using Brown's equations. Figure 3-4 shows a comparison, at the design speed, of the forward boundaries of the wetted regions as predicted using Brown's equations and as measured during the model test. The close agreements with regard to both resistance values and wetted boundaries indicates the excellence of Brown's equations for predicting the performance characteristics of this class of planing surfaces. The graphs of **Reference** 10 (which are based on Brown's equations) can accordingly be used for designing and for making accurate predictions of performance for this very large and interesting family of planing surfaces. Deadrise angles from 5 deg to 22.5 deg, and step sweepback angles from 30 deg to 70 deg are covered by the graphs in **Reference 10**.

It is interesting to note, in Figure 3-5, that over the speed range which was tested (60 to 90 mph, full-scale) the resistance consistently decreases as the speed increases. This can be explained by the fact that, as the speed increases at constant trim and load, progressively less wetted area is needed to support the weight being carried. Accordingly, the planing surface rises progressively further out of the water, the wetted length becomes shorter, and this results in an increase in the aspect ratio of the planing surface. The increase in the aspect ratio causes a progressive improvement in planing efficiency, and accordingly results in a reduction in drag. This verifies the point made in Chapter 1 that, as the design speed of an airplane configuration boat increases, the main component of the hydrodynamic hull drag ordinarily decreases.

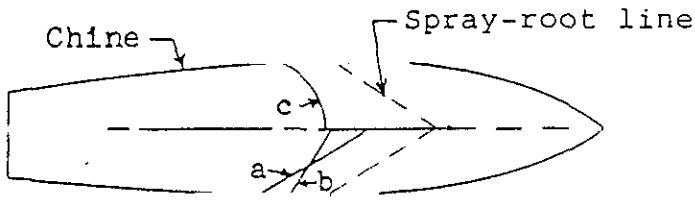

Figure 3-1 - Several Alternative Configurations for a Sweptback Step.

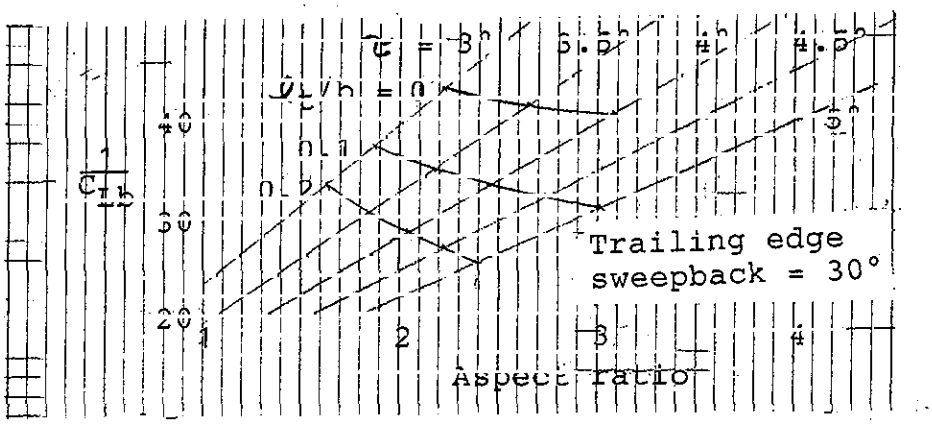

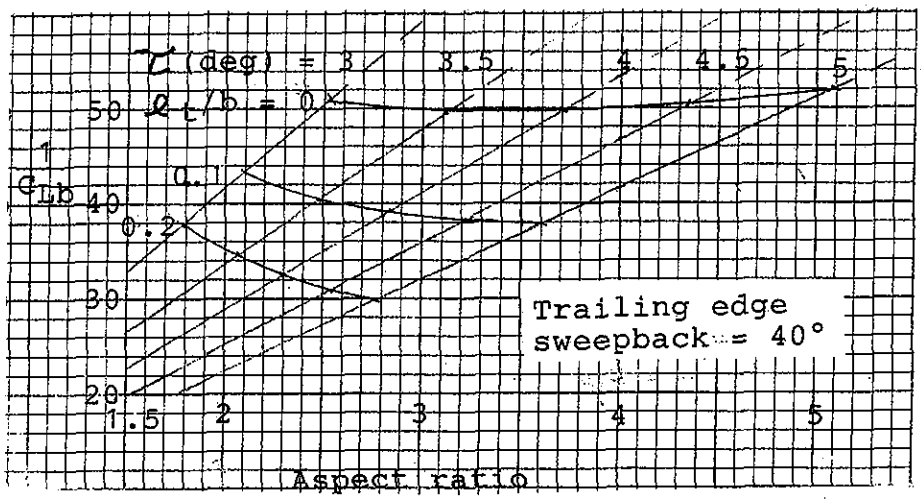

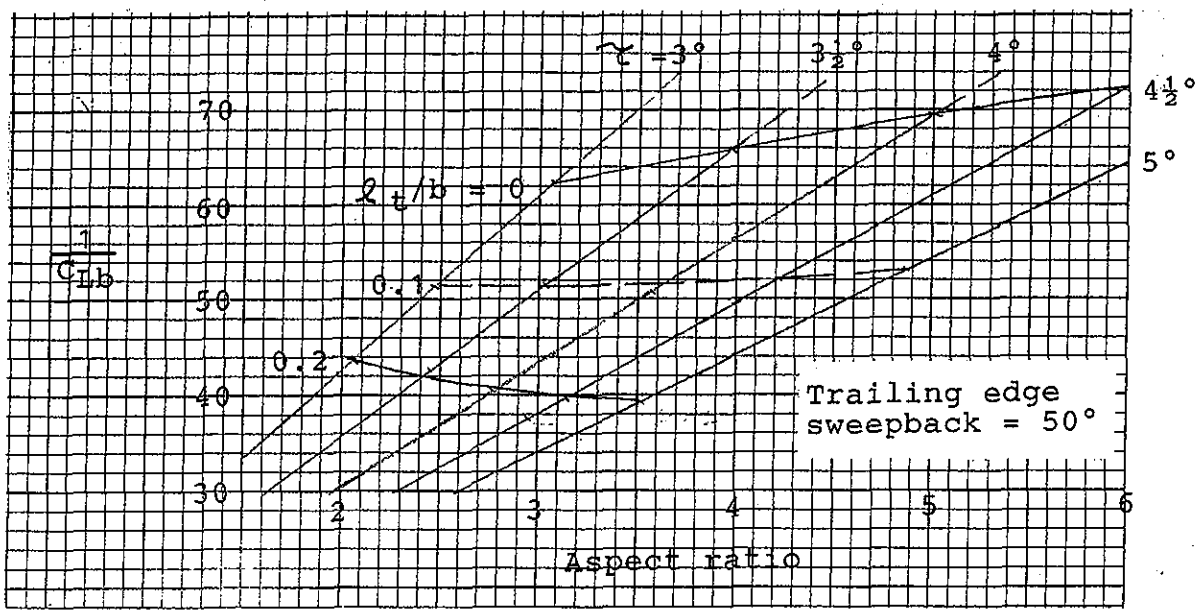

Figure 3-2 - Lift Characteristics of Planing Surfaces with 10° Deadrise and Sweptback Trailing Edges.

Brown's equations:

$$A = 2/[\ell_r/b + \ell_t/b + 0.06]$$

$$\ell_{1/4} = 0.5(\ell_r + \ell_t) + 0.045b$$

$$\ell_m = 0.5(\ell_r + \ell_t) + 0.03b$$

$$C_D = C_L \tan\tau + C_f \sec\beta$$

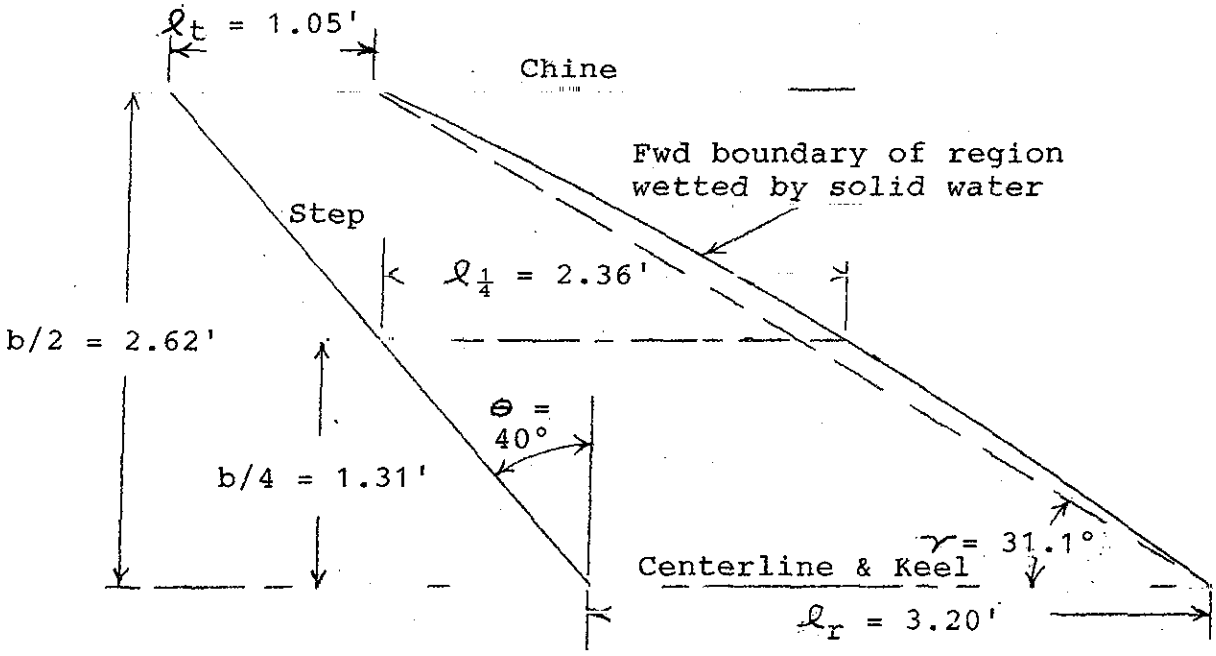

Figure 3-3 -Wetted Region of the Main Planing Surface of a Stepped Boat (and Brown's equations).

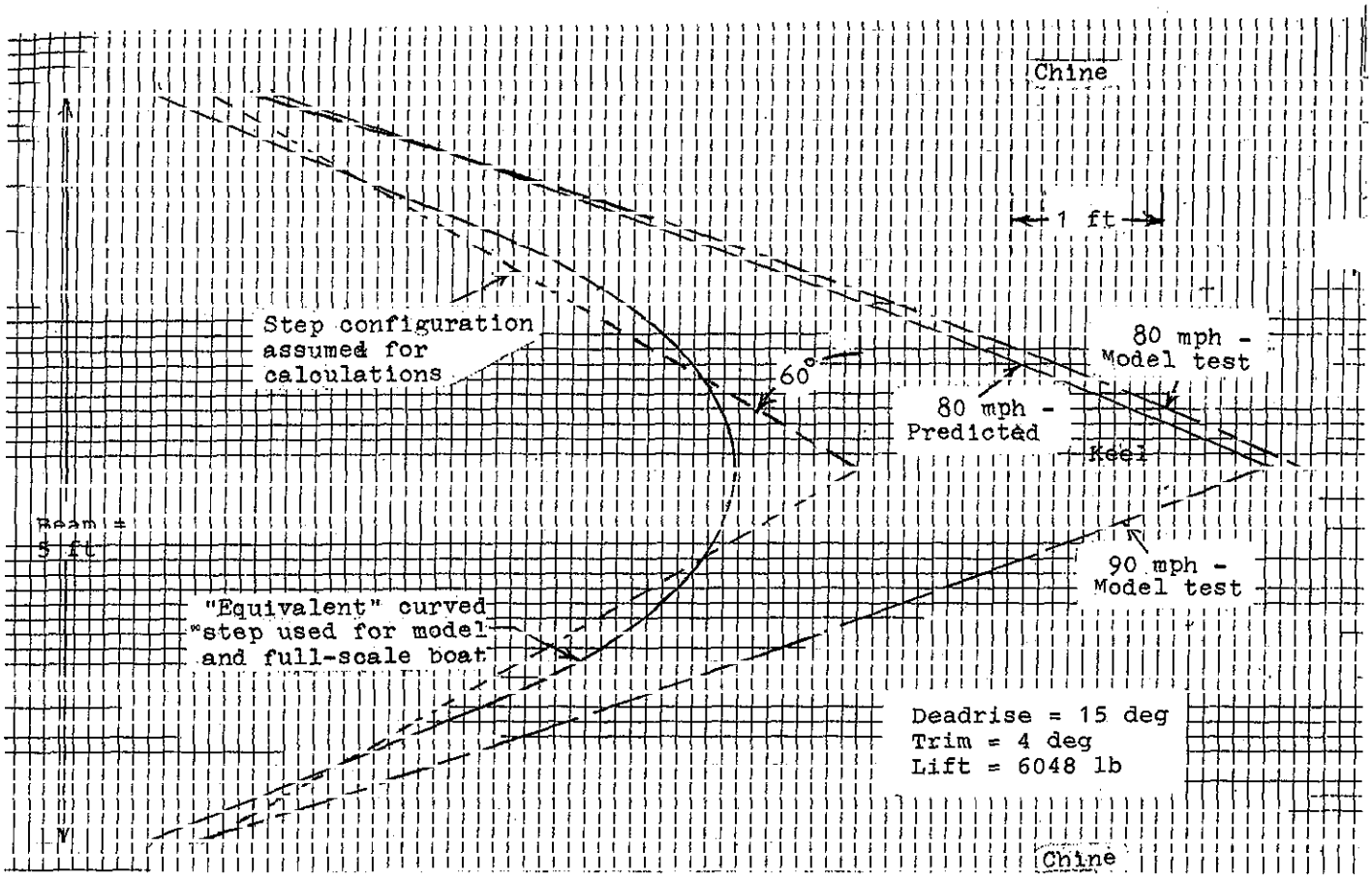

Figure 3-4 - Step Region of Main Planing Surface of Airplane-Configuration Boat Built for the British Petroleum Company. The Predicted and Experimental Forward Boundaries of the Regions Wetted by Solid Water are also Shown.

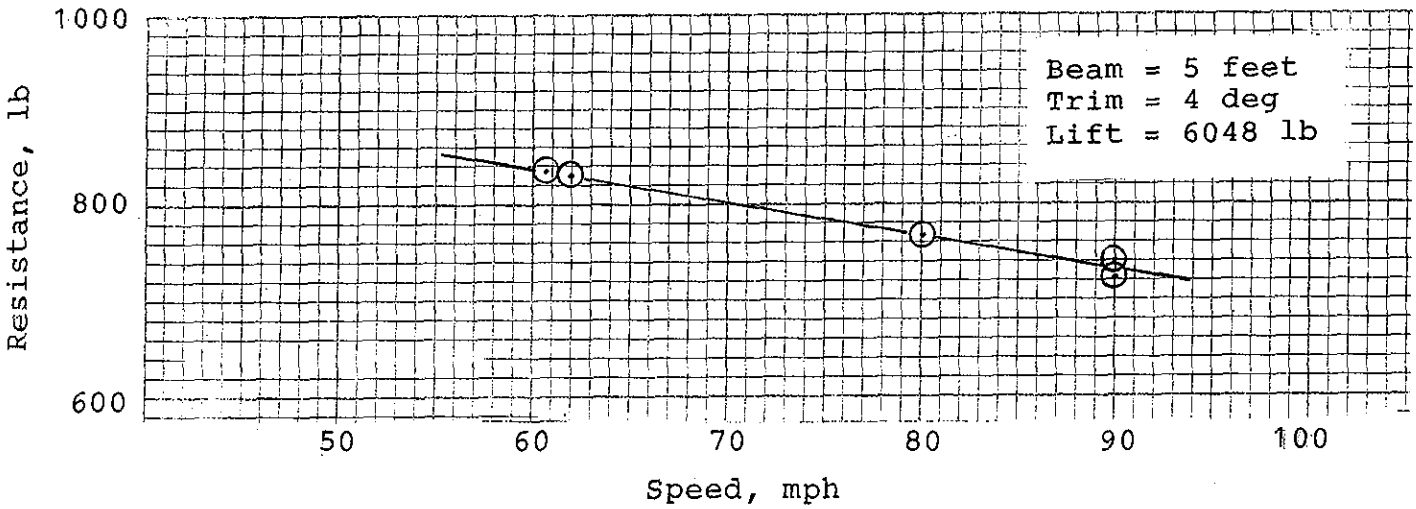

Figure 3-5 - Values of Resistance versus Speed for the Main Planing Surface of the BP Boat, as Predicted from Model Tests.

Example of the design procedure for a planing surface with a sweptback trailing edge (without camber), for a stepped boat 20ft long running in salt water.

b = 5.25ft, W = 2500lb, V = 35mph (v = 51.3fps), deadrise = 10deg, $\frac{1}{2}\rho = 1.0$.

1. Calculate that $C_{Lb} = 0.9W/(\frac{1}{2}\rho v^2 b^2) = 0.0310$; then $1/C_{Lb} = 32.3$.

2. Select 0.2 as a suitable value for the ratio of the tip-chord wetted length to the beam.

3. Select the value of the trim angle, τ, so that with the selected value of the deadrise angle, β, minimum drag will be obtained. (With β = 10deg, minimum drag will be with τ = 4deg.)

4. With $1/C_{Lb} = 32.3$, and τ = 4deg, find from among the graphs giving the lift characteristics for β = 10deg, the trailing-edge sweepback angle that will result in $\ell_t/b = 0.2$. It will be found from the appropriate graph that this result will be obtained with a trailing-edge sweepback angle (angle θ) of 40deg.

5. From the graph for β = 10deg, and θ = 40deg, read that the value of the aspect ratio, A, is 2.3.

6. Calculate the value of the ratio ℓ_r/b using the relationship (from Brown) that:

$$A = 2/(\ell_r/b + \ell_t/b + 0.06);\ \textit{finding that}\ \ell_r/b = 0.61,\ \textit{so that}\ \ell_r = 3.2\,ft$$

7. Brown found from his tests of planing surfaces with swept-back trailing edges that the forward boundaries of the regions wetted by solid water were curved convexly forward. (The shape is assumed to be that given by a second degree curve.) Brown found that:

$$\ell_{1/4} = 0.5(\ell_r + \ell_t) + 0.045b$$

For the present case, $\ell_{1/4} = 0.5\times(3.2 + 1.05) + 0.045\times5.25 = 2.36$ft.

8. A view of the wetted region of the planing surface can now be drawn as shown in Figure 3-3.

9. To calculate the drag, first calculate area $S = b^2/A = (5.25)^2/2.30 = 12.0\text{ft}^2$.

10. Assume $C_f = 0.003$.

11. Calculate $C_L = C_{Lb}\times A = 0.031\times2.30 = 0.071$.

12. Calculate C_D using the relationship from Brown that: $C_D = C_L \tan\tau + C_f \sec\beta$. Then $C_D = 0.0080$.

13. Calculate D (drag of the planing surface) $= C_D \times \frac{1}{2}\rho S v^2 = 253$lb.

14. Then, L/D of the planing surface = (2500×0.9)/253 = 8.93

Chapter 4
Design Procedure for a Planing Surface Having Camber

The similarities between designing a modern monoplane airplane, and designing an efficient stepped planing boat, have been pointed out previously. The importance of incorporating suitable camber curvature for both cases has been particularly stressed. Because of the importance of camber curvature for airplane wings, extensive theoretical and experimental work has been carried out throughout the world to find the most suitable shapes. Now, of course, all airplanes incorporate camber curvature in their wing sections, and this feature is one of the most important factors affecting the performance and efficiency of those wings.

Appropriate camber curvature can also contribute significantly to the attainment of good efficiency (i.e., high lift/drag ratios) for the case of the planing surfaces of stepped planing boats. The subject of suitable camber shapes for stepped motorboats has not received anything approaching the attention devoted to camber shapes for airplane wings. However, one outstanding research publication is available that can be utilized for designing camber shapes for stepped planing boats. This is **Reference 12,** by Virgil Johnson. The goal of Johnson's work was to develop equations defining optimum hydrodynamic camber shapes (and their performance characteristics) for the lower surfaces of supercavitating hydrofoils. Johnson succeeded in his objective, and he reported in **Reference 12** that the results of his theoretical and experimental investigation of supercavitating hydrofoils operating near the free water surface showed that substantial improvements in lift/drag ratios could be achieved over the values for flat plates. It was realized at DTMB that Johnson's work could be utilized to guide the design of optimum camber shapes for the planing surfaces of stepped boats. Johnson's equations were accordingly solved for the case of zero depth at the leading edge (which is the planing case), and the results used to prepare graphs that could be used for boat-design purposes. The graphs are for the case of the Johnson "3-term" camber, which appeared to be the camber-type promising the best performance. Comprehensive sets of the graphs for the 3-term camber are given in References 13 and 14. By means of those graphs it is possible to determine the values of lift/drag ratio and center of pressure for planing surfaces, for wide ranges of values of aspect ratio, trim angle, and amount of camber curvature. (It should be noted, however, that Johnson's equations are limited to the case of rectangular planform and zero deadrise.)

The substantial increases in attainable values of lift/drag ratio promised by Johnson's theory are shown by Figure 4-1. This figure compares calculated values of lift/drag ratio for a flat plate, with the values calculated for a surface having the Johnson 3-term camber. The aspect ratio is 2 for both cases. It can be seen that the maximum calculated value of lift/drag ratio for the flat plate was 11.5, whereas for the cambered surface it was 17.5. The extent of the anticipated improvement in lift/drag ratio is accordingly more than 50%.

The validity of the very high values of L/D predicted by Johnson's theory were

verified by testing a planing surface model which incorporated Johnson's 3-term camber. The model had a rectangular planform, zero deadrise, and an aspect ratio of 2.0. (Further particulars of the model that was tested, and also the data obtained from the testing, are given in Appendix B.) The gratifying result was obtained that the experimental values of lift/drag ratio were even higher than those predicted by the theory. This can be seen from Figure 4-1, which includes a comparison of predicted with experimental values of lift/drag ratio for a surface having the 3-term camber. The testing of the planing surface model also yielded the interesting result that the experimental values of lift coefficient corresponded very closely to the calculated values derived using Johnson's equations. Accordingly the graphs of **References13** and **14** can be relied upon to give dependable guidance for the selection of suitable values of size, aspect ratio, trim angle, and amount of camber, for the planing surfaces of stepped boats.

The graphs in **References 13 and 14** are for the case of rectangular planform and zero deadrise. In any practical design case the main planing surface of a stepped boat will have deadrise, and the planform shape will usually be swept back like the wing of a high-speed airplane. Both of these factors tend to decrease the lift and to increase the drag. Accordingly, when utilizing the graphs based on Johnson's equations, for a practical design case, it is necessary to apply suitable correction factors to account for the effects of deadrise and planform sweepback. Several planing surface models having deadrise and sweepback, as well as camber, have been tested, and the needed correction factors have been derived from the results of those tests. The factors are included in the design procedure which is provided in this chapter. The procedure for designing an efficient (cambered) main planing surface for an airplane configuration stepped boat (and for determining the drag), is given by the numbered steps of the design procedure provided at the end of this chapter. The graphs needed to facilitate the procedure are included, and also an example of the procedure.

The first step of the design procedure is to select a suitable value for the deadrise angle of the main (forebody) planing surface. That value will depend on whether the boat is intended for operation in smooth and protected waters, or in relatively rough water. For the case of a stepped boat having camber the deadrise angle will ordinarily be in the range between about 5 degrees and 15 degrees. The design angle of attack can then be determined from Figure 4-2. The shape and dimensions of the chine line in plan view will have been determined by the method explained in Chapter 1. The width of the forebody cambered planing surface can then be taken to be equal to the chine width at 45% of the bottom length from the stern. The values for the forebody deadrise and the chine width, together with the specified maximum speed and the estimated gross weight of the boat, provide the input values needed for designing the cambered main planing surface. This surface should be designed to carry 90% of the weight of the boat, with the remaining 10% carried by an adjustable hydrofoil stabilizer at the stern. Figures 4-3 through 4-7 are included as needed components of the design procedure. Figure 4-8 shows a plan view of the planing surface, and also a "balance diagram," for the design example. Figures 4-9 through 4-11 are graphs (taken from **Reference 14**) that are required for the particular design example. That is, the graphs are applicable for an aspect ratio of 2.0, and a trim

angle of 2.5 deg. The offsets for the Johnson three-term camber curve are needed for the design procedure. These are given (in dimensionless form) in Figure 4-12.

The distance of the center of pressure on a cambered planing surface forward of the trailing edge, as a proportion of the mean wetted length, is determined at step 15 of the design procedure. The significant mean wetted length (or mean hydrodynamic chord), for the case of a planing surface with taper and sweepback, is analogous to the aerodynamic "Mean Aerodynamic Chord" (M.A.C.). The M.A.C. (or, in this case, the M.H.C.) can be determined by the graphical process indicated in Figure 4-8a. Then, with the position of the center of pressure located on the plan view of the cambered planing surface, the fore-and-aft location of this planing surface, and therefore of the step, can be determined by means of a balance diagram like that shown in Figure 4-8b. That diagram is for the case of a hydrofoil-type stabilizer at the stern, like the design shown in Figure 1-3 of Chapter 1.

Design procedure for a cambered planing surface after the speed, weight, and planing surface beam have been determined.

1. Calculate the lift coefficient, $C_{Lb_\beta} = \frac{0.9W}{\frac{1}{2}\rho v^2 b^2}$

2. Select type of camber curve - Johnson 3-term.

3. Select value of deadrise angle, β.

4. Select ratios of tip chord to beam, ℓ_t/b (typically, $\ell_t/b = 0.2$), and of root chord to beam, ℓ_r/b (typically, $\ell_r/b = 0.8$).

5. Calculate aspect ratio, AR = $\frac{2}{\ell_r/b + \ell_t/b}$

6. Select appropriate value for trim angle, τ, from Figure 4-2.

7. Determine value of angle, γ. (γ is the angle between the spray-root line and the centerline, in plan view. The spray-root line is the forward boundary of the region of the bottom that is wetted by solid water, and therefore the forward boundary of the region that is to be cambered.) First, determine the value of γ for the case of a prismatic surface (without camber), from either the equation or the graph of Figure 4-3. Then add a correction factor of five degrees to that value to obtain the value for the case of a planing surface with camber.)

8. The planing surface in plan view is now fully determined. Accordingly, the following two angles can either be determined by drawing the planing surface and measuring them, or they can be determined from the figures, as indicated.

9. Determine value of ϕ from either the equation or the graph of Figure 4-4 (ϕ is angle of sweep of 50% chord line).

10. Determine value of θ from either the equation or the graph of Figure 4-5 (θ is sweepback angle of the step).

11. Determine $(C_{Lb_\beta}/C_{Lb_0})_{DL}$ from Figure 4-6. "DL" indicates Davidson Laboratory.

12. Determine $\frac{(C_{Lb_\beta}/C_{Lb_0})_{Exp.}}{(C_{Lb_\beta}/C_{Lb_0})_{DL}}$ from Figure 4-7.

    The subscript "Exp." indicates a value corresponding to the experimental value that would be obtained from a test of a cambered planing surface having the configuration of the present design.

13. Multiply value from step 11 by value from step 12 to get $(C_{Lb_\beta}/C_{Lb_0})_{Exp.}$

14. Divide C_{Lb_β} by value from step 13 to get C_{Lb_0}.

15. Enter the graphs of the performance characteristics of cambered planing surfaces having rectangular planform and zero deadrise (NSRDC Report 3147) with the value of C_{Lb_0} to determine $(L/D)_J$, $C_{L,d}$, and ℓ_{cp}/ℓ_m. The subscript "J" indicates Virgil Johnson, who developed the theory for cambered planing surfaces. (Selected examples of the graphs given in Report 3147 are included here as Figures 4-9 - 4-11. These are the particular graphs needed for the Example of the design procedure, which is given in succeeding pages.)

16. Determine $(L/D)_{Exp.}/(L/D)_J$, from Figure 4-7.

17. Multiply value from step 15 by value from step 16 to get $(L/D)_{Exp.}$.

18. Multiply value from step 17 by 0.925 to get the value of L/D for a hull with a stabilizer (including air drag).

19. Knowing the values of the beam, b, and of the ratios, ℓ_t /b and ℓ_r /b (from step 4), calculate ℓ_t and ℓ_r. These are the chord lengths, c, of the camber curves at the chine, and at the centerline, respectively.

20. A plan view of one side of the cambered planing region should be drawn. An example is given in Figure 4-8a. This figure shows the construction lines needed for defining the position and the dimension of the mean hydrodynamic chord (M.H.C.). The length of the M.H.C. should then be scaled from the drawing. Multiplying that length by the ratio ℓ_{cp}/ℓ_m (determined in step 15) gives the distance of the center of pressure (which is on the centerline of the cambered planing surface) forward of the aft end of the M.H.C.

21. Figure 8b shows an example of the type of "balance diagram" used to determine where along the length of the hull the c.p. of the cambered planing surface should be located. The appropriate longitudinal position for the step can then also readily be determined.

22. Knowing ℓ_r (this is the chord length of the camber curve at the centerline), and the value of $C_{L,d}$ (from step 15), the offsets for the camber curve at the centerline of the cambered region can be determined by utilizing either the tabulated values or the equation given in figure 4-12. Taking ℓ_t as the chord length, c, of the camber curve at the chine, the camber curve for that location can be determined in a similar manner.

23 The cambered region between the camber lines at the centerline and at the chine is defined by an array of straight lines connecting points on those lines which are located at equal percentage points of their chord-line lengths. For example, a

straight line connecting the point on the centerline camber curve located at 35% of its chord-line length with the point on the chine camber curve located at 35% of its chord-line length will coincide with the cambered surface, and accordingly will assist in defining it. Another way of explaining the case is to say that the configuration of the cambered region is such that the shapes of the camber curves in all of the buttock planes are geometrically similar.

Example - cambered planing surface for the case of a 20-ft boat running in salt water.
L_p = 20 ft, b = 5.25 ft, W = 2500 lbs, V = 35 mph (v = 51.3 fps), $\rho/2$ = 1.0

1. $C_{Lb_\beta} = 0.9W/(\frac{1}{2}\rho v^2 b^2) = 0.031$
2. Assume Johnson three-term camber curve
3. Take β = 10 deg
4. Take $\ell_t/b = 0.2$
5. Take $\ell_r/b = 0.8$
6. From equation, AR = 2.0
7. Take τ = 2.5 deg (from Figure 4-2)
8. Calculate γ for no camber from equation; add 5 deg for camber case. Then γ = 21.3 + 5 = 26.3 deg
9. See Figure 4-8 for a plan view of the planing surface, and also a "balance diagram"
10. Calculate ϕ from equation. ϕ = 55 deg
11. Calculate θ from equation. θ = 39.5 deg
12. To correct for effect of deadrise on lift, determine C_{Lb_0} from Figure 4-6 (equals 0.04). Then $(C_{Lb_\beta}/C_{Lb_0})_{DL} = 0.031/0.04 = 0.775$. ("DL" indicates Davidson Laboratory.)
13. For ϕ = 55 deg, read $\dfrac{(C_{Lb_\beta}/C_{Lb_0})_{Exp.}}{(C_{Lb_\beta}/C_{Lb_0})_{DL}} = 0.843$, from Figure 4-7. (The subscript "Exp." indicates a value corresponding to the experimental value obtained from a test of a cambered planing surface.)
14. Then $(C_{Lb_\beta}/C_{Lb_0})_{Exp.} = 0.775 \times 0.843 = 0.653$
15. $C_{Lb_0} = 0.031/0.653 = 0.0475$
16. From Report 3147, $(L/D)_J$ = 12.9 (Alternatively, use Figure 4-9, taken from Report 3147.)
17. From Figure 4-7, $(L/D)_{Exp.}/(L/D)_J = 0.895$
18. Then $(L/D)_{Exp.} = 0.895 \times 12.9 = 11.5$
19. Multiply value from 18 by 0.925 to get the value for a hull with a stabilizer (including air drag).
20. From Report 3147, for $C_{Lb_0} = 0.0475$, AR = 2.0, and τ = 2.5 deg, read $C_{L,d}$ = 0.045, and $\ell_{cp}/\ell_m = 0.62$. (Alternatively, use Figures 4-10 and 4-11, which are taken from Report 3147.)
21. As indicated on Figure 4-8a, the chord lengths of the camber curves of the cambered region are 4.2 ft (50.4 in) at the keel and 1.05 ft (12.6 in) at the chine.
22. By drawing the indicated construction lines on Figure 4-8a , the position of the M.H.C. is determined, and its length is found to equal 2.95 ft. Multiplying that dimension by the value of 0.62 for the ratio ℓ_{cp}/ℓ_m gives a value of 1.83 ft for the distance of the center of pressure on the cambered planing surface fwd of the

aft end of the M.H.C.

23. Assume for the present case that, on average, the C.G. of the boat will be located at 50% of the length, L_P. The "balance diagram" shown in Figure 8b then indicates the procedure for determining the appropriate longitudinal location on the hull of the c.p. of the cambered planing surface. At the high-speed design point the cambered planing surface is intended to carry 90% of the weight of the boat. This result will be attained if the cambered planing surface is located such that its center of pressure is 11.11 ft forward of the stern of the boat. The "point" of the step (i.e., the intersection point of the step with the keel) is found, by scaling from the drawing, to be 0.93 ft aft of the c.p. Accordingly, on the plan view drawing of the boat the point of the step should be positioned at (11.11 ft - 0.93 ft) = 10.18 ft forward of the aft end of L_P.

24. Knowing the chord length of the camber curve at the keel (50.4 in), and the value of $C_{L,d}$ (0.045) the offsets of that camber curve can be determined by utilizing the tabulated values given in Figure 4-12. For example, the offset for the camber curve at 55% of the chord-line length from the leading edge (i.e., at x/c = 0.55) equals $50.4 \times 0.045 \times 0.0715 = +0.16$ in. The offset at the aft end of the cambered region (which corresponds to the step position) equals $50.4 \times 0.045 \times -0.1698 = -0.38$ in. This offset dimension will probably not be adequate to be taken as the dimension for the depth of the step. Instead the depth of the step should be equal to about 1% of the chine beam, or equal to about 0.6 in.

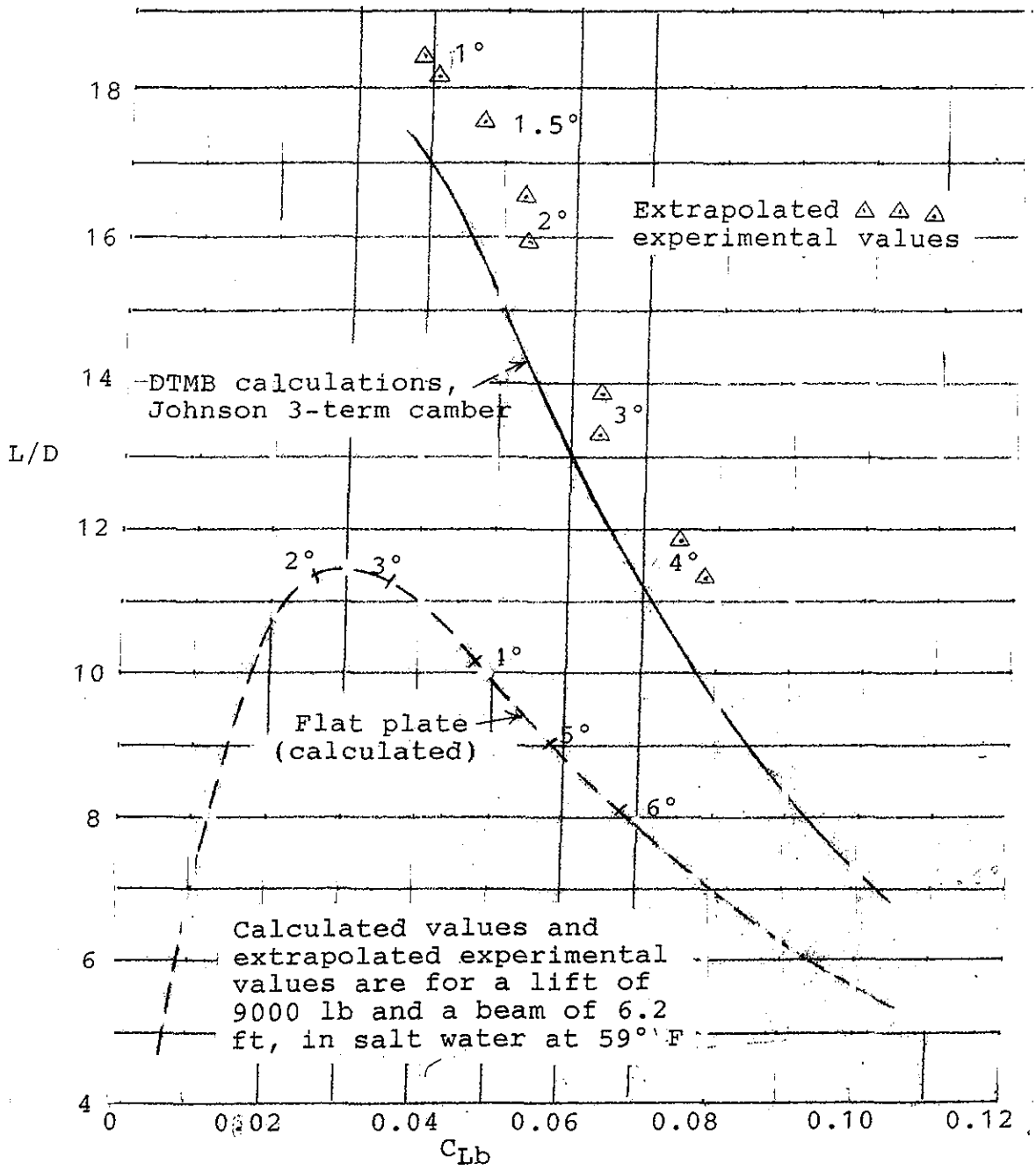

Figure 4-1 - Comparison of Calculated and Experimental Values of Lift/Drag Ratio for a Cambered Planing Surface Having the Johnson 3-Term Section. Comparison also with a Flat Plate. Aspect Ratio = 2.0

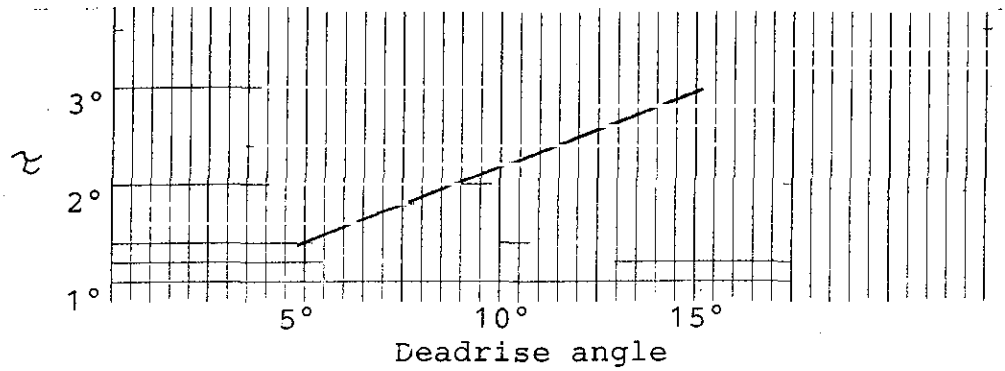

Figure 4-2 - Approximate Relationship Between Deadrise Angle and Design Angle of Attack for a Cambered Planing Surface.

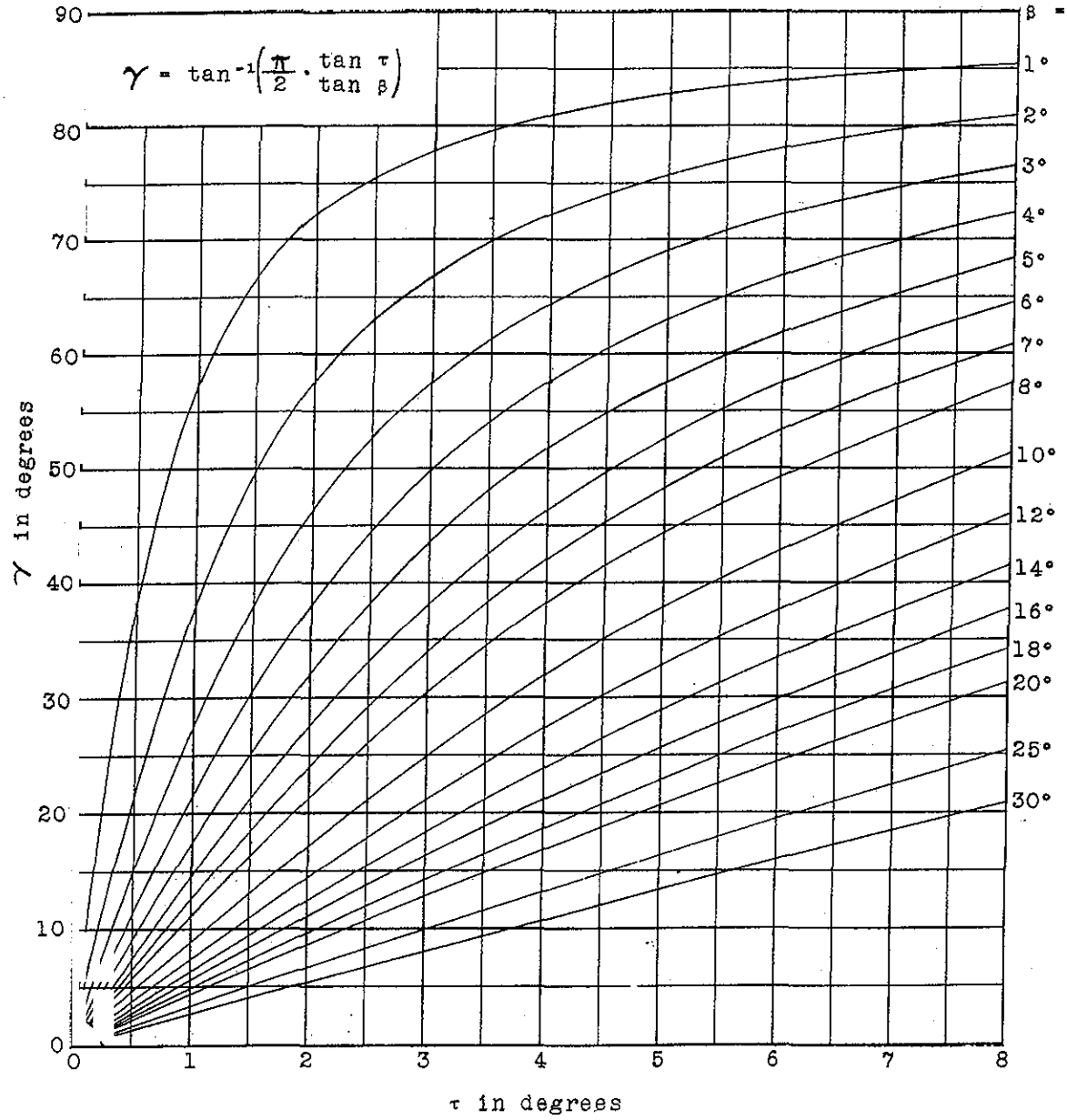

Figure 4-3 - Angle Gamma (γ) Between Spray-Root Line and Centerline, in Plan View, For Prismatic Planing Surfaces.

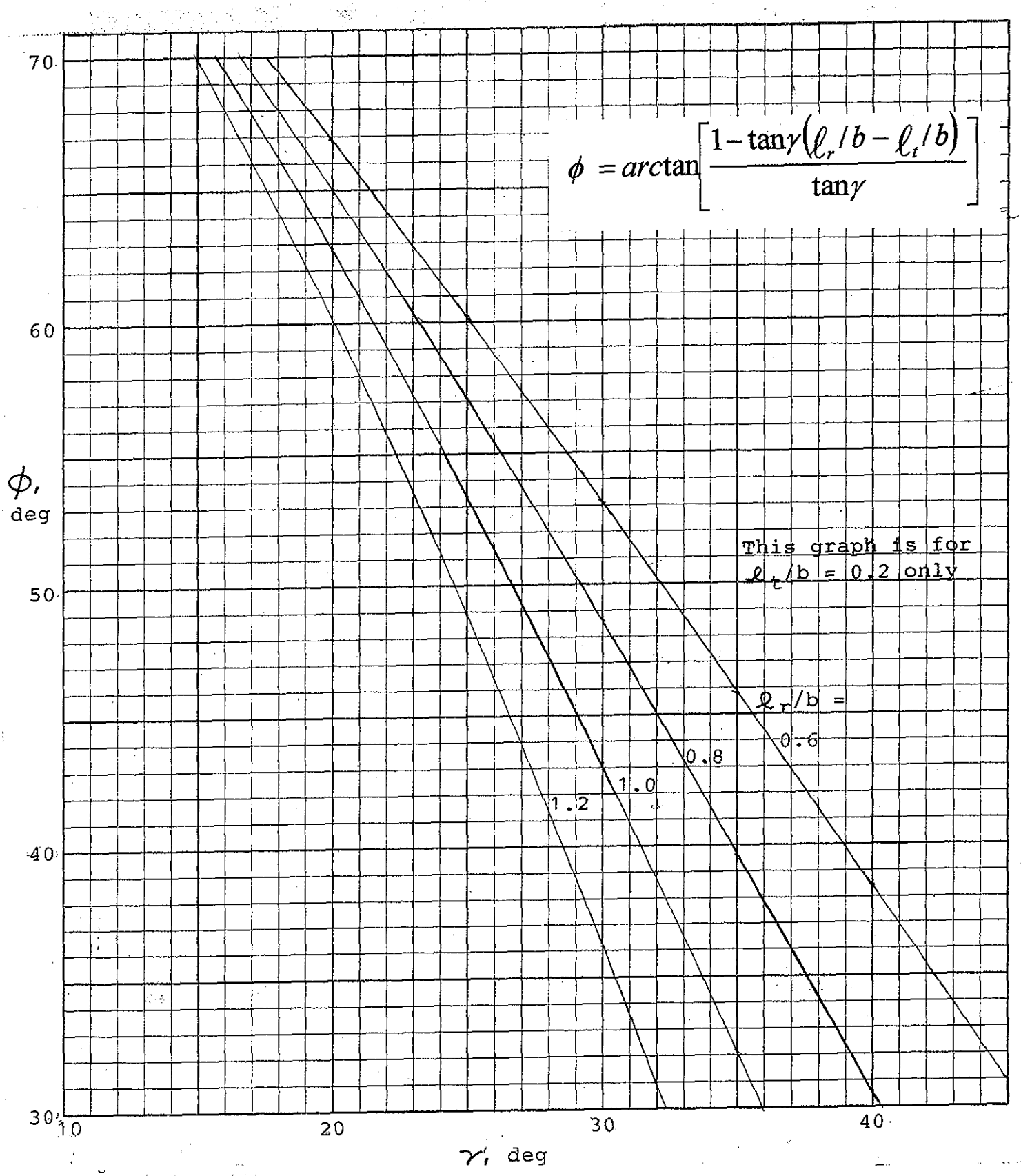

Figure 4-4 - Angle of Sweep of 50% Chord Line (Angle ϕ), Versus Angle Between Spray-Root Line and Centerline in Plan View (Angle γ), for ℓ_t/b = 0.2.

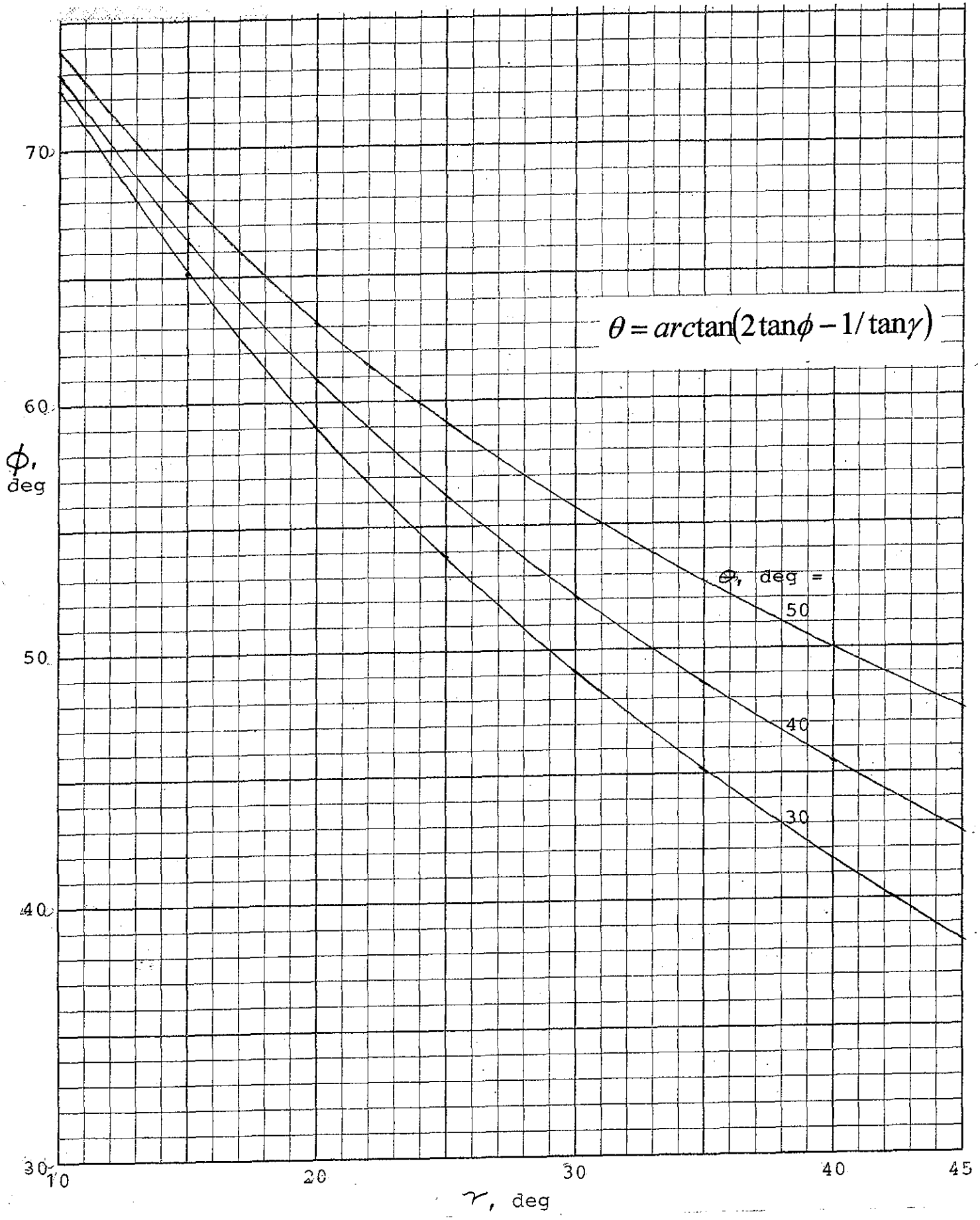

Figure 4-5 - Curves of Step Sweepback Angle as a Function of Angles γ and ϕ.

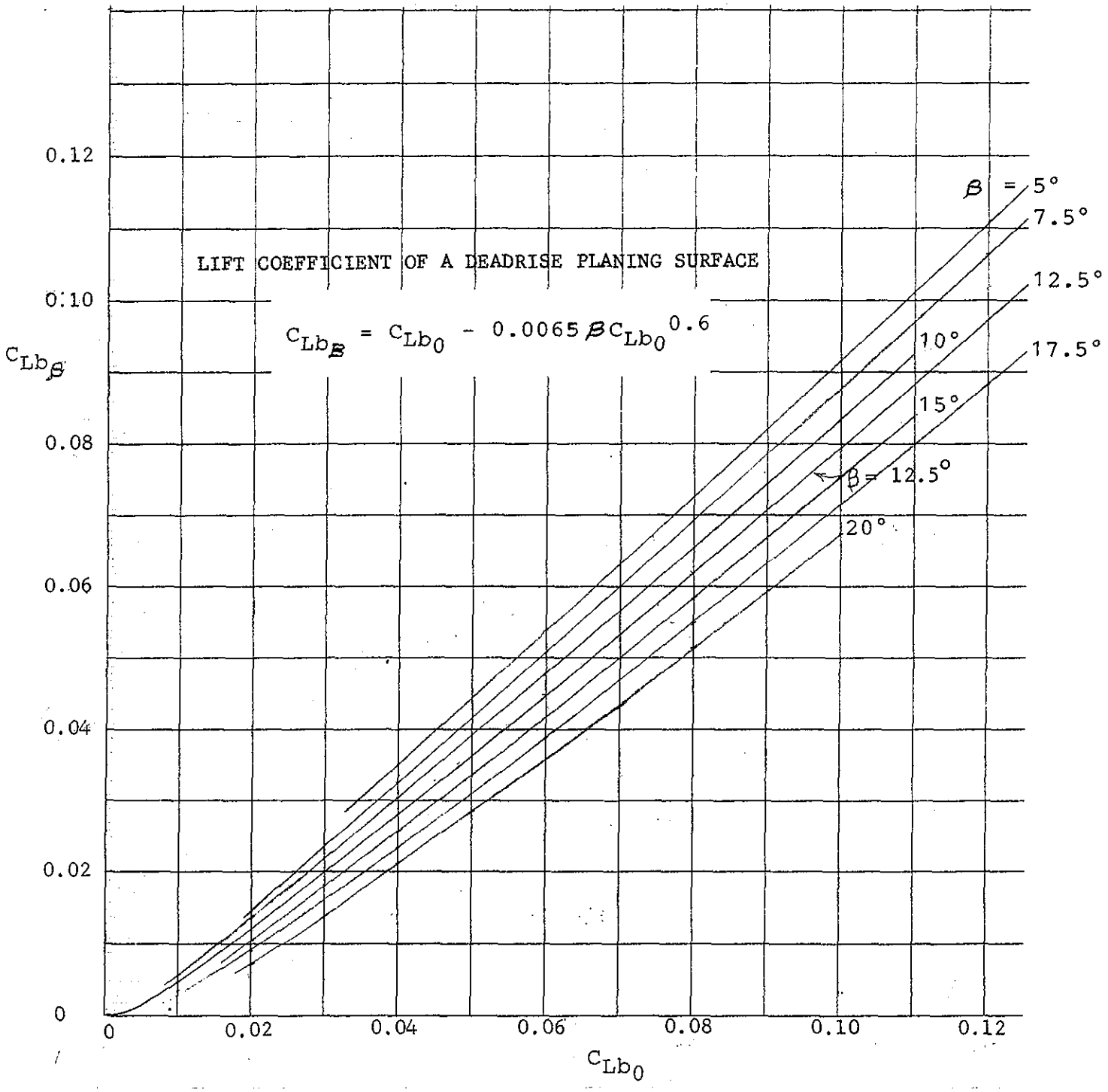

Figure 4-6 - Lift Coefficient with Deadrise versus Lift Coefficient without Deadrise for Prismatic (Uncambered) Planing Surfaces - from the Davidson Laboratory.

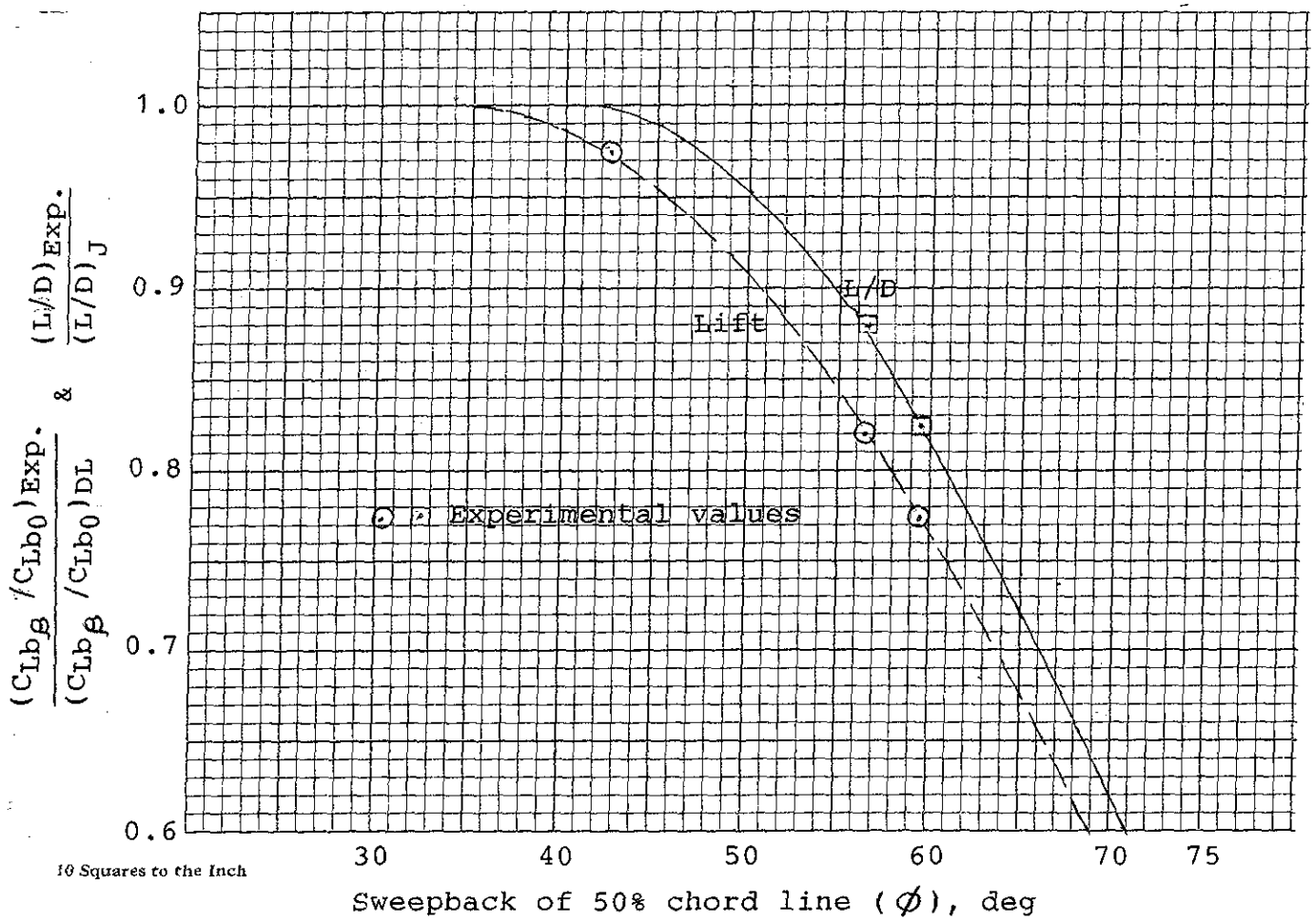

Figure 4-7 - Cambered Planing Surfaces - Corrections for Sweepback Angle (Φ) to Lift and L/D.

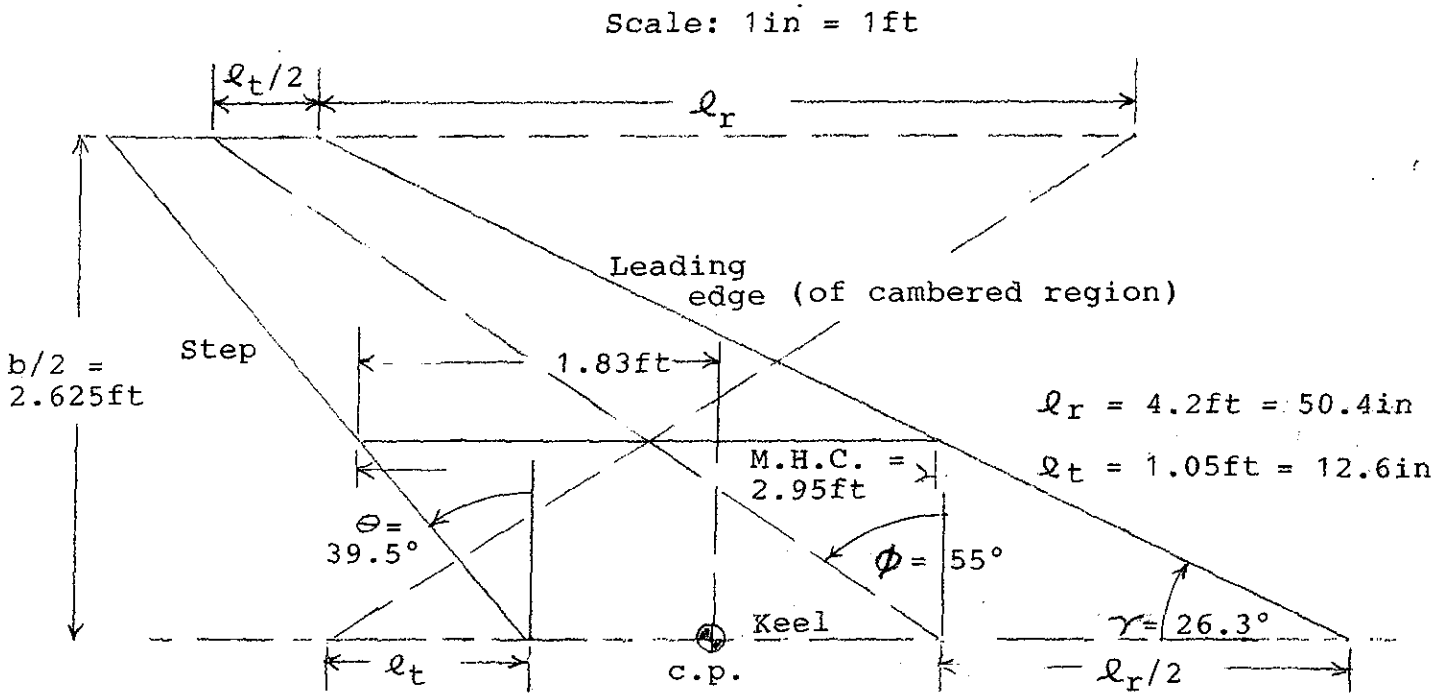

8a - Plan View of the Planing Surface, with Construction Lines for Determining the Location and Length of the Mean Hydrodynamic Chord (M.H.C.).

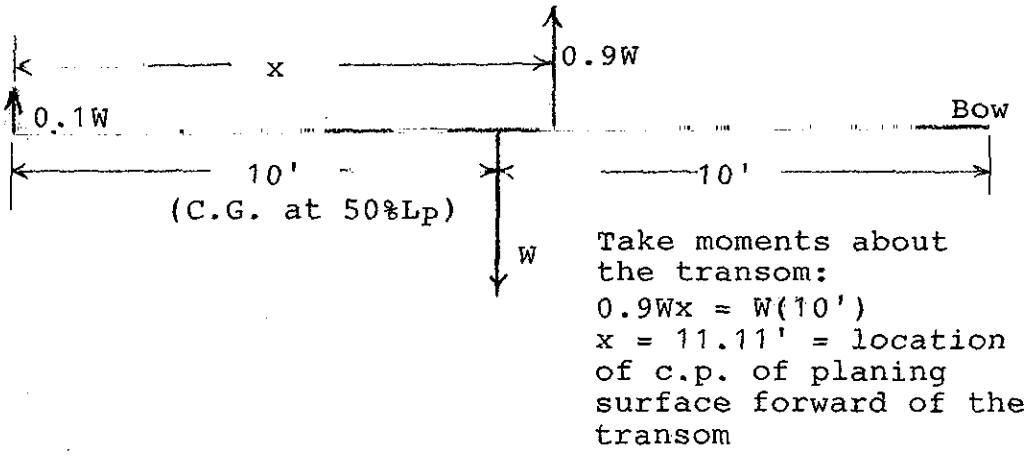

8b - Balance Diagram for the Case of a 20' Boat with an Adjustable Hydrofoil at the Transom Which Provides 10% of the Lift.

Figure 4-8 - Plan View and Balance Diagram for Example Calculation.

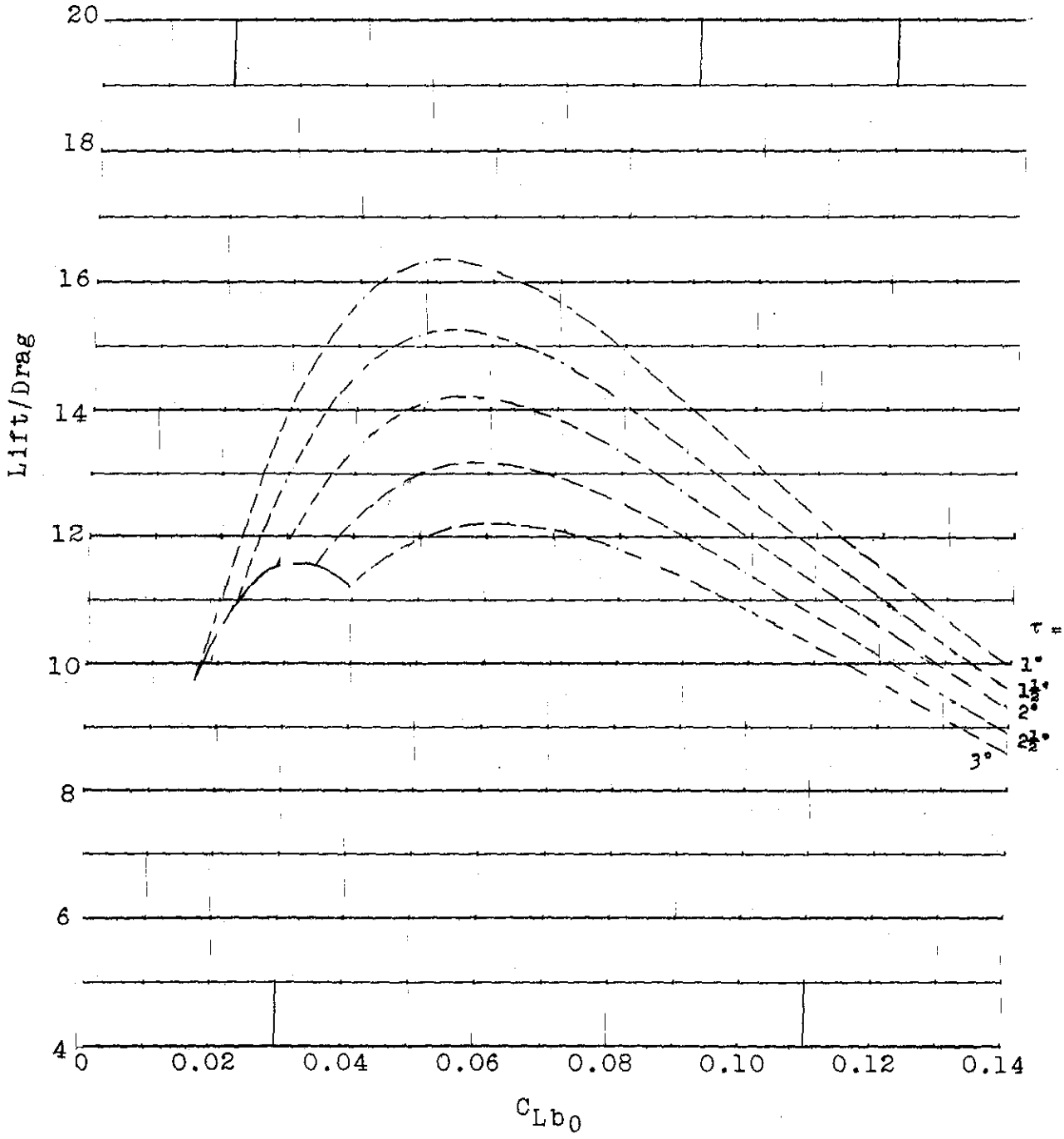

Figure 4-9 - Lift/Drag versus C_{Lb_0} for Rectangular Planing Surfaces Having the Johnson Three-Term Section and Zero Deadrise, $R_e = 10^7$, Aspect Ratio = 2.0.

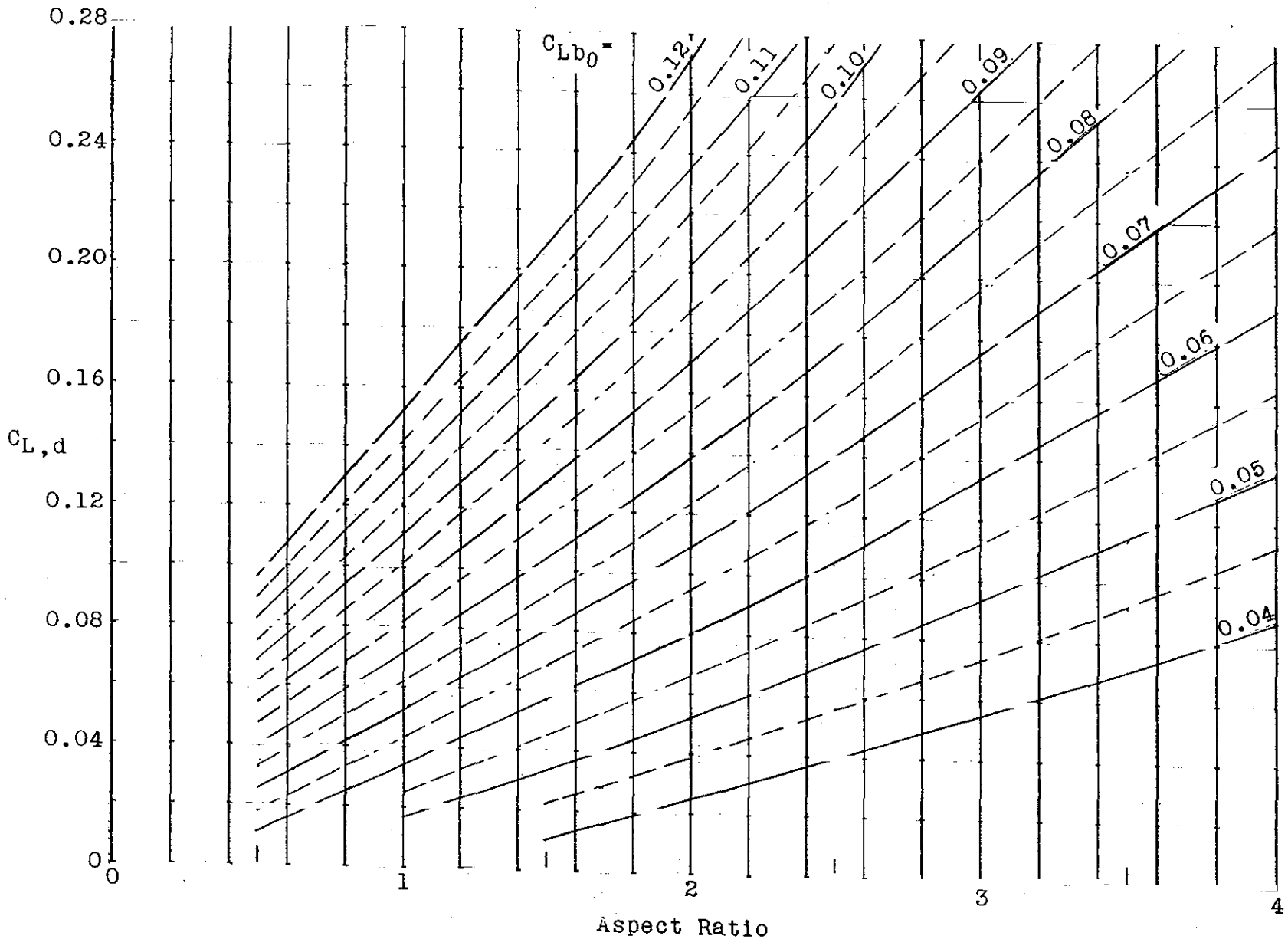

Figure 4-10 - $C_{L,d}$ versus Aspect Ratio for Rectangular Planing Surfaces Having the Johnson Three-Term Section and Zero Deadrise, $\tau = 2\frac{1}{2}°$.

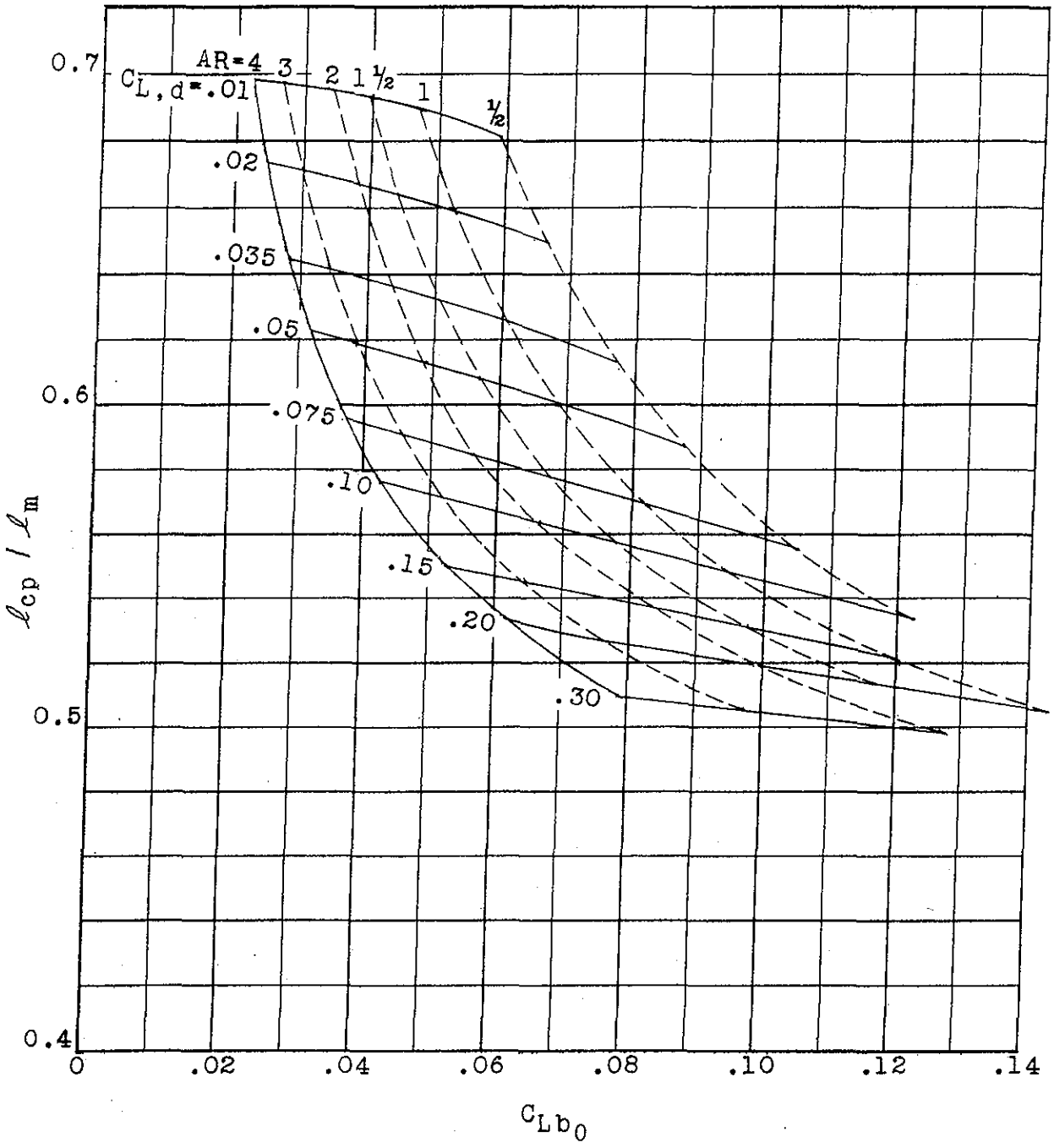

Figure 4-11 - Location of Center of Pressure versus C_{Lb_0} for Rectangular Planing Surfaces Having the Johnson Three-Term Section and Zero Deadrise, $\tau = 2\frac{1}{2}°$.

Equation of the Johnson three-term camber curve:

$$\frac{Y}{C_{L,d}} = \left(-20X^{3/2} + 80X^{2} - 64X^{5/2}\right) \times \frac{1}{7.5\pi}$$

$$X = \frac{x}{c} \qquad Y = \frac{y}{c}$$

$\frac{x}{c}$	$\frac{y}{c \cdot C_{L,d}}$
0.0	0.0
0.02	-0.0012
0.04	-0.0022
0.06	-0.0026
0.08	-0.0024
0.10	-0.0015
0.15	0.0034
0.20	0.0113
0.25	0.0212
0.30	0.0322
0.35	0.0433
0.40	0.0536

$\frac{x}{c}$	$\frac{y}{c \cdot C_{L,d}}$
0.45	0.0623
0.50	0.0686
0.55	0.0715
0.60	0.0704
0.65	0.0645
0.70	0.0530
0.75	0.0353
0.80	0.0108
0.85	-0.0214
0.90	-0.0618
0.95	-0.1110
1.00	-0.1698

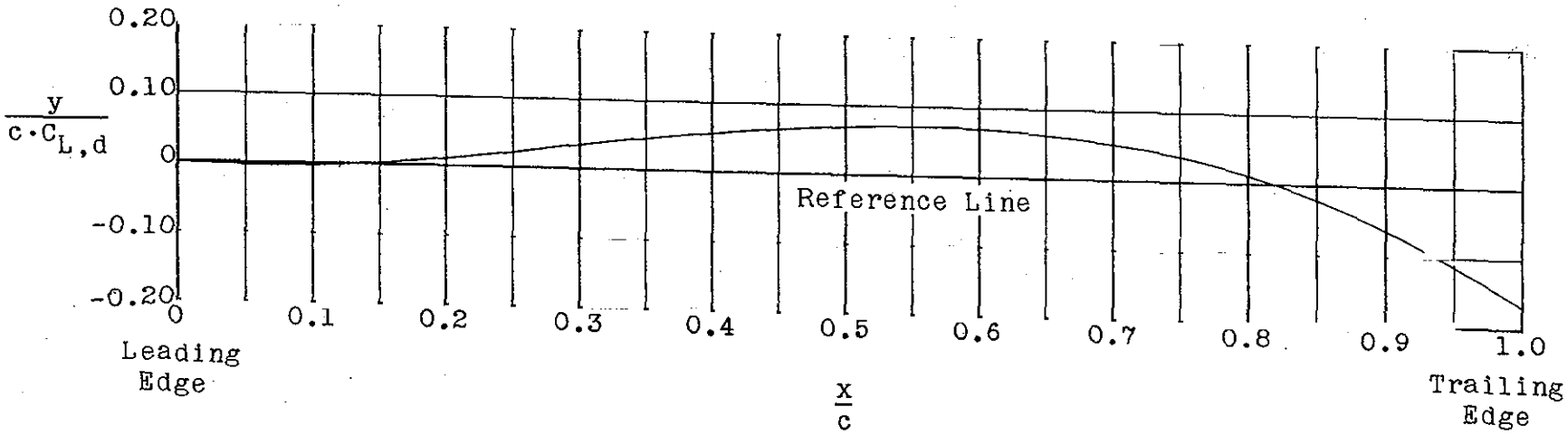

Figure 4-12 - Dimensionless Offsets of Johnson Three-Term Camber Curve

Chapter 5
Design of the Step and Afterbody, and Drag at the Hump

Important considerations in the design of a satisfactory airplane-configuration stepped boat are the fact that the resistance in the lower part of the speed range tends to be higher than for a conventional unstepped boat, and, also, there is invariably a pronounced "hump" in the curve of resistance versus speed. It is desirable that the resistance not be unduly high in the lower part of the speed, in order to give a satisfactory range at a low "cruising speed." Furthermore, it is essential that the "hump" resistance be less than the available propulsion thrust, and by a sizeable margin (20% would be adequate), so that the boat can be accelerated to the designed planing speed. Suitable details of design for the step and the afterbody are needed for achieving those important ends. The fact that the resistance of a conventional unstepped boat is relatively low in the speed range being considered suggests that when converting to the stepped type it will be helpful to keep the magnitudes of any changes to a minimum. The necessary changes are the introduction of a step, and the tilting of the afterbody up with respect to the forebody. Evidently both the depth of the step and the angle to which the afterbody is tilted should be kept to a minimum. The correctness of this view has been confirmed by the testing of a variety of models and full-scale boats of the airplane-type. It has been found that a depth of step equal to only about one percent of the chine beam will ordinarily be adequate. Such a small depth of step not only contributes to low drag at slow speeds, but also facilitates continuity of the longitudinal structural members. A depth of step at the keel equal to the trailing edge camber line offset for the centerline section of a Johnson 3-term camber will on occasion be adequate. Step depth for the 8-foot long Model No. 5115 (shown in Appendix A) was 0.17 in., which is approximately 1 % of the chine beam at the step. It is appropriate to maintain an approximately constant depth of the step across the bottom of the hull. It is important that the edges of the step be sharp. If the step sweep-back angle is large (more than about 20 degrees) vent pipes should be provided, as indicated in Figure 1-3, to assist the separation of the flow from the afterbody.

There are two main requirements governing the design of the afterbody for an efficient stepped planing hull. At high speed the hull afterbody should be entirely clear of the surface of the water so that it will be un-wetted and will not contribute to the drag. The needed lift aft should then be provided by an efficient, adjustable, trim-control device. In the lower part of the speed range, however, lifting support aft is needed from the afterbody of the hull as well as from the trim-control device (the dynamic lift of the latter derives from the forward speed of the boat, and is therefore very much reduced at low speed). The after part of the afterbody should accordingly be in contact with the wake from the forebody in the lower part of the speed range so that it can contribute both buoyant and planing lift. This lifting support is essential to minimize the magnitude of the drag at the "hump." Both of the afterbody requirements will be met if the angle between the forebody and afterbody keels is such that the afterbody keel is close to being horizontal when the hull is running at its design angle of attack. In the case of Model 5115, for example, the angle between the forebody and afterbody keel lines was 2 .5 degrees, and the running trim angle at high speeds was 3.2 degrees. At planing speeds

there is typically a downwash of the flow leaving the step of about 2 degrees, and this will give adequate clearance of the afterbody above the water surface. The form of the afterbody bottom should consist simply of two flat surfaces meeting at a suitable deadrise angle. The deadrise angle of the afterbody should be less than that of the forebody, in order to give an approximately constant depth of the step across the bottom. (In the case of the hull form shown in Figure 1-3, the deadrise of the forebody was 12.5 degrees and the deadrise of the afterbody was 10.7 degrees, and this gave an approximately constant depth of step.) After the forebody (including the cambered planing surface) has been designed, and the afterbody keel angle has been selected, a value for the afterbody deadrise angle that will give a constant depth of step can readily be arrived at during the succeeding steps of the drafting process.

A value for drag at the hump can be estimated by means of Figure 5-1. This figure presents experimental values of resistance at the hump from tests of Model 5115 at different weights and LCG positions. It has been learned from previous testing of models of stepped seaplane hulls that experimental values of resistance at the hump tend to collapse along a single line when plotted against the dimensionless ratio, $\frac{\nabla}{(LCG)^2 b}$ where ∇ is the volume of water displaced at rest, LCG is the distance of the center of gravity forward of the stern, and b is the width over the spray strips at the location of the center of gravity. Accordingly the hump-drag data for Model 5115 have been plotted against that coefficient. In the case of a new design the value of the coefficient can be calculated from the values of W, LCG, and b, in the early stages of a design, and a value for the resistance/weight ratio at the hump can then be determined from Figure 5-1. The available data indicate that the speed at the hump for an airplane-type boat will correspond to a value of F_{∇} of approximately 2.25. A complete resistance curve for one particular airplane-type design (represented by Model 5115) is given in Figure 5-2. This resistance curve can be utilized to construct a resistance curve for the hump-speed region for other similar designs. The procedure recommended is to multiply the values of R/W from Figure 5-2 (at a number of values of F_{∇}) by the ratio of the hump R/W for the new design (determined from Figure 5-1) to the hump R/W from Figure 5-2 (equals 0.12). The resistance at high speed will be derived as a part of the design procedure for the forebody planing surface of the new design, and the curve of hump-speed resistance can then be faired to connect with this new value of the resistance at high speed to give a relatively complete curve of resistance versus speed.

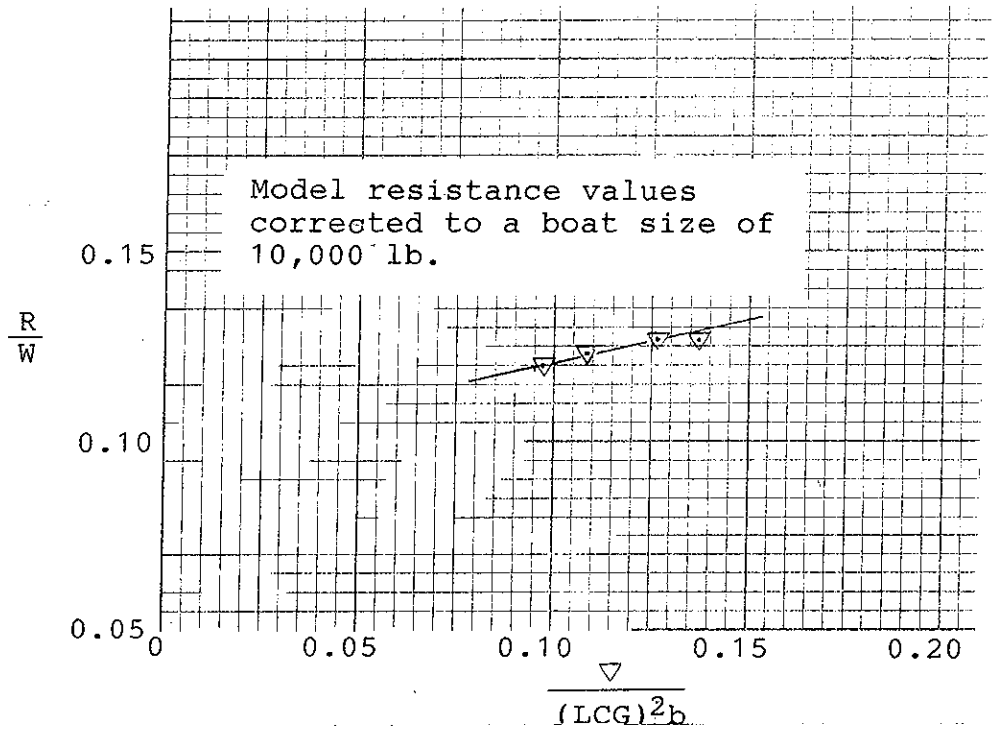

Figure 5-1 - Values of Resistance at the Hump from Tests of Model 5115 at Different Weights and LCG Positions.

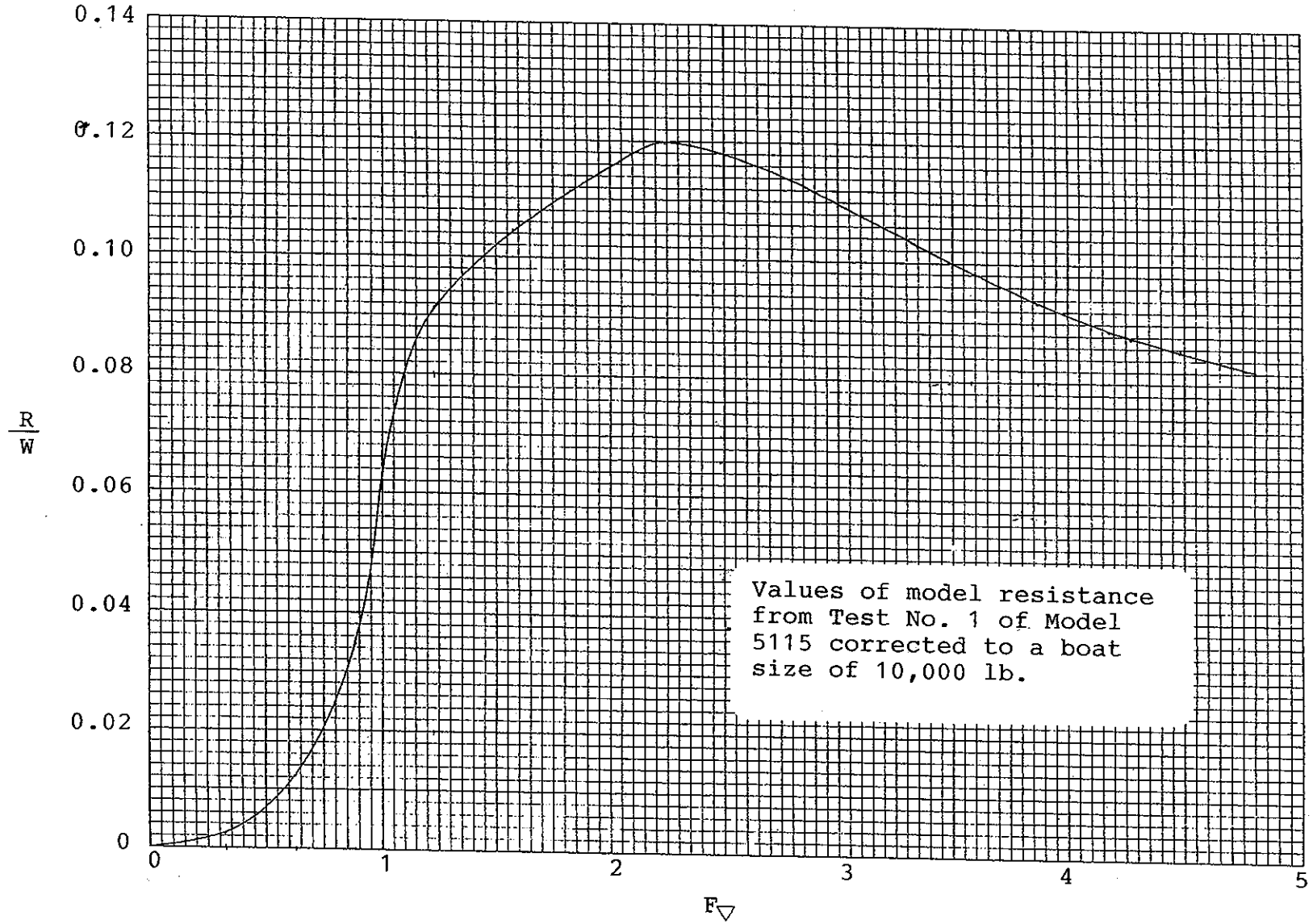

Figure 5-2 - Curve of Resistance versus Speed for an Airplane-Configuration Stepped Boat Represented by Model 5115.

Chapter 6

A Surface-Piercing Vee Hydrofoil as the Trim-Control Device for A Stepped Planing Boat

Superior planing boat performance can be achieved with a stepped configuration in which a cambered main planing surface located near amidships carries approximately 90% of the weight, and an adjustable lifting surface at the stern carries the remainder of the weight, and in addition, provides a means of controlling the boat's trim angle. The resistance of such a configuration (at planing speeds) is chiefly determined by the resistance of the cambered main planing surface. An important factor for keeping this major drag component to a minimum, at different boat weights and speeds, is having the ability to trim the main planing surface to the angle giving the least drag, by means of the stern trim-control device.

The type of stern trim-control device that particularly recommends itself is a surface piercing Vee hydrofoil. This should be adjustable vertically in order to be able to vary the amount of its submersed area, and therefore the amount of its lift. Towing tank tests of some surface-piercing Vee hydrofoils, and also their successful utilization for several hydrofoil boats, provide background information on which suitable foil designs can be based. Data from some of the towing-tank tests of surface-piercing Vee hydrofoils that have been made are given in **Reference 3**. Those tests were made in the old NACA seaplane towing tank. The purpose of the testing was to determine the effects of angle of dihedral and depth of submersion on the performance of hydrofoils. The foils tested had the NACA 16-509 section shape. That shape had been previously developed as one of a series of airfoil section shapes which would have a pressure distribution as nearly constant as possible. Accordingly, when used as a hydrofoil, the section can be run at a particularly high speed before it will cavitate. The 16-509 designation indicates that the section is designed to have optimum characteristics at a lift coefficient of 0.5, and that it is 9% thick.

The hydrofoils for which the data are given in **Reference 3** each had a chord length of 5 inches and a span of 30 inches. They were rectangular in planform, with square tips. The dihedral angles tested were 10, 20, and 30 deg. The foils were tested at different depths, and over ranges of speeds and angles of attack. Tests of the hydrofoil having 30-deg dihedral, in the half-submerged condition, and when submerged to the foil tips, produced some particularly promising results. Those favorable results were obtained at angles of attack close to zero deg. (This was to be expected since the design angle of attack for the 16-509 airfoil section was zero deg.) The hydrofoil with 30-deg dihedral is shown (with the two test water levels also shown) in Figure 6-1. The test results are given in Figures 6-2 and 6-3. It can be seen that in the half-submerged condition (aspect ratio then equaled 3.0), values of lift/drag ratio in the range of 14 to 16 were obtained, for speeds up to 60 fps. When the foil was submerged to its tips (aspect ratio then equaled 6.0), L/D values in the range of 18 to 25 were obtained, for speeds in the range of 40 to 60 fps. (The strut tares were subtracted from the drag values in the case of the latter configuration.) Values of L/D for the foils having the three different dihedral angles, at a speed of 40 fps, when half-submerged, were compared in **Reference 3**. The maximum values of L/D for that case were 6 for the foil with 10 deg dihedral, 12.5 for the foil with

20 deg dihedral, and 16 for the foil with 30 deg dihedral. A clear implication from this comparison is that the optimum dihedral angle (giving the highest values of L/D) would probably be greater than 30 deg.

Cavitation was observed to occur on the foils reported on in **Reference 3**, during the test runs at the higher angles of attack. The speeds and angles of attack at which cavitation occurred are indicated in the report. No cavitation was observed on the 30-deg dihedral foil at the low angles of attack which are of interest for design purposes, and for which the lift and drag data are given in Figures 6-2 and 6-3. The marked decreases in the lift coefficients, and the increases in the drag coefficients, with increase in speed, which are shown in those figures are therefore surprising. There is, of course, a corresponding marked decrease in the values of L/D with increase in speed. This deterioration in performance is presumably to be attributed to flexing of the strut-foil assembly from the hydrodynamic forces, resulting in an unfavorable distortion of the foil configuration. Details of the strut-foil assembly are accordingly of interest. Both struts and foils were machined from "hard brass." The struts were biconvex in section, approximately 28 inches long, and tapered toward the hydrofoil. At the point of attachment to the upper surface of the hydrofoil, the struts had a chord of 2.9 inches and a thickness of 3/8 inch; at the top, the chord of each strut was 4 inches and the thickness was ¾ inch. The center line of each strut intersected the upper surface of the foil at the half-chord point. The method of attaching the struts to the hydrofoil is not explained in the report. It is probably also of significance, with regard to the likelihood of flexing, that when the struts were vertical the angle of attack of the hydrofoil was 6 deg. Accordingly, when the foil was running at the angle of attack of zero degree (the design angle for the foil section, and the angle giving the maximum values of L/D) the struts were raked back at an angle of 6 deg. It can be concluded that measures that would reduce the amount of flexing of surface-piercing Vee-foils mounted on actual motorboats would markedly improve the values of L/D attainable at high speeds.

The promising test results reported in **Reference 3,** for the foil having 30 deg dihedral, suggested the likelihood that there would be practical applications for surface-piercing Vee-hydrofoils. Also, as noted, the results indicated that the optimum dihedral angle would be greater than the 30 deg angle that had been tested. Accordingly, several companies and individuals have experimented with higher dihedral angles, and have designed and built boats that were supported by either three or four Vee-hydrofoils having approximately 40 deg dihedral angle. Noteworthy among these were Gordon Baker and Tom Lang. Many interesting particulars about the hydrofoils of Baker and Lang can be found in **References 16-18.** Both Baker and Lang utilized the NACA 16-510 section for their hydrofoils. (This was essentially the same as the section that had been used for the NACA tests, but with the thickness ratio increased from 9% to 10%.) Also, both formed their aluminum Vee-hydrofoils from straight lengths that had been produced by extrusion of the material through a die. A typical Baker foil (with the dihedral angle that he preferred of 42 deg) is shown in Figure 6-4. Lang concluded that, "... the maximum efficiency of surface piercing hydrofoils should occur at a dihedral above 30 deg and probably below 45 deg." Numerous additional helpful recommendations regarding the

shape, manufacture, and mounting of surface-piercing Vee-hydrofoils can be found in **References 16-18.**

The excellent performance of the hydrofoil boats of Baker and Lang indicate that a suitable foil for a trim-control device would be one that closely followed their successful practice. The type of hydrofoil that recommends itself, therefore, is a V-foil of 40 deg dihedral angle, with the same NACA 16-510 section that was used by both Baker and Lang. Their practice should be followed also by starting with a straight extrusion (formed by extruding aluminum through a die of the specified section shape) and then bending the extrusion into a form such as that shown in Figure 6-4.

The patents of Baker and Lang (**References 16 and 17**) indicate that the design high-speed running condition for their hydrofoils was with the Vee portion half-submerged. It seems appropriate to assume the same high-speed design condition of foil submergence for the case of a hydrofoil being utilized as a stern trim-control device. This is the condition shown for the case of the airplane-type boat depicted in Figure 1-3.

It is unfortunate that the program of testing reported on in **Reference 3** did not include tests of a hydrofoil with 40 deg dihedral. However, straight-line extrapolation of the data for the foils with 20 deg and 30 deg dihedral should give approximate values for a foil with 40 deg dihedral. The appropriate angle of attack to adopt for design cases is zero deg. This is the design angle of attack for the 16-510 foil section; and, consistent with this, the data from the tests of the foil with 30 deg dihedral show that the maximum L/D's were attained at, or close to, that angle (see Figures 6-2 and 6-3). Now, at zero deg angle of attack, an aspect ratio of 3, and a speed of 50 fps, the test value of C_L for the foil having 20 deg dihedral was 0.10. The test value of C_L for the foil having 30 deg dihedral, at the same conditions, was 0.19 (see Figure 6-2). Extrapolation of the foregoing two values of C_L to 40 degrees dihedral gives a value for C_L of 0.28. Also, Reference 3 reports a C_L value of 0.22 for the foil with 20 degrees dihedral, at zero degree angle of attack, an aspect ratio of 6, and a speed of 50 fps. Extrapolating as before gives a value of C_L of 0.32 for a foil with 40 degrees dihedral at an aspect ratio of 6. The foregoing numbers suggest that for the case of a foil with an aspect ratio of 4 when running at its high-speed design point it would be appropriate to assume that the applicable value of C_L would be close to 0.30. The C_L values arrived at by the foregoing extrapolations will probably tend to be high. However, there is the compensating factor that the lower corner of the foil is to be rounded, as shown in Figure 6-4, instead of having the type of sharp corner shown in Figure 6-1. Any remaining discrepancy between the C_L value assumed when designing a foil, and the value realized in practical operation can be catered for, without suffering a significant decrease in foil L/D, by adjusting the foil angle of attack.

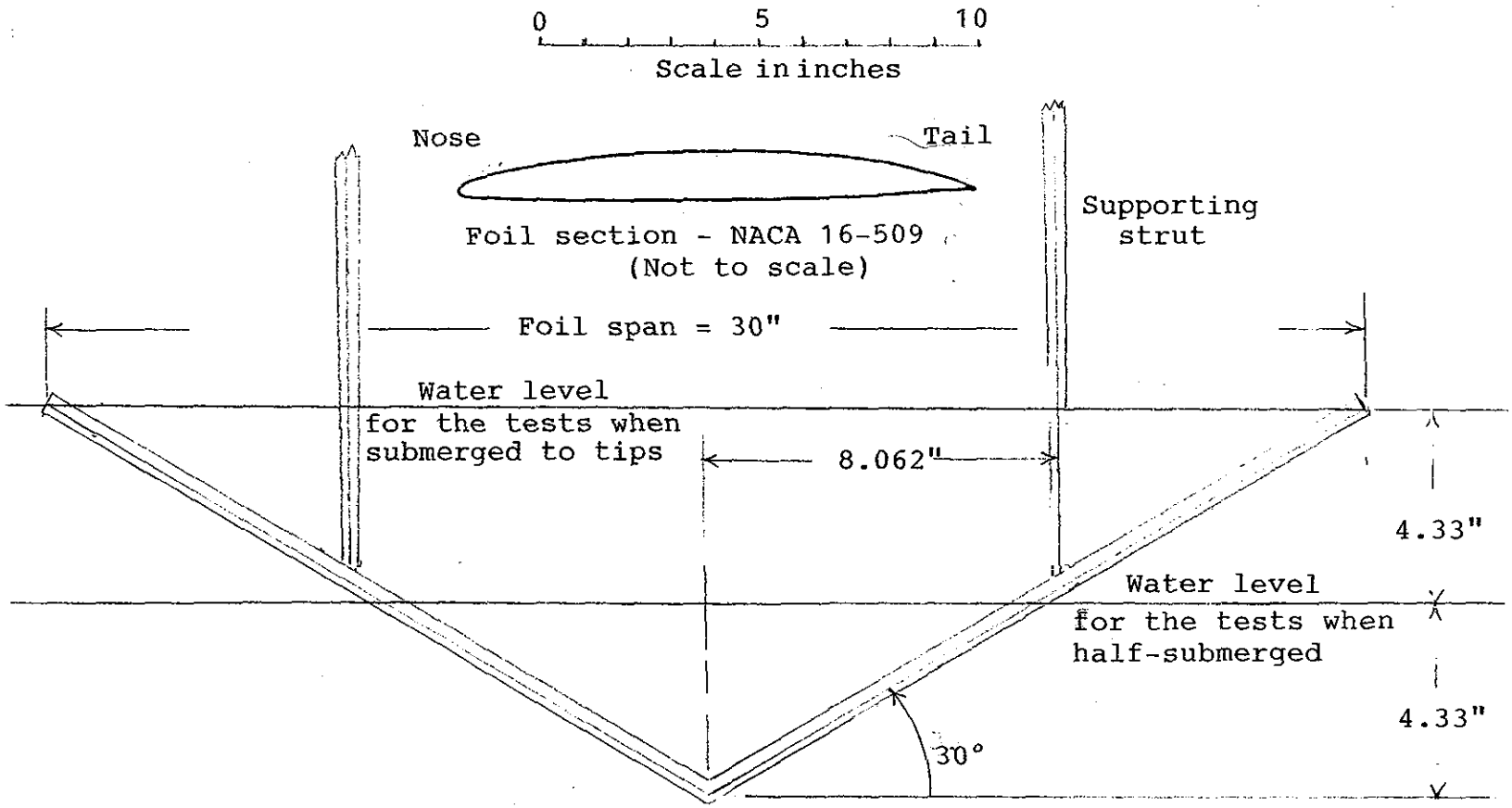

Figure 6-1 - 30-deg Dihedral Hydrofoil Showing the Water Levels for Two Test Conditions.

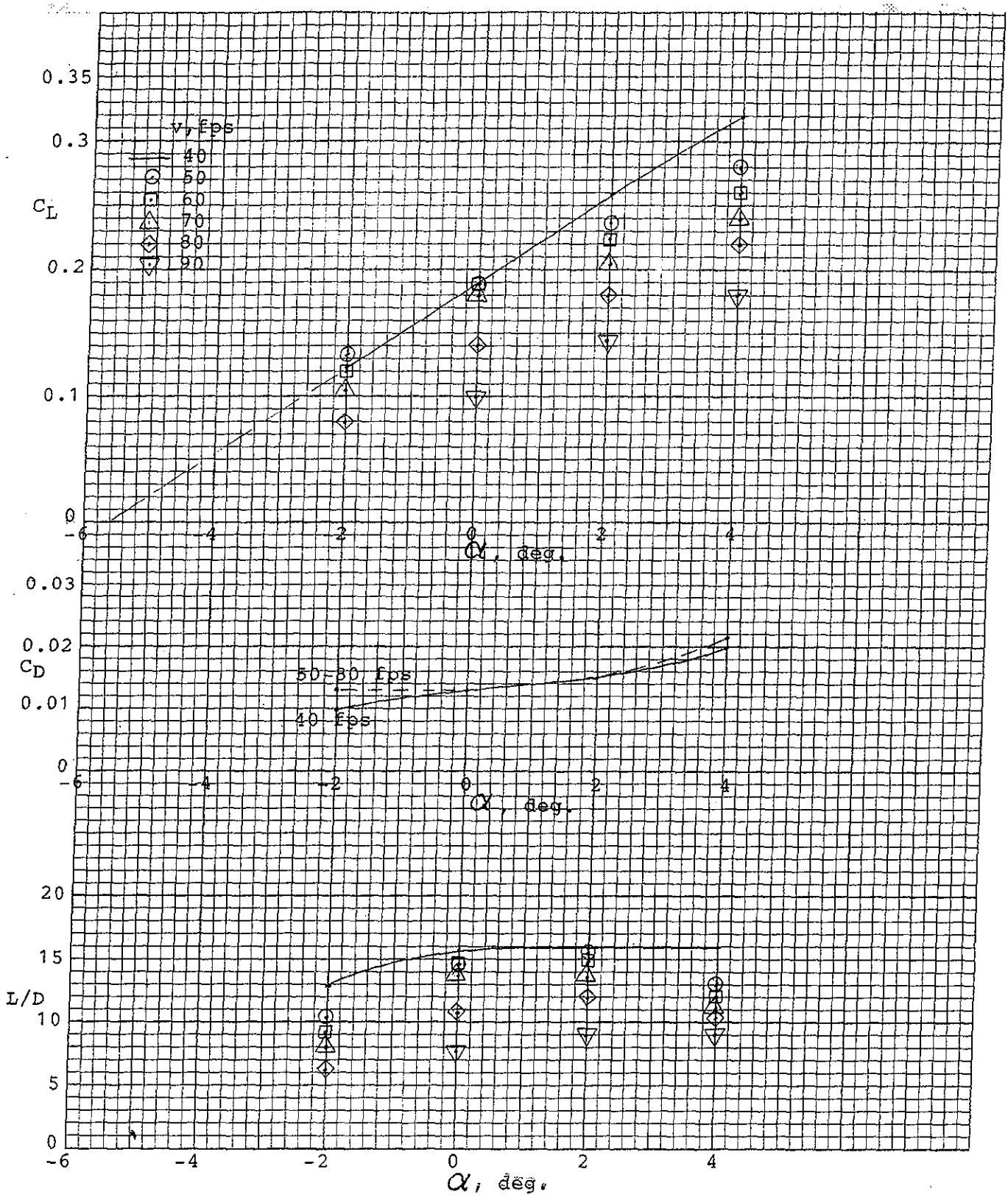

Figure 6-2 - Values of Lift Coefficient, Drag Coefficient, and Lift/Drag, for 30-deg Dihedral Hydrofoil when Half-Submerged. Aspect Ratio = 3.0.

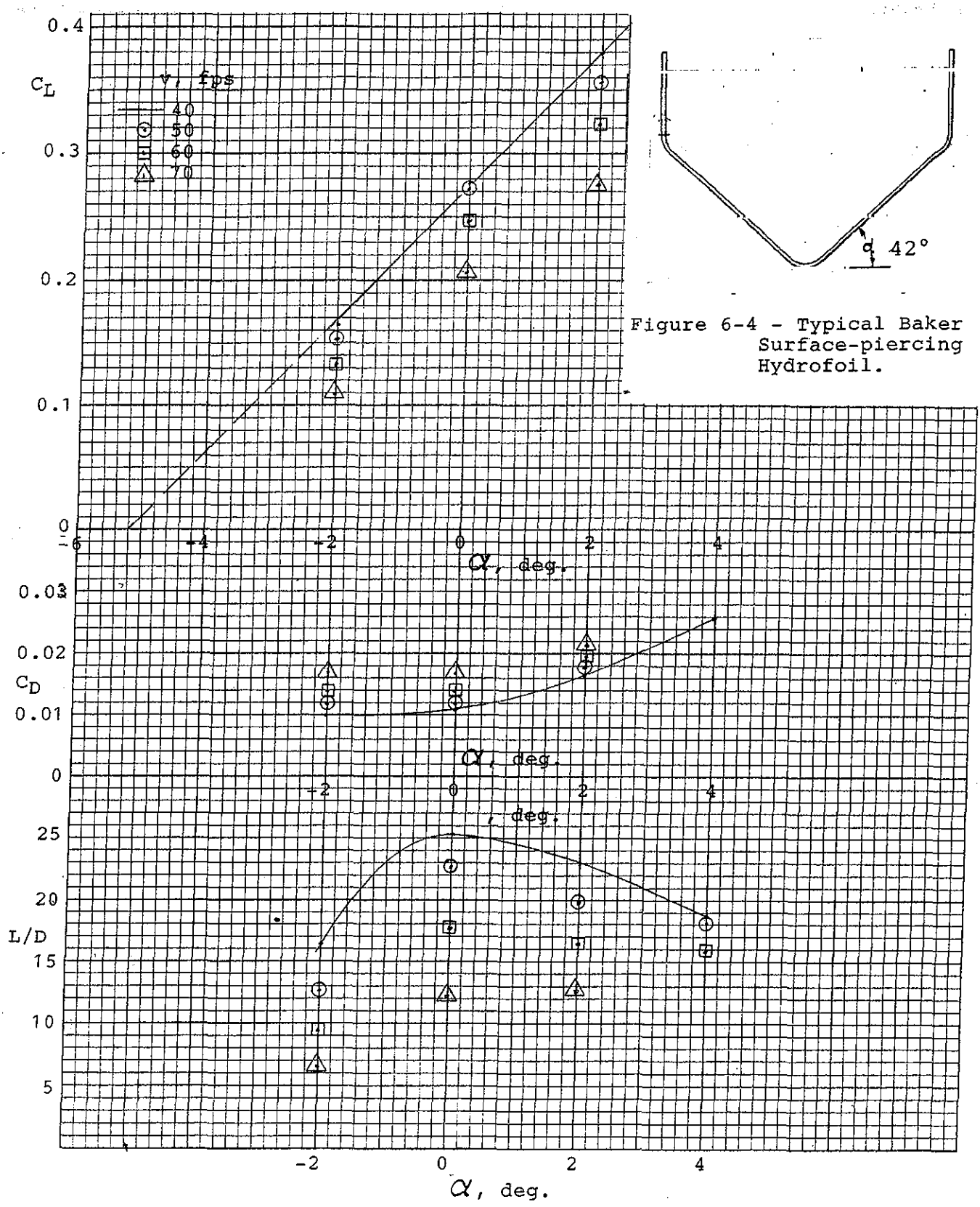

Figure 6-3 - Values of Lift Coefficient, Drag Coefficient, and Lift/Drag, for 30-deg Dihedral Hydrofoil when Submerged to the Tips. Aspect Ratio = 6.0.

Figure 6-4 - Typical Baker Surface-piercing Hydrofoil.

Appendix A
Drawings and Test Results for DTMB Model 5115

This appendix givens details of the configuration and the test results for a model of a stepped hull having a cambered planing surface near amidships, and an adjustable planing stabilizer at the stern. Drawings of the hull and the stabilizer are given in Figures A-1 and A-2. The planing (lower) surface of the stabilizer was a portion of a cylinder. Longitudinal sections thorough the stabilizer were straight-line wedges with the bases aft and the leading edges rounded. Additional details of a stabilizer of this type have been given in Reference 19. The stabilizer was adjustable, up or down, by means of an air-spring actuator, along the approximately-vertical axis shown in Figure A-1. The mode of operation for this configuration was to utilize the vertical positioning of the stabilizer so as to attain, at each speed, a running trim angle for the boat that resulted in the least drag. Testing of both models and full-scale boats of this type has shown that at low speed the lowest drag is attained with the stabilizer retracted against the bottom of the stern extension of the hull. The lower surface of the stabilizer is then parallel to the afterbody keel (and accordingly at an angle of -2.5 deg with respect to the baseline). This is the position shown in Figure A-1. When the stabilizer is moved down it rotates about the pivot shown through an angle of 4.5 deg. In the lowered position the stabilizer is accordingly at an angle of +2 deg with respect to the baseline. Experience with both models and full-scale boats has shown that, as the speed is progressively increased beyond the low speed range, progressively lower positions of the stabilizer are appropriate for maintaining minimum drag. Tabulated values of the data from one of the tests of Model 5115 are given in Figure A-3. Included are values for the stabilizer position at each test speed that resulted in the least drag. The test results for Model 5115 are given in graphical form in Figure A-4.

Dynaplane boat, $L_P/B_{PX}=4.06$
NSRDC Model No. 5115

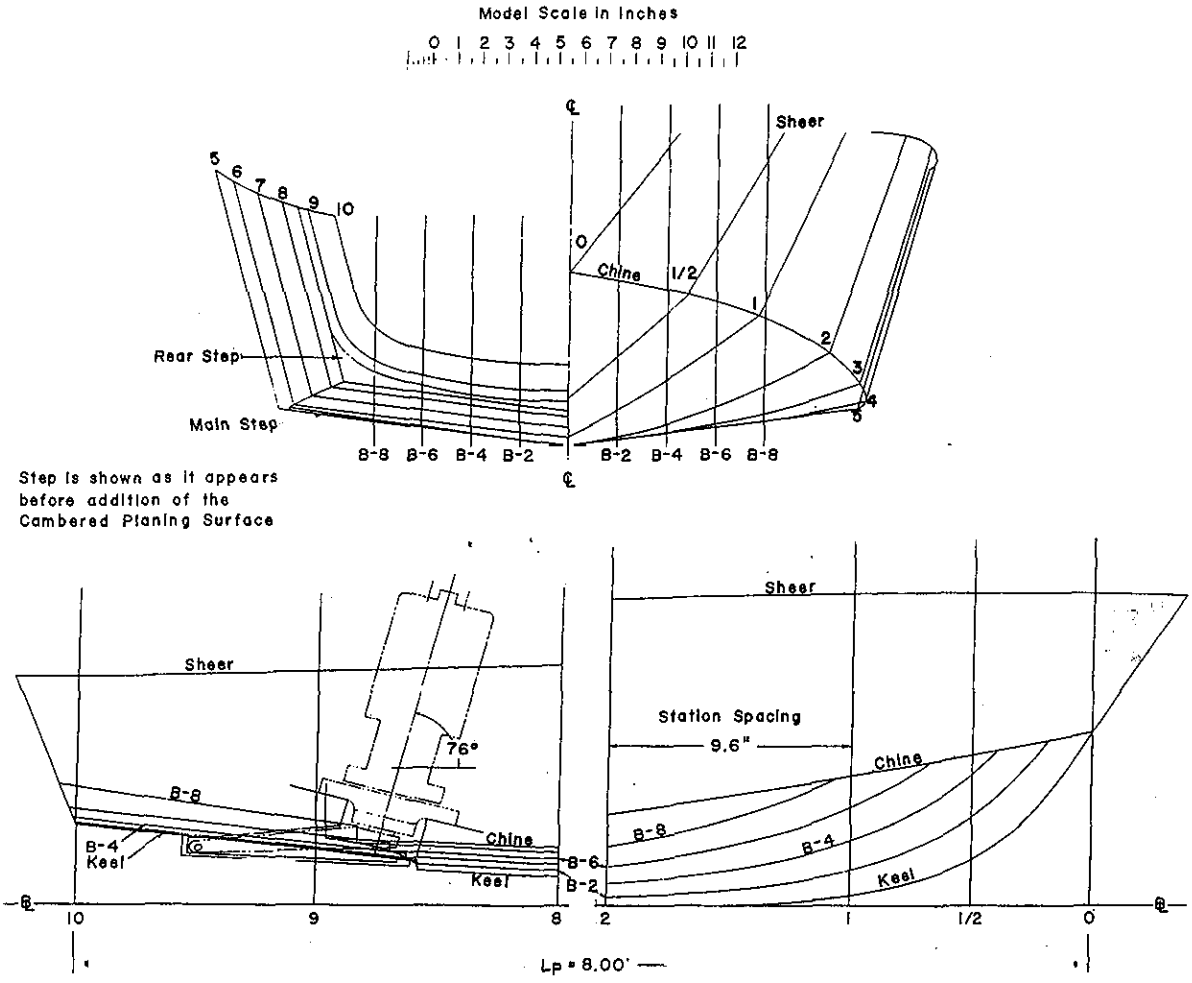

Figure A-1 - Model 5115 - Body Plan Drawing, Profile Drawings of Bow and Stern, and Centerline Section of Stabilizer in Retracted Position.

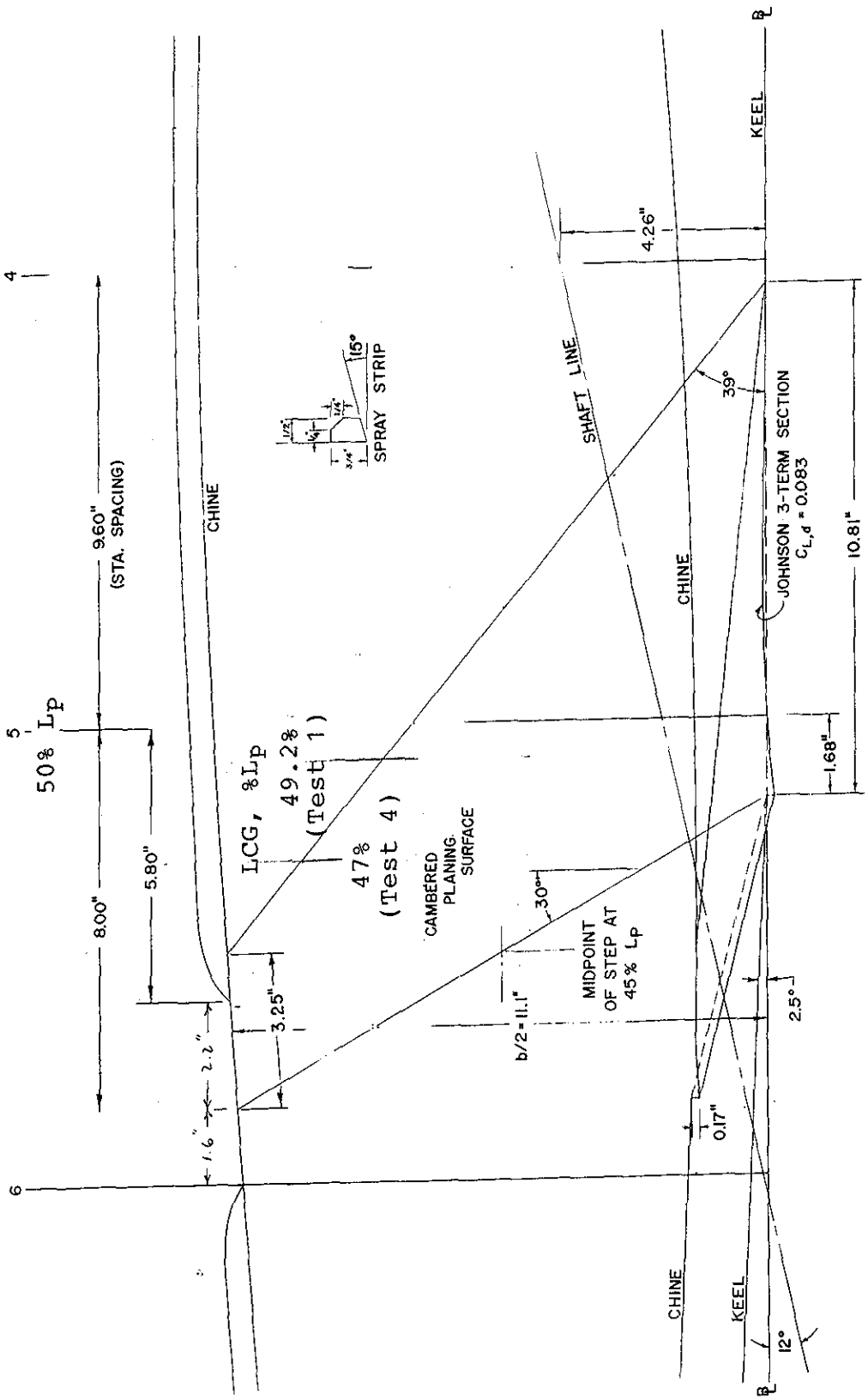

Figure A-2 - Plan and Profile Views of Amidships Region of Model 5115, Showing the Step and the Cambered Planing Surface.

Boat Dynaplane

Model Number 5115

Appendages Plum Stabilizer and Spray Strips

Laboratory NSRDC (Langley Field)

Basin High-Speed

Basin Size 2880 x 24 x 12 ft

Model Length 8 Feet

Test 4 Date

Water Temperature 42F

Specific Weight 63.4 lb/ft^3

Model Material Wood and Plastic

Model Finish Paint

Turbulence Stimul. None

Remarks: Model was towed in the shaft line shown in the profile drawing. Test was made in brakish water having a density of 1.9727 lb-sec^2/ft^4. and a kinematic viscosity of 1.6372 ft^2/sec.

Planing Bottom Dimensions and Coefficients

L_P 8.00 ft

B_{PX} 1.970 ft

B_{PA} 1.608 ft

A_P 12.84 ft^2

$A_P/\nabla^{2/3}$ 7.00

$L_P/\nabla^{1/3}$

L_P/B_{PA} 4.98

L_P/B_{PX} 4.06

LWL Dimensions and Coefficients

L

B_X

H

L/B_X

$L/\nabla^{1/3}$

C_B

C_P

C_W

Model Test Condition

W, lb 157.6 τ_0 1.0° α_0 1.0°

LCG location 45.1 in. forward of Station 10

(LCG location 1.7 percent L_P aft of centroid of A_P)

Model Test Results

V, knots	R_t, lb	Forebody: Solid water wetted lengths fwd of main step, ft — Keel	Forebody: Solid water wetted lengths fwd of main step, ft — Chine	S_{fb}, ft^2	Afterbody: Solid water wetted lengths fwd of rear step, ft — Keel	Afterbody: Solid water wetted lengths fwd of rear step, ft — Chine	S_{ab}, ft^2	Stabilizer down, in.	Change of trim, deg	CG rise, in.	F_∇
0	0	---	---	---	---	---	---	0	0	0	0
1.21	0.38	---	2.8	---	---	---	---	0	0	-0.15	0.31
2.30	1.38	---	2.9	---	---	---	---	0	0	-0.29	0.59
3.51	5.98	---	3.9	---	---	---	---	0	0.2	-0.48	0.90
4.97	16.12	3.6	3.0	7.7	2.7	2.2	5.55	0	3.5	-0.48	1.27
5.98	17.71	---	2.8	---	---	---	---	0	4.1	-0.14	1.53
7.26	20.10	2.7	2.2	4.9	2.1	1.6	4.4	0	4.8	0.72	1.86
8.40	21.17	---	2.2	---	---	0.8	---	0.59	4.3	0.91	2.15
9.56	21.62	1.9	1.6	3.5	1.0	-0.2	1.7	0.65	4.7	1.73	2.45
10.72	20.67	1.6	1.3	2.9	0.6		1.2	0.70	4.6	1.79	2.74
12.02	19.34	1.2	0.95	2.2	0.3		0.65	0.70	4.4	2.48	3.07
13.09	18.34	1.0	0.75	1.8			0.4	0.77	4.1	2.67	3.35
14.08	17.59	0.9	0.6	1.45			0.3	0.89	3.6	2.93	3.60
15.24	16.90	1.2	0.6	1.75			0.4	1.62	2.9	2.61	3.90
16.68	16.02	0.9	0.4	1.25			0.25	1.32	2.7	3.02	4.26
17.12	16.08	1.1	0.4	---			---	1.88	2.4	3.45	4.38
17.54	15.71	1.0	0.3	1.25			0.2	1.52	2.4	3.00	4.48
18.04	15.59	---	---	---			---	1.55	2.3	2.97	4.61
18.37	15.57	0.9	0.2	1.05			0.2	1.53	2.2	3.20	4.70
18.84	15.85	0.8	0.2	---			---	1.52	2.3	3.08	4.82

Figure A-3 - Test Conditions and Tabulated Test Results for Test Number 4 of Model 5115.

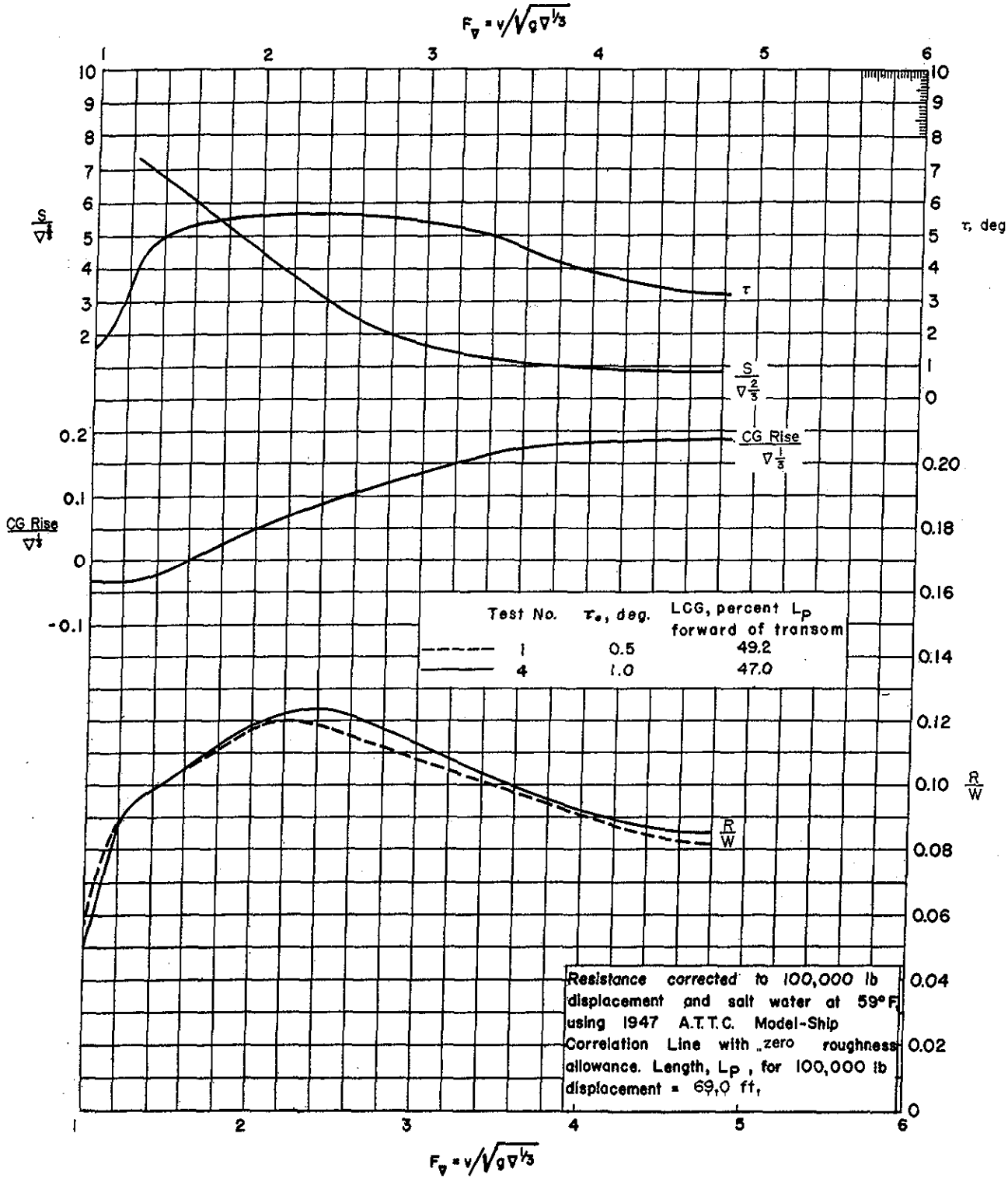

Figure A-4 - Test Results for Model 5115, in Dimensionless Form.

Appendix B

Results of Tests of a Planing Surface Model with the Johnson 3-Term Camber

In **Reference 12** Virgil Johnson predicted that high values of lift/drag ratio could be attained for supercavitating hydrofoils operating near the free water surface by utilizing his "3-term" type of camber curvature. It was evident that Johnson's theory should be applicable for planing surfaces as well as for submerged surfaces. Therefore a planing surface model (of rectangular planform and zero deadrise), which incorporated the 3-term camber, was built and tested, in order to substantiate the applicability of Johnson's equations for the planing case. Details of the test, and the results obtained, were reported in **Reference 13**. Drawings of the model are given in Figure B-1. As can be seen, the cambered region was 6 inches long by one foot wide. The aspect ratio was accordingly 2.0. The value of $C_{L,d}$ for the cambered region (this defines the amount of camber) was 0.075. The graphs derived from Johnson's equations, for the planing case, had shown that with an aspect ratio of 2, and for trim angles in the practical range of 2 deg to 3 deg, this value of $C_{L,d}$ would result in the maximum values of lift/drag ratio (see Figure B-2.). The forward end of the cambered region of the model was tangent to the flat region ahead of it. (The "Reference Line" shown in Figure B-1 is also tangent to the camber line at its forward end.) Trim angle was taken to be the angle with the horizontal of the flat center portion of the model. The model was made of transparent Plexiglas, and longitudinal markings were provided on the bottom, so that the wetted lengths when running could be observed.

The model was tested in the high-speed basin of DTMB, on Carriage 3, using the towing gear shown in Figure B-3. Test runs were made with the model fixed in trim but free to heave. Runs were made at a number of trim angles, and at a number of speeds for each trim angle. All the runs were made with the model carrying a load of 70 lb. Each test run was started with the model out of the water, and when the carriage had attained the desired test speed the model was lowered into the water so that the 70-lb load on the model (applied by the counterbalance rig shown in the figure) was balanced by the hydrodynamic lift. The drag was then measured, and the length of the bottom of the model that was wetted by solid water was observed visually. The test runs at the various speeds and trim angles resulted in a range of conditions of wetted length. The wetted-length condition of particular interest was, of course, that at which the wetted length of the model coincided with the length of the cambered region. A particular aim of the testing, therefore, was to determine, at each trim angle, the speed that would give that specific condition, and then to record the drag at that condition. Drag and bottom wetted length were also recorded, however, for those test runs at which the wetted length was greater or less than the length of the cambered region, and those values are included here.

Air drag values were measured with the model attached to the towing gear. Those measurements were made for a range of speeds and angles of attack, with the trailing edge of the model one inch above the water surface. There was no significant variation of the air drag with change of model angle of attack. The air drag values were subtracted

from the measured total drag values to give the net values of hydrodynamic drag which are reported here

The experimental values of lift coefficient for the model, for the test points at which the wetted length coincided with the cambered length, are compared with the calculated values of lift coefficient in Figure B-4. It can be seen that there is very close agreement between the experimental and the calculated values. It is presumed therefore that dependable values for the lift of cambered planing surfaces for a range of values of aspect ratio, angle of attack, and amount of camber, are given by Johnson's equations. A comprehensive set of graphs presenting those values of lift is given in **Reference 14.**

The calculated values of drag coefficient are compared with the experimental values in Figure A-5. This shows that the experimental values of drag were below those calculated from Johnson's equations. In planning the testing it had been considered that the combination of moderately high Reynolds numbers, short time between runs, and painted scales on the bottom of the planing surface model would ensure turbulent flow for all of the test conditions. However, in view of the low drag values that were measured, an experiment was made to determine if they were caused by partial laminar flow. A surface piercing cylindrical strut 1/16 inch in diameter was positioned in the water ahead of the model in such a manner that the turbulence generated was approximately the width of the model at its wetted leading edge. This produced no significant change in drag. Therefore the laminar flow explanation for the drag discrepancy was rejected. Values of lift/drag ratio calculated from Johnson's equations can therefore be presumed to be conservatively low.

The resulting finding that the values of lift/drag ratio from experiment are even higher than those which were calculated by utilizing Johnson's equations is evidently valid. The two sets of values are compared in Figure B-6. (Figure B-7 is included to show how the values of L/D for the model varied with the extent of the bottom wetted-length.) Figure B-8 compares values of L/D from calculation and from experiment when both sets of values have been extrapolated up to a size representative of a full-scale boat. This figure also includes a curve of L/D values for a flat plate (calculated), in order to show the great improvement in performance that can be achieved by the utilization of camber.

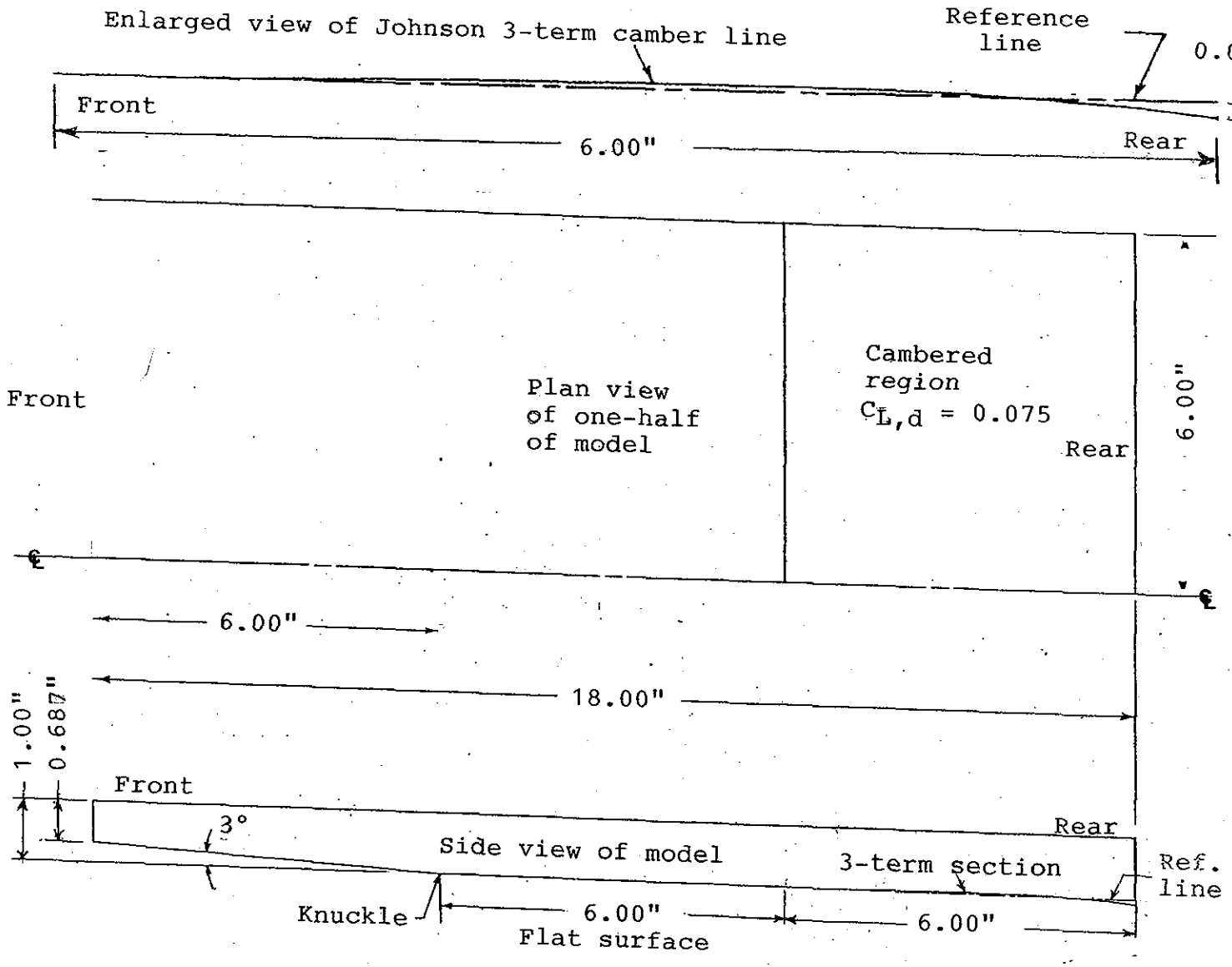

Figure B-1 - One-Foot Wide Model Incorporating Johnson 3-Term Camber in its After Six Inches

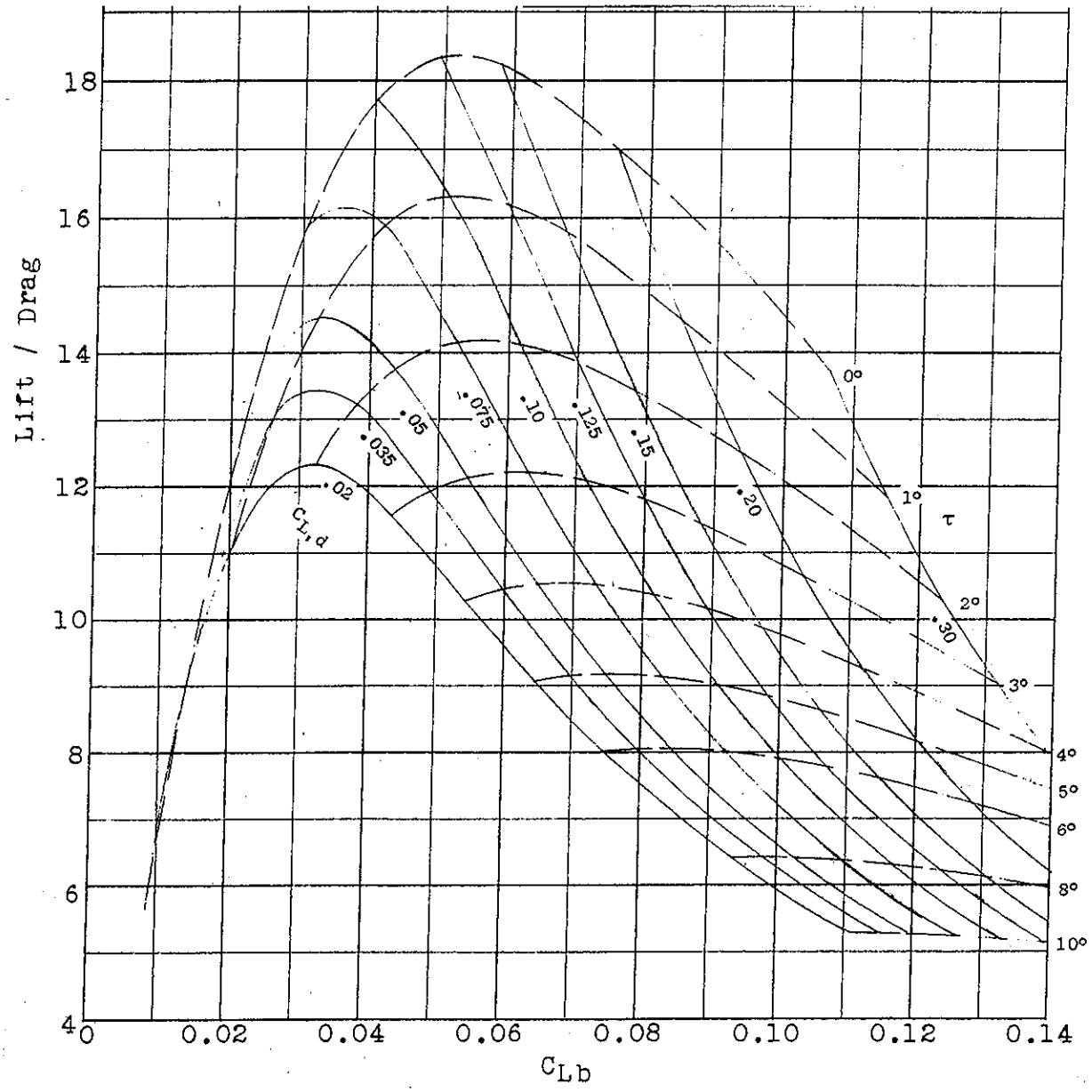

Figure B-2 - Calculated Values of Lift/Drag Ratio Versus C_{Lb} for Ranges of Values of Trim Angle and $C_{L,d}$. Johnson 3-term Section, Aspect Ratio = 2.0, C_f = 0.00293.

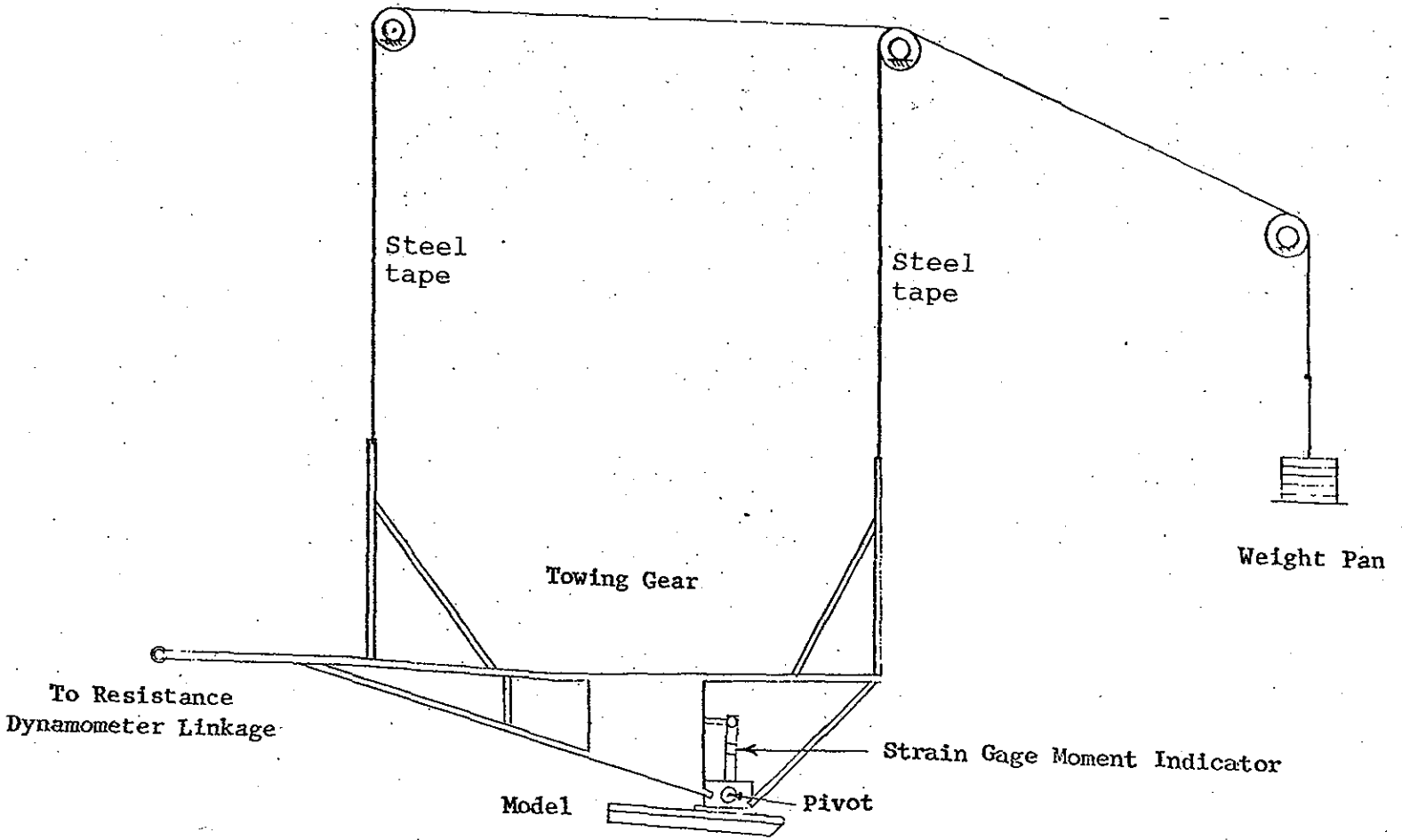

Figure B-3 - Towing Gear Used for Testing Planing Surface Model.

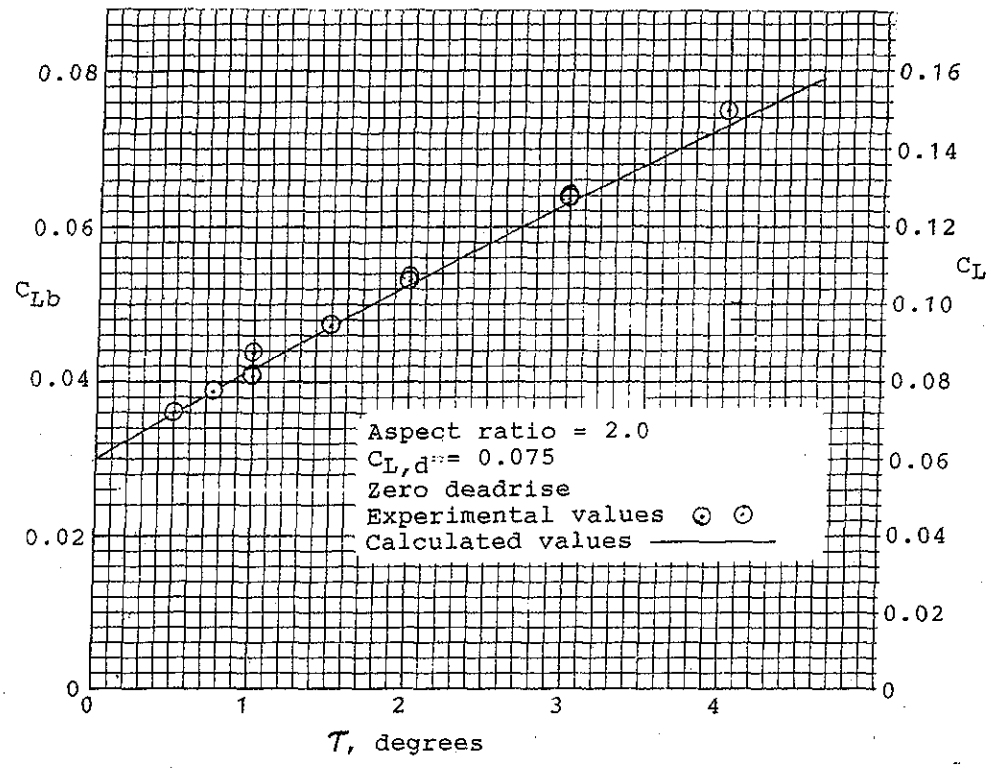

Figure B-4 - Comparison of Calculated and Experimental Values of Lift Coefficient for a Cambered Planing Surface Having the Johnson 3-Term Section. Beam = 1.0 ft, lift = 70 lb.

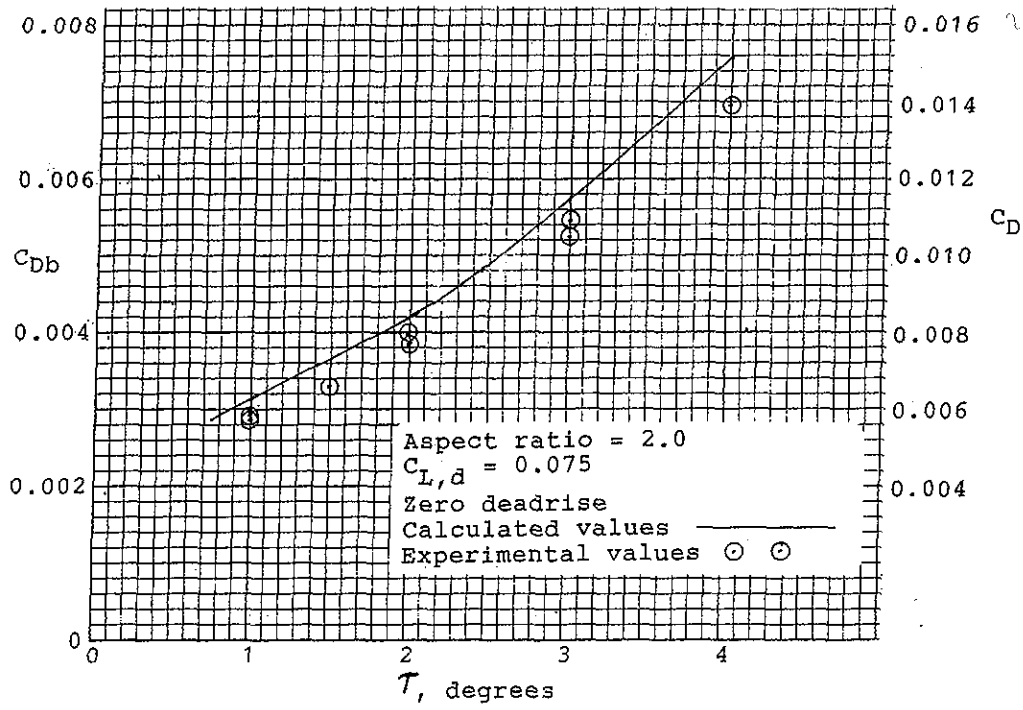

Figure B-5 - Comparison of Calculated and Experimental Values of Drag Coefficient for a Cambered Planing Surface of Rectangular Plan Form Having the Johnson 3-Term Section. Beam = 1.0 ft, lift = 70 lb.

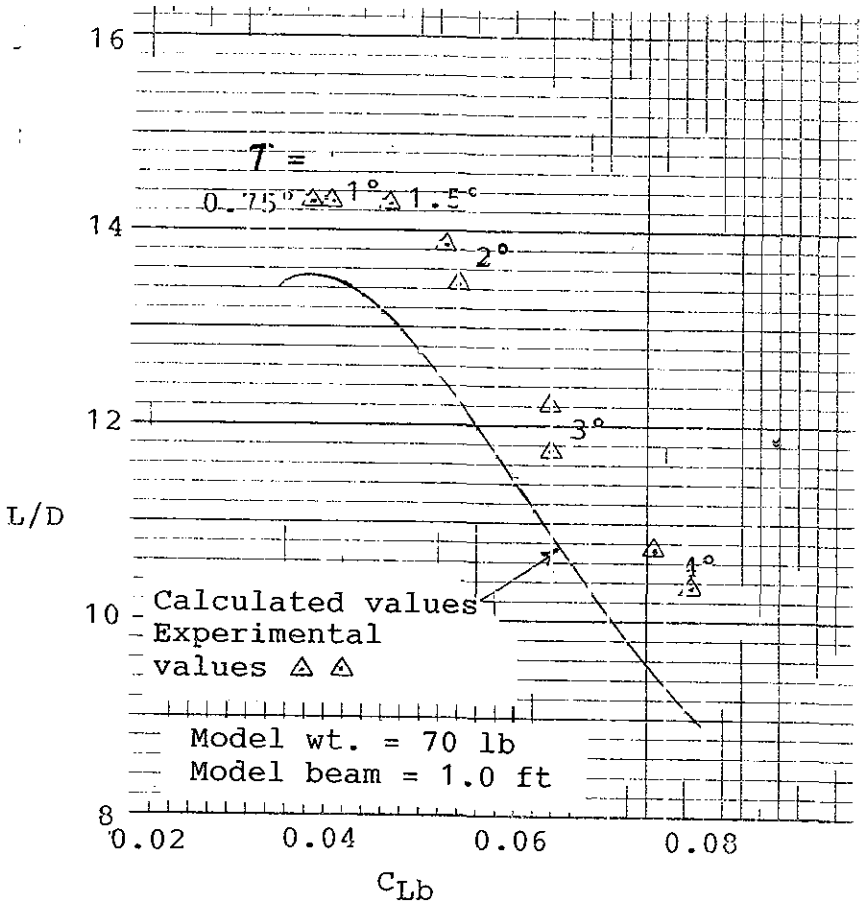

Figure B-6 - Comparison of Calculated and Experimental Values of Lift/Drag for a Model of a Cambered Planing Surface Having the Johnson 3-term Section. AR = 2.0, $C_{L,d}$ = 0.075.

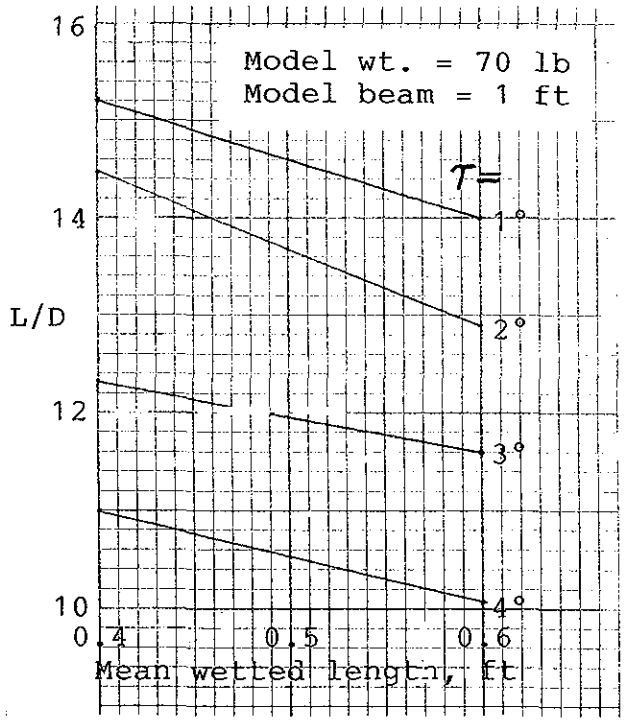

Figure B-7 - L/D Versus Wetted Length for Model That is Cambered for 0.5 ft of its Length.

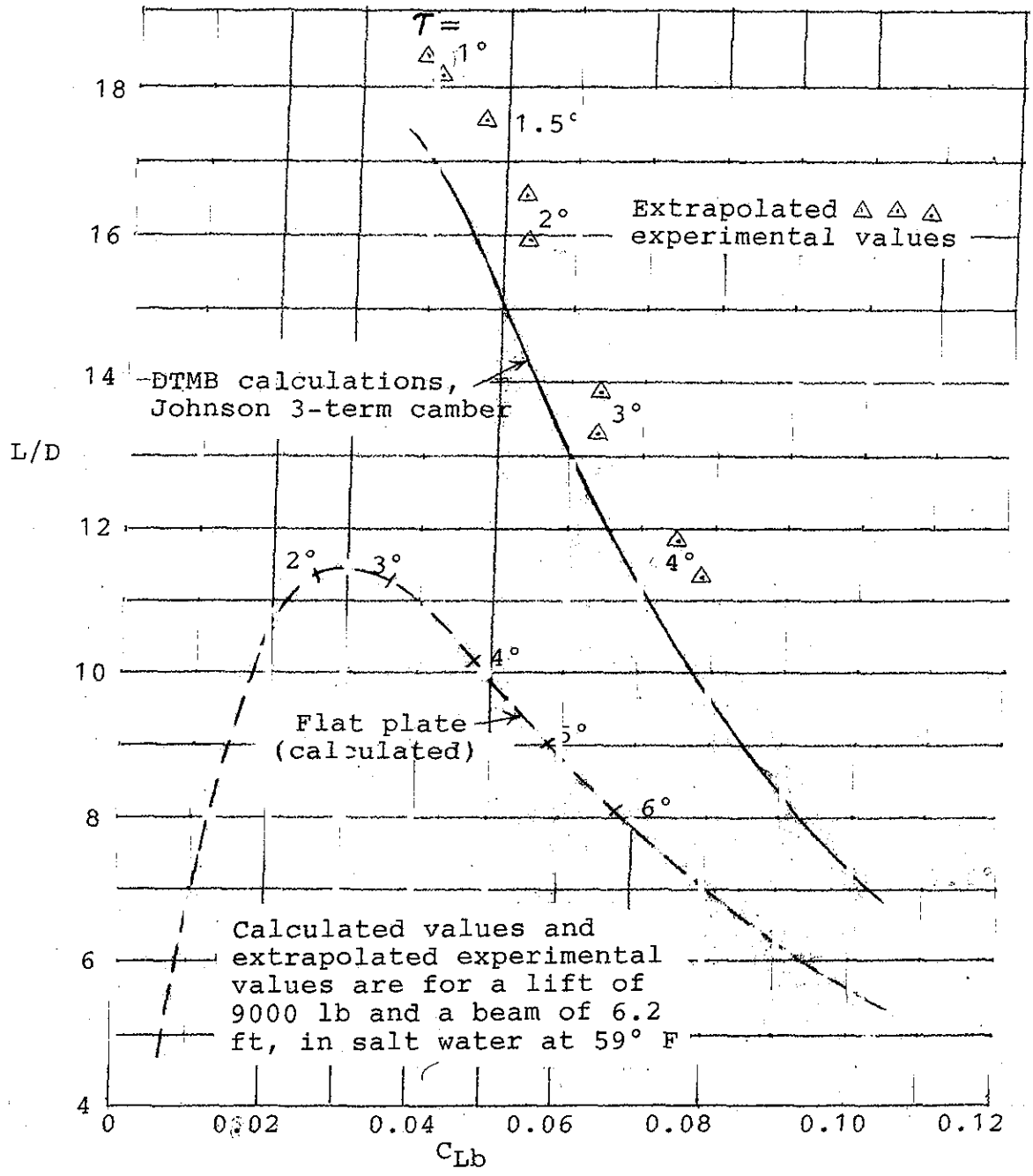

Figure B-8 Comparison of Calculated and Experimental Values of Lift/Drag Ratio for a Cambered Planing Surface Having the Johnson 3-Term Section. Comparison also with a Flat Plate.

References

1. Clement, E.P., and Blount, D.L., "Resistance Tests of a Systematic Series of Planing Hull Forms," Transactions, SNAME, 1963.

2. Rodstrom, R., Edstrand, H., and Bratt, H., "The Transverse Stability and Resistance of Single-Step Boats When Planing," Swedish State Shipbuilding Experimental Tank publication Nr 25 (1953).

3. Benson, J.M., and Land, N.S., "An Investigation of Hydrofoils in the NACA Tank, I - Effect of Dihedral and Depth of Submersion," NACA W.R. L-758, Sept, 1942.

4. Shuford, C.L., Jr., "A Theoretical and Experimental Study of Planing Surfaces Including Effects of Cross Section and Plan Form," NASA Report 1355 (1958).

5. Clement, E.P., and Pope, J.D., "Stepless and Stepped Planing Hulls - Graphs for Performance Prediction and Design," DTMB Report 1490 (Jan 1961).

6. Clement, E.P., and Koelbel, J.G., Jr., "Effects of Step Design on the Performance of Planing Motorboats," Fourth Biennial Power Boat Symposium, SE Sect., SNAME (Feb 1991).

7. Savitsky, D., and Breslin, J.P., "On the Main Spray Generated by Planing Surfaces," ETT Report No. 678 (Jan 1958).

8. Clement, E.P., "A Lifting Surface Approach to Planing Boat Design," DTMB Report 1902 (Sep 1964).

9. Brown, P.W., "An Analysis of the Forces and Moments on Re-Entrant Vee-Step Planing Surfaces," Davidson Laboratory Letter Report 1142 (May 1966).

10. Clement, E.P., "Graphs of the Performance Characteristics of Prismatic Planing Surfaces With Sweptback Trailing Edges - for Use in Stepped-Boat Design," Publ. by author.

11. Clement, E.P., and Desty, D.H., "The BP Dynaplane High-Speed Research Boat," Conference on High Speed Surface Craft, Brighton, England (Jun 1980).

12. Johnson, V.E., Jr., "Theoretical and Experimental Investigation of Supercavitating Hydrofoils Operating Near the Free Water Surface," NASA Technical Report R-93, 1961.

13. Moore, W.L., "Cambered Planing Surfaces for Stepped Hulls - Some Theoretical and Experimental Results," DTMB Report 2387 (Feb 1967).

14. Clement, E. P., "Graphs for Designing Cambered Planing Surfaces Having the Johnson Three-Term Camber Section, Rectangular Planform, and Zero Deadrise," Naval Ship Research and Development Center Report 3147, Oct, 1969.

15. Clement, E.P., and Koelbel, J.G., Jr., "Optimized Designs for Stepped Planing Monohulls and Catamarans," HPMV-92, Intersociety High Performance Marine Vehicles Conference and Exhibit, Washington, D.C., Jun, 1992

16. Baker, J.G., U.S. Patent No. 2,856,877, Oct. 21, 1958, "Hydrofoil System for Boats".

17. Lang, T.G., U.S. Patent No. 3,094,960, June 25, 1963, "Hydrofoil for Water Craft".

18. Lang, Tom, "The Up-Right Hydrofoil Kits," Website of The International Hydrofoil Society (www.foils.org) 1 Sep 2000.

19. Clement, E.P., and Koelbel, J.G., Jr. "Progress During the Past Century Toward the Development of Efficient, Load-Carrying, Stepped Planing Boats," Fifth Biennial Power Boat Symposium, SE Sect., SNAME, Feb, 1993